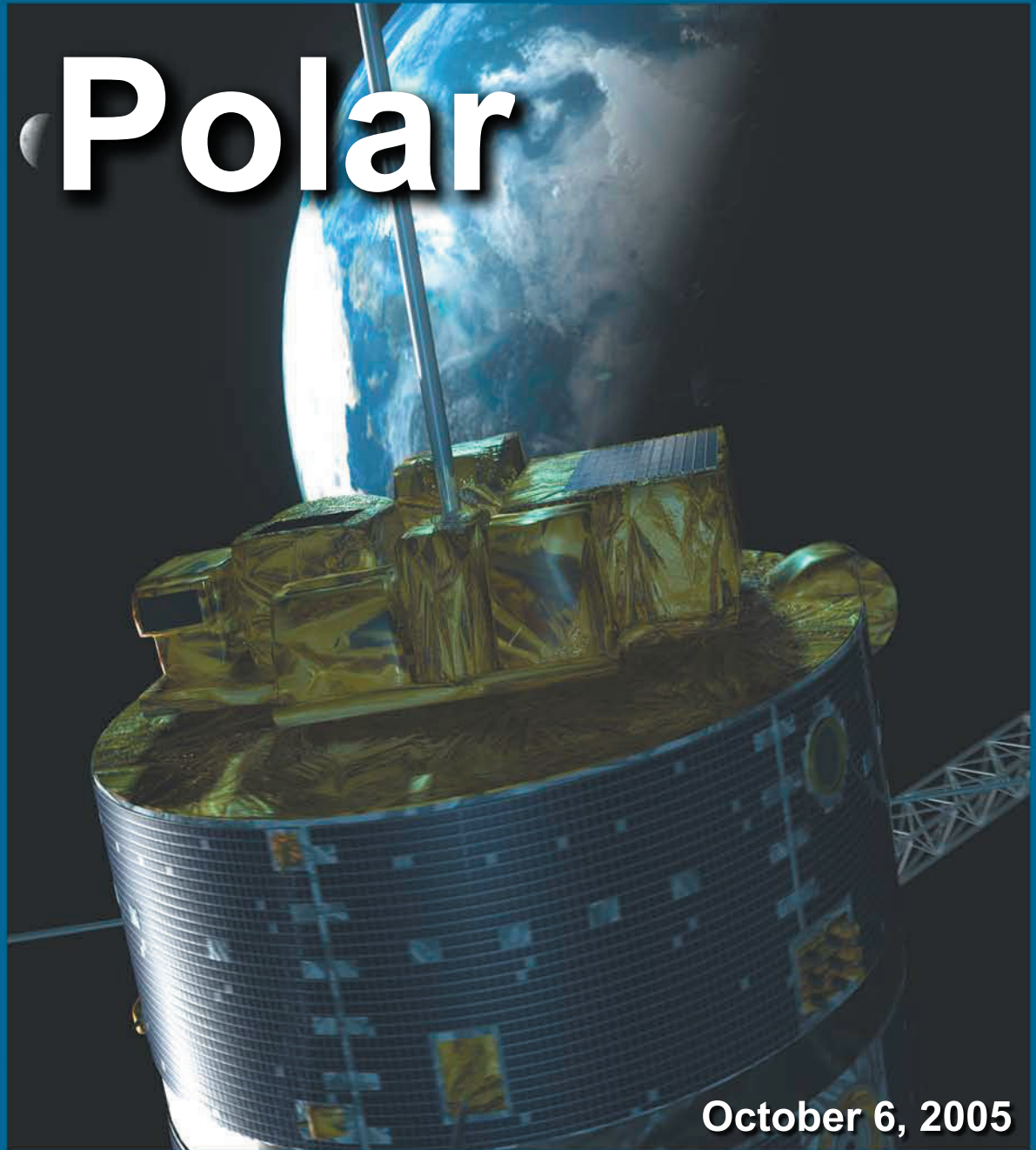
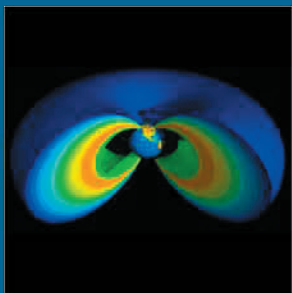
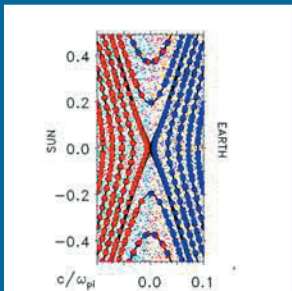
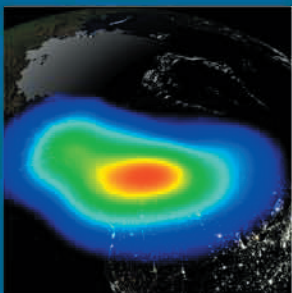
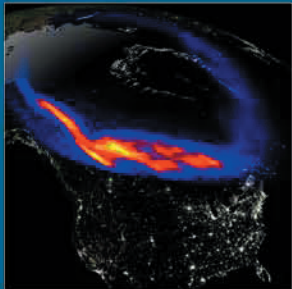
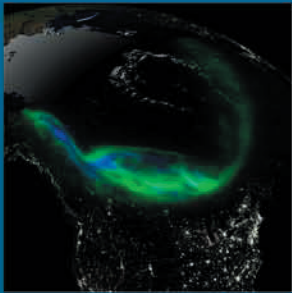
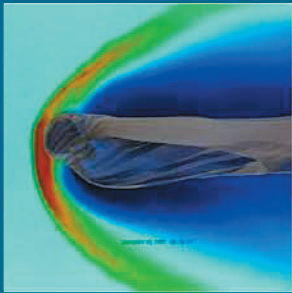


Polar



October 6, 2005



National Aeronautics and Space Administration

Goddard Space Flight Center
Greenbelt, Maryland 20771

Bernard Blake, CEPPAD, Aerospace Corporation
Theodore Fritz, CMMICE, Boston University
Donald Gurnett, PWI, University of Iowa
Ching Meng, MDI, Johns Hopkins University
Thomas Moore, TIDE, NASA
Forrest Mozer, EFI, Univ. of California, Berkeley
George Parks, UVI, Univ. of California, Berkeley
William Peterson, TIMAS, Univ. of Colorado
Christopher Russell, MFE, Univ. of California, Los Angeles
Michael Schulz, PIXIE, Lockheed Martin
Jack Scudder, HYDRA, University of Iowa
John Sigwarth, VIS, NASA
Martin Walt, SEPS, Stanford University

John Sigwarth, Project Scientist, NASA
Mark Adrian, Deputy Project Scientist, NASA
Nicola Fox, Operations Scientist, Johns Hopkins University

Contents

Executive Summary/Overview	1
1. Introduction	3
2. Science Objectives	7
2.1. Polar radiation belt science in the 2006–2007 interval: A return to the core of the outer zone during the descent to solar minimum	7
2.2. Auroral electron acceleration and ion outflow region	10
2.3. Microscale and macroscale physics of the high-latitude dayside region	13
2.4. Polar and the Sun-Solar System Connections Great Observatory	19
2.5. What have we learned from Polar?	20
3. Technical and Budget	26
3.1. Status of the space assets	26
3.2. Status of the combined Polar-Wind-Geotail ground system	28
3.3. Data availability	29
3.4. Polar budget	30
4. Education and Public Outreach	31
4.1. Accomplishments	31
4.2. E/PO products	32
4.3. New E/PO efforts	33
Appendices	
Appendix A: References	35
Appendix B: Acronym List	41
Appendix C: Polar-Provided Community Support	43
Appendix D: Young Scientists Benefitting from the Polar Mission	49

Polar Facts:

Launch:	February, 1996
Current Orbit:	1.7 × 9.4 R _E , 83.7° inclination 16° line of apsides precession/year 18.5-hour period
Spacecraft:	All subsystems healthy
Instrumentation:	Two imagers (visible and UV), healthy 3D electric and magnetic fields, healthy Eight charged particle sensors, healthy (the wave experiment, one imager, and two charged particle sensors no longer fully operational)
Predicted EOM:	March 2007

Executive Summary

In its tenth year of successful operation, the Polar mission is positioned and configured to take advantage of new opportunities for discovery and observation in collaboration with the updated assets of the Sun–Solar System Connection (S³C) Great Observatory. As Polar’s orbit evolves throughout the period covered in this proposal, Polar will make passes through the radiation belts that are progressively closer to Earth as the Sun approaches solar minimum. Meanwhile, perigee moves into the high-latitude northern hemisphere, placing Polar in the high reaches of the auroral acceleration region. Finally, Polar’s apogee moves to high southerly latitudes where encounters with the high-latitude magnetopause and investigations of high-latitude reconnection will occur. During periods of the orbit when imaging is not possible, Polar’s telemetry stream is reallocated from the imagers to the fully three-dimensional fields and particles instruments. Telemetry in this “science mode 2” allows unequalled determination of the scale size and occurrence of reconnection.

The Polar science objectives for the proposed continuation of the Polar mission are in line with the research focus areas defined by the S³C roadmap. The direct relations between the Polar science investigation objectives and the research focus areas are highlighted in Table E.1.

In the S³C Great Observatory, Polar serves a key role as the inner magnetospheric mission within 9 R_E geocentric altitude. Natural synergies exist between Polar and the flotilla of the S³C Great Observatory. The radiation belt investigations will

benefit from the global views obtained with IMAGE and the soon-to-be-launched first of the TWINS pair; while these missions will benefit from the ground truth provided by the Polar passes through the radiation belts and plasmasphere. The high temporal investigations of the 1- to 2-R_E altitude auroral acceleration region will complement the observations by FAST through the lower acceleration region below 0.8-R_E altitude. In addition, conjunctions with Polar and FAST, the newly activated Double Star and DMSP spacecraft will provide exceptional opportunities to investigate the behavior along the same field line. The ground-based imaging and magnetometer chain component of the THEMIS mission will be operational throughout the proposed extension and will benefit from early scientific collaborations with Polar. Auroral observations from IMAGE and TIMED will be utilized to complete the picture. Polar and the THEMIS spacecraft (launch in October 2006) will benefit from natural synergies, with Polar providing auroral sector imaging and high-time-resolution fields and particles observations and THEMIS covering the magnetotail. Polar’s proposed high-latitude magnetopause investigations provide an exciting opportunity to begin to evaluate the relative importance of antiparallel and component reconnection. As Polar’s passes through the southern cusp region rise in altitude, Polar becomes the fifth member of the Cluster Mission, providing a long base line for comparison when in the same hemisphere and an opportunity to investigate interhemispherical differences with Polar in the southern hemisphere

Table E.1 Connection of the polar science objectives to the research focus areas of the 2005 S³C Roadmap.

Polar Mission Science Objectives	Connection to S ³ C Roadmap
1. Polar Radiation Belt Science in the 2006–2007 interval: A return to the core of the outer zone during the descent to solar minimum	F2.1 How are charged particles accelerated to high energies? F2.2 How are energetic particles transported? H2.2 How do energetic particle spectra, magnetic and electric fields, and currents evolve in response to solar disturbances? J1.1 What are the variability and extremes (worst case) of the radiation and space environment that will be encountered by future human and robotic explorers, both in space and on the surface of target bodies? J1.2 How does the radiation environment vary as a function of time and position, and how should it be sampled to provide situational awareness for future human explorers? J4.1 To what extent does the hazardous near-Earth radiation environment impact the safety and productivity of human and robotic explorers?
2. Auroral electron acceleration and ion outflow region	F2.1 How are charged particles accelerated to high energies? F2.4 How are planetary thermal plasmas accelerated and transported? F3.3 How do the magnetosphere and the ionosphere-thermosphere (IT) systems interact with each other? H2.1 What role does the electrodynamic coupling between the ionosphere and the magnetosphere play in determining the response of Geospace to solar disturbances? H2.3 How do the coupled middle and upper atmosphere respond to external drivers and with each other?
3. Microscale and Macroscale Physics of the High-Latitude Dayside Region	F1.1 What are the fundamental physical processes of reconnection on the small scales where particles decouple from the magnetic field? F1.2 What is the magnetic field topology for reconnection at the Earth and at what size scales does magnetic reconnection occur on the Sun?

and Cluster in the northern hemisphere. To achieve maximum science return, all of the S³C Great Observatory Missions will utilize the observations from the upstream solar wind monitors such as Wind and ACE.

The Polar mission is currently experiencing unprecedented demand for data in all forms. Because most of the Polar data are easily accessible online, without the need for Principal Investigator team involvement, it is not easy to monitor the broad range of Polar data users; however, a partial list of scientists and educators that have used the Polar data is included in Appendix C.

The Polar spacecraft remains in good operational health, with 9 of 11 instruments continuing to acquire observations (see Table 1.1). However, with this proposal, the Polar mission will have a definite end. We propose to expend all remaining fuel during the final maneuver in October 2006 to achieve operations through March 31, 2007. In addition, the inert gas pressurizing the fuel tanks will be expelled to achieve the additional impulse after the fuel has been exhausted. The

performance of these thrusters in this low- to no-fuel situation is of interest to spacecraft engineers for many projects as they look forward to the future end of fuel reserves on their projects. Some time in the spring of 2007, the spacecraft is expected to overheat due to the Sun shining on the radiators connected to the spacecraft batteries.

This proposal requests a modest 1-year extension for Polar operations ending on March 31, 2007, the expected spacecraft end of life. This demise will occur after completion of a significant fraction of the 2007 magnetopause crossing season. We are also requesting a 1-year ramp down period for finalization of data analysis and data archiving activities. A high return in science value will be achieved for this modest increment in funding.

The criteria for continuation of the Polar mission were given in the call for Senior Review Proposals. Table E.2 is an aid for the review panel in finding the relevant sections of the Polar proposal.

Table E.2 Mapping of review criterion to sections in the proposal.

Criterion	Proposal Section	Comment
1. Relevance to S ³ C and the Great Observatory	1, 2.4	Polar science is closely aligned with the goals of the S ³ C Roadmap and plays a vital role in the Great Observatory
2. Impact of scientific results as evidenced by citations, press releases, etc.	2.5, 4	Five press releases
3. Spacecraft and instrument health	1, 3.1	9 of 11 instruments operational
4. Productivity and vitality of the science team (e.g., publishable research, training of younger scientists, education and public outreach)	2.5, 4, App. D	962 papers published 185 undergraduate and graduate students and post docs E/PO programs
5. Promise of future impact and productivity (due to uniqueness of orbit and location, solar cycle phase, etc.)	1, 2.1, 2.2, 2.3	Polar orbit continues to track south to the key location for studying radiation belts, auroral acceleration, and reconnection in conjunction with other S ³ C assets
6. Broad accessibility and usability of the data	3.2, 3.3, App C	Data statistics, list of Polar data users (more than 350 individual users of Polar data)

1. Introduction

Polar is in its tenth year of successful operation and has explored the northern half of the magnetosphere and a significant fraction of the southern hemisphere. The Polar spacecraft is one of NASA's few magnetospheric assets providing system science input to the Great Observatory. The data collected during this tour of the magnetosphere have been exploited by those studying the radiation belts, ring current, auroras, storms and substorms, ultra-low frequency (ULF) waves, magnetospheric compressions, magnetopause, plasmasphere, ionospheric plasma outflow, cusp and near-tail.

The success of Polar in exploring the magnetosphere is largely due to its long dwell time at apogee. Polar's precession of the line of apsides over the course of the mission has enabled detailed studies of key magnetospheric regions. Because of its complete complement of instruments, Polar science objectives have been able to evolve to take advantage of these orbital changes, resulting in a stream of exciting scientific accomplishments (detailed in section 2.5).

Initially, Polar's apogee lay above the high-latitude northern hemisphere. This allowed the first tri-spectral global images of the northern lights, and the discovery of thermal ion plasmas at high altitudes. From its vantage point at high

latitudes, Polar had a panoramic view of the entire ring current that allowed the first, time-dependent, global observations of the asymmetric properties of the ring current via energetic neutral atom (ENA) imaging. As the mission continued, Polar's precession of the line of apsides brought it into the equatorial plane and a whole new set of objectives was pursued. The long dwell time at apogee enabled observations near the magnetopause for extended periods, critical for studying the subsolar magnetopause. Polar is the only magnetospheric spacecraft with 3-axis electric field measurements, which has allowed the mapping of the electric field structure near the reconnection X point to determine the strength of flows in this region. Polar's apogee sweep through the magnetospheric regions has allowed sampling of the radiation belts over a wide range of L-value. In addition to the spatial coverage, the temporal coverage is approaching a full solar cycle (Fig. 1.1).

The precession of Polar's apogee into the southern hemisphere and the availability of data from other magnetospheric satellites, such as IMAGE and Cluster, have opened a wealth of new research areas. Fundamental issues concerning the behavior of the magnetosphere can now be addressed in the context of our earlier northern hemisphere observations. Using

New factors motivating continued operations of the Polar spacecraft

Throughout the remaining Polar mission operations, the science team will continue to exploit orbit evolution, flexible telemetry options, and constellation spacecraft:

- Precession of apogee into the southern polar region: During this precession the Polar orbit will sweep through the heart of the outer radiation belt at distances from 2 to 7 R_E during the declining phase of the solar cycle.
- Reallocation of telemetry: To provide significantly higher resolution measurements of in situ vector electric and magnetic fields, the Polar science team has reconfigured telemetry allocations maximizing our science return.
- Observations during the declining phase of the solar cycle
- Addition of constellation spacecraft: With the addition of complementary spacecraft such as Cluster, TIMED, and IMAGE to the inner-magnetospheric constellation and ACE, TRACE, SOHO, and RHESSI observing the Sun and solar wind, significant, new collaborating data sets are now available, allowing more in-depth analysis of geo-effective events from their origins to Earth's upper atmosphere.

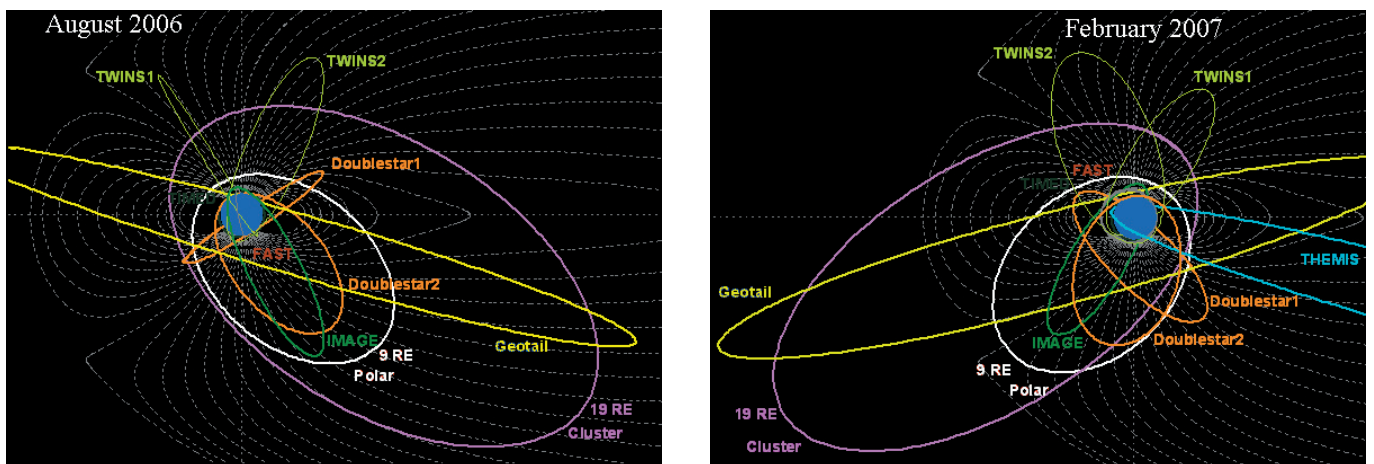


Fig. 1.1 Polar's perigee is now proceeding through the high-latitude northern hemisphere, providing increasingly good opportunities for high-temporal-resolution investigations of the auroral acceleration region, burst mode sampling of the high southern latitude magnetopause boundary layers, and successively deeper cuts into the inner magnetosphere for 7 to 2 R_E , which are ideal for diagnosing energetic particle injection and acceleration mechanisms.

our new science mode 2 (reallocating the science-data telemetry from the imagers to in situ instruments), we have provided significantly higher time resolution measurements of in situ vector electric and magnetic fields. This improved sampling has substantially benefited the study of kinetic processes, especially during magnetopause crossings.

In this final epoch of its life, Polar will, in a sense, return to its origins, apogee at high latitudes to reach the cusp region, and perigee near the auroral oval, but with critical differences:

- The return to the heart of the outer radiation belt that will occur in a significantly different context: new collaborating space assets of complementary observations (especially IMAGE observations of the plasmopause and ring current populations) and at a different phase of the solar cycle when the probability of encountering large electron flux enhancements will increase
- Comparison of the high-spatial-resolution plasma, electric, and magnetic field measurements within and above the auroral acceleration region with large-area high-resolution optical observations of the aurora from the THEMIS All-Sky Imager network over all of Canada and Alaska
- The new high-time-resolution, 3D electric field measurements from Polar together with the availability of Cluster data for high latitude/cusp studies of the micro- and macrophysics of reconnection.

Approval of continued Polar operations into the second quarter of FY2007, the expected end of the spacecraft's operational life, will permit continued acquisition of unique and unprecedented data leading to even greater and more in-depth insights into the processes that transport solar mass, energy and momentum into near-Earth space.

Approach

Through judicious use of our fuel supply, we have been able to extend the Polar mission lifetime through March 2007. The spin axis is now permanently oriented normal to the ecliptic, but this orientation has not impaired our ability to address the science objectives. The main impact of operations at ecliptic-normal spin orientation has been a reduced duty-cycle of Earth-viewing opportunities for the imagers (4 to 6 hours per 18-hour orbit). As noted above, we have re-portioned the science-data telemetry when the imagers cannot see the Earth to provide a higher sampling rate for selected in situ measurements. Because the high-time-resolution electric field measurements are crucial for the success of our proposed science objectives, we have developed a comprehensive maneuver plan for the remainder of the mission. We will use our remaining fuel to maximize the time spent at appropriate sun angles to minimize the impacts of the spacecraft shadowing on the electric field instrument (EFI) antenna. The final maneuver in October 2006 will deliberately exhaust all of the remaining fuel in the fuel tanks to put the spacecraft at an optimal sun angle for continued operations for the final months. In addition, expending all of the remaining fuel on the final maneuver will give engineers an unprecedented opportunity to observe the effectiveness of the thrusters as the fuel runs

out and the remaining inert gas is expelled from the fuel tanks. This information will be valuable to planners of other NASA missions nearing the end of their fuel reserves.

The spacecraft remains healthy, with all subsystems operating nominally. The three batteries have successfully serviced the spacecraft through the longest eclipses of the mission. Polar has lost one of its two digital tape recorders through failure of the recorder's power supply, but despite this loss, the Polar mission continues to acquire data with greater than 90% coverage; the remaining tape recorder is fully capable of servicing the Polar mission. The despun platform continues to operate nominally with no degradation of performance. Most of Polar's instruments remain healthy despite our radiation exposure (see Table 1.1 and Section 3.1).

Polar as a key component of the Great Observatory

The strategic objective addressed in the current Sun-Solar System Connection (S³C) roadmap is "intrinsically one of connections . . . extending over vast distances to produce dramatic effects throughout the solar system." As a result of its ever-changing location within the magnetosphere, Polar has provided connection between ground and space measurements, studies of coupling processes between the various regions of geospace, and a valuable global perspective on the magnetosphere as a whole. Thus Polar has played a key role in connections studies for the past decade, first as part of the International Solar-Terrestrial Physics (ISTP) fleet of spacecraft and now with a new flotilla of satellites, each contributing to the Great Observatory.

The proposed Polar science investigations highlight Polar's role in the S³C Great Observatory. Understanding the details of energization of radiation belt particles to megaelectron volt levels and modeling of the radiation belts will be important for human and robotic explorers leaving low Earth orbit on their way to the Moon and Mars. The organized interaction of the magnetic and electric fields with particles, as in the auroral acceleration region, is important for its impact on our home in space (the Earth) and may have important implications for particle acceleration elsewhere in the solar system and the universe. Finally, reconnection plays a fundamental role in the acceleration and transport of plasmas in the Earth's magnetosphere and on the surface of the Sun. Currently, Earth's magnetosphere provides the only accessible laboratory for directly observing reconnection. Knowledge gained from Polar's high-time-resolution observations of the high-latitude dayside reconnection region will be applied to reconnection on the Sun.

The Polar team has made comprehensive contributions to public awareness of the science of Sun-Solar System Connections, both with the development of products valuable to education and public outreach (E/PO) and with many direct contacts between its scientists and the public at formal and informal gatherings. We have an exciting set of E/PO objectives planned for the remainder of the mission to ensure that Polar's legacy will live on well beyond its operational lifetime.

New scientific objectives

Polar radiation belt science in the 2006–2007 interval: A return to the core of the outer zone during the descent to solar minimum

Problems:

- Why are multi-MeV electrons apparently lost during the initial phases of major geomagnetic storms? Are electromagnetic ion cyclotron (EMIC) plasma waves a major storm-time loss process for outer zone relativistic electrons?
- How does the inner portion of the outer zone evolve during the descent to solar minimum?
- What determines the effectiveness of a given geomagnetic storm as a relativistic electron accelerator?

Opportunities and unique assets:

- Approach to solar minimum is the time of the most intense radiation belt enhancements.
- Polar is in the ideal location to acquire radiation belt data, as the equatorial crossing of Polar will move into the high-intensity core of the radiation belt.
- Data from a more robust fleet of collaborating spacecraft are now available to compare phase space densities of energetic particles.

Expected results:

- Characterize the evolution of the inner portion of the outer radiation belt as a function of solar cycle descent.
- Discover the mechanisms through which the energy of scattered radiation belt electrons is dependent upon storm intensity and/or characteristics.

Lead instruments:

CEPPAD, CAMMICE, EFI, MFE

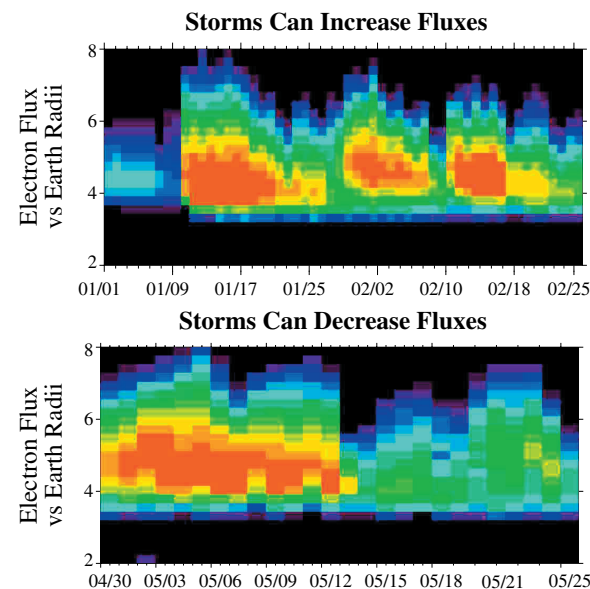


Fig. 1.2 Examples of the widely different response of relativistic outer zone electrons to magnetic storms. Flux levels after a storm can be enhanced (top) or depressed (bottom) compared with conditions before the storm. This emphasizes the need to understand and quantify both acceleration and loss processes, which can occur simultaneously during the storm period [after Reeves *et al.* 2003].

Auroral electron acceleration and ion outflow region

Problems:

- What are the energy sources at the top of the auroral acceleration region?
- Where (e.g., at what intermediate altitude) are auroral electrons accelerated?
- What fraction of energy available in the convection electric field is converted to precipitating electron energy?
- What are the physical processes that lead to ion outflow from the ionosphere?

Opportunities and unique assets:

- Utilize magnetic conjunctions with high-resolution auroral images and magnetometer observations from the THEMIS ground-based network.
- Use high-temporal-resolution Polar data from the middle to the high reaches of the auroral acceleration region.
- Combine the Polar data with high-resolution data from FAST in the lower altitudes in the auroral acceleration region, with Double Star at intermediate altitudes, with DMSP auroral observations at low altitudes, and with the THEMIS spacecraft in the magnetotail.

Expected results:

- Determine the energy partitioning from the auroral energy sources to the energized auroral electrons in the inverted-V and other auroral acceleration regions.
- Determine the full extent of the auroral electron acceleration region (i.e., altitude and MLT regime) and the fraction of energization with altitude.
- Characterize the physical processes causing ion outflow from the ionosphere

Lead instruments:

Hydra, TIDE, TIMAS, EFI, MFE

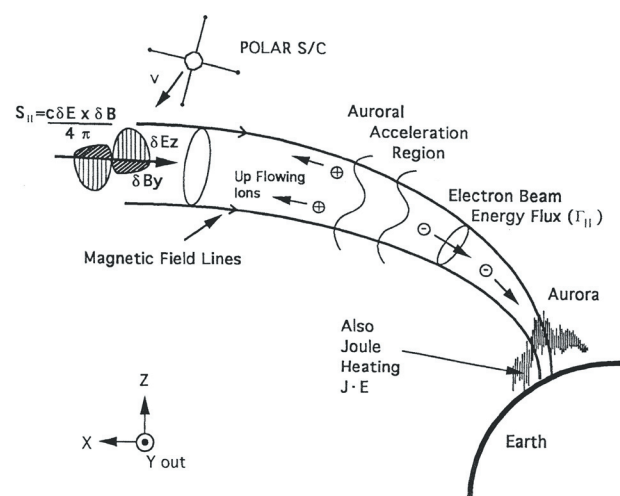


Fig. 1.3 Illustration of a magnetic flux tube conjugate to the auroral acceleration region with incident Poynting flux and its conversion to energized particles and joule heating of the ionosphere (wavelength of wave fluctuations not to scale), from Wygant *et al.* [2000].

Microscale and macroscale physics of the high-latitude dayside region

Problems:

- Microscale: How do the occurrence and nature of separatrix/diffusion region crossings vary as a function of latitude and external IMF magnetic geometry?
- Microscale: What are the electron demagnetization mechanisms that allow component reconnection at high latitudes? Do these mechanisms include thin layers of strong electric field enhancements (EFEs) that have been observed at lower latitudes?
- Macroscale: How does the orientation of the magnetic field in the magnetosheath impact the relative fraction and rates of antiparallel reconnection versus component reconnection in the presence of a guide magnetic field?
- Macroscale: What is the spatial/temporal coherence of the dayside magnetosphere under steady solar wind conditions?

Opportunities and unique assets:

- Polar's orbit will provide long dwell time at apogee near the high-latitude dayside magnetopause.
- High-temporal-resolution fields and particles will be observed with new science mode 2 telemetry.
- Polar is the only operating spacecraft with 3D electric field measurements that are required for identifying reconnection regions in the vicinity of the cusp.
- Polar and Cluster provide a unique opportunity to study large-scale structure of the dayside magnetosphere.

Expected results:

- Characterize the filamentary nature of reconnection leading to the formation of electron diffusion regions.
- Understand the fundamental properties of reconnection based upon distinguishing between antiparallel and component merging scenarios.

- Understand the large-scale structure of plasmas in the dayside magnetosphere

Lead instruments:

Hydra, EFI, MFE, TIMAS, CEPPAD, CAMMICE

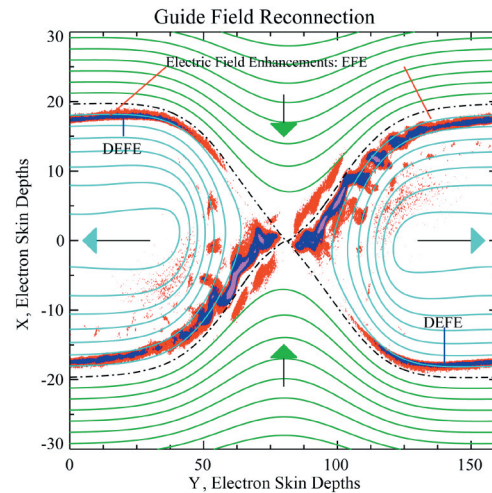


Fig. 1.4 Electric field enhancements (EFE) allow component reconnection to proceed in a low β_e plasma with a guide field, as recently observed from Polar using science mode 2 data. These thin EFE layers enable collisionless magnetic reconnection along a substantial arc of the separatrices away from the crossing point. Unusually thin locales of EFEs capable of demagnetizing the thermal electrons are labeled DEFEs, as indicated (Figure courtesy of W. Daughton).

Table 1.1 Status of the instrumentation onboard Polar. Extensive spacecraft subsystem and instrument subsystem redundancies have preserved an extremely robust set of measurement capabilities.

Instrument	Capability	Status
MFE: Magnetic Fields Experiment	DC – 54 Hz vector magnetic field	Normal
EFI: Electric Fields Instrument	3D electric field, thermal electron density: 80 Hz, 1600 Hz	Normal
PWI: Plasma Wave Instrument	Spectral and wave vector characteristics: 0.1 Hz to 800 kHz	Infrequent operations
CAMMICE: Charge & Mass Magnetospheric Ion Composition Experiment		Not operational
MICS Sensor	Energetic ion composition: 6 keV/q to 400 keV/ion	Normal
HIT Sensor	Energetic ion composition: 100 keV/q to 60 MeV/ion	Normal
CEPPAD: Comprehensive Energetic Particle Pitch-Angle Distribution		Not operational
IES & IPS sensor	25 to 400 keV ions and electrons	Normal
HIST sensor	High energy ions and electrons, $E_e > 350$ keV and $E_p > 3.25$ MeV	Normal
SEPS sensor	Loss cone measurements	Not operational
Hydra: 3D Electron and Ion Hot Plasma Instrument		Normal
DDEIS sensors (2)		Normal
PPA sensors (2)	3D electron and ion distributions (2 to 35 keV/q)	Normal
TIMAS: Toroidal Imaging Mass-Angle Spectrometer	3D mass separated ions: 15 eV to 25 keV	Normal
TIDE: Thermal Ion Dynamics Experiment	2D ions: 0 to 500 eV/q	Normal, no mass separation
UVI: Ultraviolet Imager	Far ultraviolet auroral imager: 130.4, 135.6, 140-160, 160-175, 175 to 190 nm	Normal
PIXIE: Polar Ionospheric X-ray Imaging Experiment	X-ray auroral imager: 2 to 60 keV	Not operational
VIS: Visible Imaging System	3 low-light cameras: 124 to 149, 308.5, 391.4, 557.7, 589.0, 630.0, 732.0 nm	Normal

2. Science Objectives

The current proposal spans the approach to solar minimum, characterized by large transient equatorial holes in the corona of the Sun. These structures are associated with long-lived, high-velocity solar wind streams that produce recurrent geomagnetic storms and the largest fluxes of damaging MeV radiation belt electrons. The innovative reallocation of the Polar spacecraft telemetry allows high time-resolution measurements of the electric and magnetic fields and particles. In conjunction with other assets within the S³C Great Observatory, we propose to use these high-resolution Polar observations to accomplish the following general goals for the extended phase:

- The return to the heart of the outer radiation belt during the declining phase of the solar cycle, when large electron flux enhancements occur more frequently than in previous phases of the mission, in conjunction with the existing assets such as IMAGE and Cluster and new anticipated assets such as TWINS and THEMIS, which were not available early in the Polar mission.
- Understanding the auroral acceleration process using a comparison of the high spatial and temporal resolution plasma, electric and magnetic field measurements with large-area high-resolution optical observations of the aurora from the THEMIS All-Sky Imager network over all of Canada and Alaska, with the expanded SuperDARN network, and (after its launch in October 2006) with the THEMIS spacecraft.
- High-latitude dayside investigation of the micro- and macrophysics of reconnection using high-time-resolution 3D field and particle measurements, together with data from Cluster and Double Star.

2.1. Polar radiation belt science in the 2006–2007 interval: A return to the core of the outer zone during the descent to solar minimum

Overview: The processes leading to the acceleration, transport, and loss of high-energy electrons is of fundamental scientific importance. Previous work suggests that the effect of geomagnetic storms on radiation belt fluxes is a delicate and complicated balance between the effects of particle acceleration and loss [Reeves *et al.* 2003]. Most electron acceleration sites can only be remotely observed but, in the case of the Earth’s magnetosphere, in situ measurements can be made, and Polar has been a key tool recently for making such measurements.

The Living With a Star (LWS) program has begun, with its focus on science having significant societal benefit. Energetic electrons are the primary radiation threat in most Earth orbits. Space system designers require more accurate radiation models; the use of large margins to cover ignorance is no longer acceptable. Scientific quality observations over a long period not only provide a better understanding of the average space environment, but also greatly increase the confidence in “worst-case” environments that are needed for many purposes

including human space missions, internal dielectric charging mitigation, and sensor background engineering. *Increased knowledge of energetic electron dynamics has immediate LWS applications, and will be a precursor science for the upcoming Radiation Belt Storm Probes mission.*

Polar was launched at solar minimum, and the argument of perigee was such that Polar traversed the equatorial region of the heart of the outer zone for 3 to 4 years. Later, motion of the argument of perigee led to a Polar orbital track that did not traverse the central regions ($2 < L < 5$), and therefore the critical equatorial measurements could no longer be made. Fortunately, in 2006 Polar will return to the equatorial regions of the outer zone during the descent to solar minimum, that time period in the solar cycle just before the Polar launch. Measurements at equatorial latitudes are important because the most intense fluxes are generally found near the equator, and that is the only place where all particles trapped on a magnetic field line can be observed.

Polar returns to the magnetic equator in the core of the radiation belts with new scientific assets, such as IMAGE and the soon-to-be-launched TWINS, available for key complementary measurements. Table 2.1 highlights some new missions that will provide important context for ongoing Polar observations. Polar is the only spacecraft operating in the inner magnetosphere with a full complement of energetic particle instruments that provide angular distributions of the energy spectra and vector magnetic and electric field measurements. Figure 2.1 shows that $L = 2$ to 5 is a prime crossroads for the radiation belts and the plasmopause. If the late 2005 through 2007 interval is anything like 1994–1996, Polar should see several large enhancements of the energetic outer-zone electrons.

Why are multi-MeV electrons apparently lost during the initial phases of major geomagnetic storms? Are electromagnetic ion–cyclotron (EMIC) waves a major storm-time loss process for outer zone relativistic electrons?

General problem: During the main phase of nearly every magnetic storm, trapped relativistic electron fluxes are observed to drop dramatically, as shown in Fig. 2.2 [Reeves *et al.* 2003]. This characteristic feature begs for an explanation.

Recent advances: Originally, the decrease in electron flux during the main phase of magnetic storms was thought to be an adiabatic response, nicknamed the “Dst effect” [Dessler and Karplus 1961, Kim and Chan 1997]. However it has become evident that there are real, significant particle losses during the main phases of magnetic storms [Reeves *et al.* 2003, O’Brien *et al.* 2004]. One mechanism that may explain this loss is wave–particle interactions that result in pitch-angle scattering into the loss cone. Two wave populations have been identified as likely candidates: very-low-frequency (VLF) chorus [Lorentzen *et al.* 2001, O’Brien *et al.* 2004, Thorne *et al.* 2005] and EMIC waves [Horne and Thorne 1998, Albert 2003]. Previous studies using Polar and SAMPEX have helped to estimate the VLF losses.

Table 2.1 New additions to the geospace constellation since Polar's last visit to the core of the outer zone.

Mission	Launch	Highlights
IMAGE	2001	Plasmasphere images, Waves
Cluster-II	2000	Waves, particles, fields
MEO-1	2001	Dosimeters, Crosses magnetic equator at L = 2.5, five electron channels above 1 MeV
HEO-4	2005	Dosimeters, ESA, ENA, Crosses magnetic equator at L = 2
TWINS	2005	ENA (TWINS is aboard HEO-4)
GEO	Several on-orbit	5-6 spacecraft instead of 3 prior to 2001, extensive electron and ion measurements from plasma energies to several MeV, <i>cf.</i> http://leadbelly.lanl.gov
GPS	Several on-orbit	up to 8 energetic electrons, 100s of keV to few MeV, measurements down to L = 4 on equator

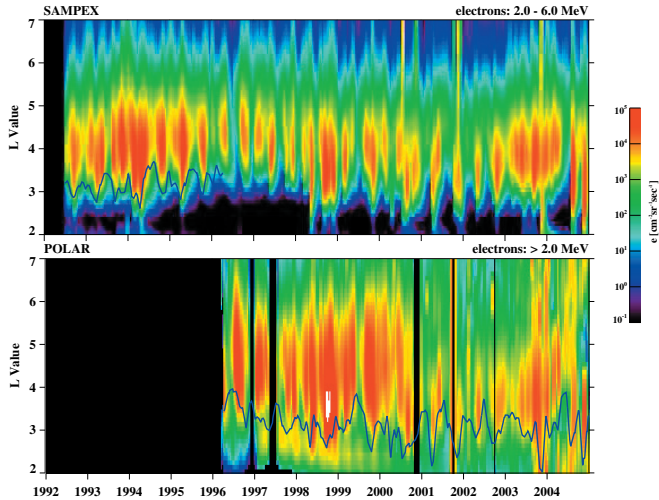


Fig. 2.1 A plot of relativistic electrons as seen by SAMPEX and Polar – combined observations spanning more than a solar cycle. The minimum L of the plasmopause is over-plotted. The 2005–2006 interval should resemble 1993–1994 (prior to Polar launch), when significant solar wind driving led to a strongly enhanced outer zone.

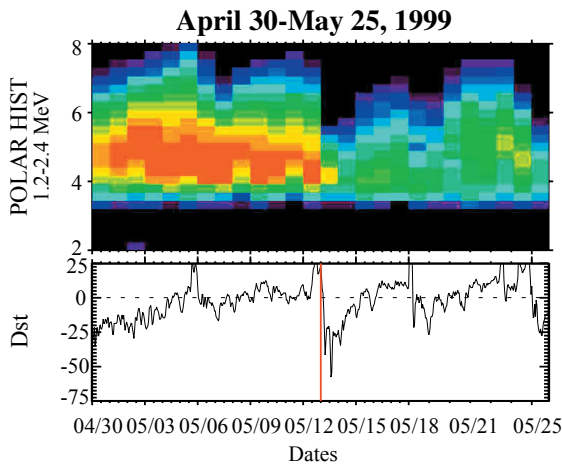


Fig. 2.2 Some magnetic storms dramatically deplete the entire outer zone. In this example, a moderate storm in Dst produces a very large depletion of the energetic electron fluxes [Reeves *et al.* 2003].

New opportunities and specific goals: The period 2006–2007 marks the first time since the launch of IMAGE that Polar will be in the right place to comprehensively observe the high-energy electron response to magnetic storms and EMIC waves. EMIC waves interact preferentially with higher-energy

electrons in plasmaspheric plumes. Figure 2.3 shows that only for higher energy electrons can EMIC waves resonate with the bulk of the equatorially trapped particles, whereas for lower energy electrons EMIC waves can only resonate with particles already near the loss cone [Summers and Thorne 2003]. The CEPPAD/HIST instrument, which is the only science-quality NASA asset measuring electrons in the 2- to 10-MeV range, is ideal for evaluating the loss of electrons via EMIC wave interactions. In concert with the HIST measurements of changes in the particle fluxes, IMAGE EUV (launched after Polar's last visit to the core of the outer belt) can provide global specification of the location of plasmaspheric plumes, where freshly injected ring current ions interact with the cold plasma to produce strong EMIC waves.

A vital component to the determination of wave-particle losses of radiation belt electrons will be the use of MFE data correlated with CEPPAD/HIST measurements. VLF chorus consists of whistler-mode electromagnetic waves with frequencies of hundreds of Hz to several kHz, while EMIC waves have associated magnetic component bursts that have spectral components on the order of 1 mHz (e.g., Fraser *et al.* [2005]). Thus, ≤ 1 -mHz bursts in association with CEPPAD/

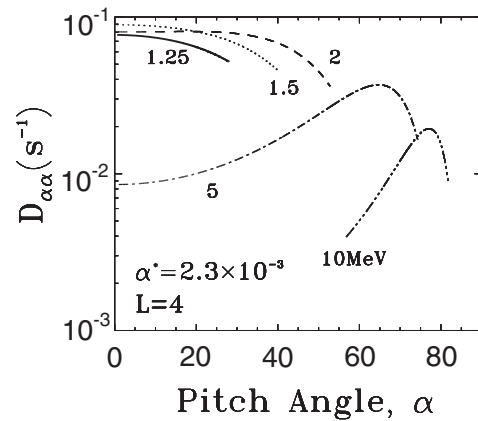


Fig. 2.3 A plot of the pitch-angle diffusion coefficient vs. particle pitch angle at L = 4 for several electron energies. EMIC waves can interact with electrons having energies above about 1 MeV [Summers and Thorne 2003]. Below about 2 MeV, EMIC waves can interact only with particles that mirror far from the magnetic equator. Thus the curves for electrons of 2 MeV and less terminate no higher than a pitch angle of 60°. The dependence of the pitch-angle diffusion coefficient upon electron energy and equatorial pitch angle means that EMIC waves can effectively scatter equatorially mirroring electrons only if they have energies of several MeV.

HIST observations of reduced flux of 3- to 10-MeV electrons would suggest loss due to EMIC waves, whereas spectrally broad, reduced electron flux would not be compatible with EMIC-wave scattering.

Expected results: Global IMAGE measurements of the plasmopause location are vital to the interpretation of the in situ changes in the relativistic electron fluxes observed by Polar. A lower plasmopause indicates stronger convection and a penetration of VLF waves to lower L. A good correlation of relativistic electron enhancements with a lower plasmopause would provide support for the importance of VLF waves. Power spectra calculated for either the 25-Hz sampled MFE data or the 54-Hz Hydra sampled MFE data are clearly capable of detecting or indicating the presence of EMIC bursts. Correlations with the relativistic electron observations will reveal the significance of the EMIC waves in pitch-angle scattering energetic electrons.

How does the inner portion of the outer zone evolve during the descent to solar minimum?

General problem: Unlike the region near geosynchronous orbit ($L = 6.6$), the energetic electron population in the inner portion ($L = 2$ to 3.5) of the outer zone responds only to some magnetic storms (see Fig. 2.2). Current theory suggests that this selectivity is controlled by plasmopause location or the strength of radial diffusion. However, a paucity of relevant measurements has limited study of this problem.

New opportunities and specific goals: During Polar's previous visit early in the mission, the fleet of spacecraft available for correlative observations was considerably different. As illustrated in Table 2.1, new assets that were not present during the earlier visit will now enable a vastly superior study of this region. Polar data, acquired with its high-quality scientific instrumentation, will be crucial. Other missions will supply more limited data, but these data will be critical in providing context and broad-scale observations. MEO-1 (2001-026) has a high residence time in the region $2.5 < L < 4$. It has provided continuous coverage since launch in 2001 and is equipped with energetic particle/dosimeter sensors. HEO-4, scheduled for launch in late 2005, will cross the magnetic equator at $\sim L = 2$, providing spatial coverage well inside the regions that will be traversed by Polar, with dosimeters and an electrostatic analyzer for measuring plasma electrons and ions. The HEO-4 plasma instrument will measure ions and electrons from 50 eV to 30 keV; the electrostatic analyzer (ESA) has the standard top-hat configuration. This ESA will have a data rate of 50 kilobits/s. The dosimeters measure the electrons fluxes from >300 keV, >1.5 MeV, and >3 MeV, as well as total dose and protons between 6 MeV and 50 MeV. Of crucial importance, IMAGE can now provide global snapshots of the plasmopause position (e.g., Goldstein et al. [2003]).

Expected results: The many widely spaced spacecraft will provide the relativistic electron data needed to understand the global response of the magnetosphere to a given storm, and in particular how the inner portion of the outer zone has responded.

The high-scientific-quality particle and fields measurements, acquired by Polar in the heart of the outer zone, can then be used for detailed analysis with confidence provided the overall global response of the magnetosphere in terms of energetic electrons is known. This global response will be measured by a fleet of complementary spacecraft (Table 2.1). The phase-space-density versus the first adiabatic invariant (μ) spectrum around GEO and at Polar will be examined to determine if the shape is consistently the same. If so, this is strong evidence for a single accelerator acting across the entire outer zone. If the shapes are different, then we can determine the energy filtering that goes on at lower L relative to higher L, and this should give us some indication of the acceleration mechanism at lower L. Experience (cf. Fig. 2.1) indicates that significant events will occur during 2006–2007.

What determines the effectiveness of a given geomagnetic storm as a relativistic electron accelerator?

General problem: Many aspects of geomagnetic storms as relativistic electron accelerators are not well understood. For example, fewer storms affect higher-energy electrons (2 to 8 MeV) than lower energies (0.5 to 2 MeV). A variety of wave-particle interactions from ULF to VLF are under consideration as the cause of relativistic electron acceleration in the outer zone [Summers et al. 1998, Elkington et al. 2003, Liu et al. 1999]. Each of these mechanisms presents some selectivity in energy. Just as the EMIC waves mentioned above interact differently with electrons of different energies, so too do the ULF and VLF waves proposed as accelerators of electrons. One proposed VLF acceleration mechanism depends on energy, with stronger energy diffusion at higher energies up to 10 MeV [Summers and Ma 2000].

New opportunities and specific goals: Opportunities to study the response of these multi-MeV electrons to magnetic storms have been few. CEPPAD/HIST is uniquely capable of measuring electrons up to about 8 MeV. The fluxes of these higher-energy electrons are highest in the core of the outer zone. During Polar's return to this region, we will have a unique opportunity to study the dynamic of this energetic population with a variety of coordinated measurements not available during the earlier visit and during a new phase in the solar cycle: descent to minimum. In the previous visit, Polar observed that the multi-MeV electrons respond to fewer storms than do the lower-energy electrons (Fig. 2.4). In Fig. 2.5 we see that the phase-space density at $L = 3.0$ is roughly similar in shape to that at GEO after a major magnetic storm. This suggests that a single mechanism is active all the way from $L = 3.0$ to GEO. By comparing the response at the core of the outer zone to that at higher L, and by putting those densities into context using IMAGE, Cluster-II, HEO-4, TWINS, GEO, and MEO-1 data, we can determine why only some storms affect the multi-MeV electrons and what physical mechanism is responsible.

Expected results: The large number of satellites monitoring energetic electron populations throughout the

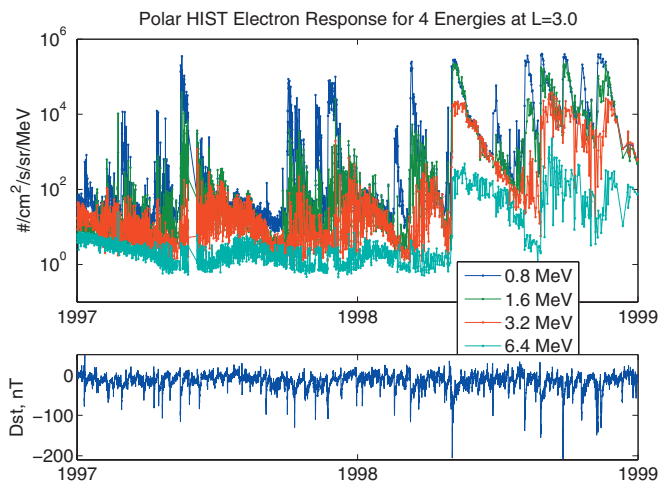


Fig. 2.4 Only some storms affect the 6.4 MeV electrons, whereas many storms affect the 1- to 2-MeV electrons.

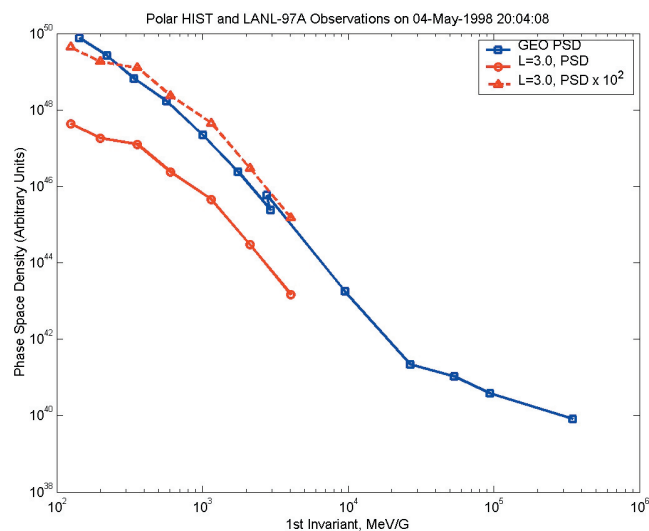


Fig. 2.5 In this example, the spectral shape at the inner edge of the outer zone resembles that at the outer edge, suggesting that a single unifying process affects the entire outer zone.

outer zone, coupled with the detailed particle and fields measurements from Polar, will enable us to address the storm geoeffectiveness question from an electron accelerator point of view. Understanding what makes a storm geoeffective, of course, is critical for space weather predictions. We will be able to observe in detail under what circumstances the magnetospheric electron accelerator reaches lower L and thereby test theoretical suggestions. Is the correlation best for bigger storms, or more compression, or the presence of strong waves, or perhaps preconditioning by recent past events? We do know that the situation is complex and that there is no simple, universal answer. The comprehensive observations only now possible will be vital for progress in understanding.

Section 2.1 summary: *Mission extension through March 2007 will enable compelling new science, especially significant because of the beginning of the LWS era. The return to the heart of the outer zone will occur in a significantly different context: a more robust fleet of assisting observations and a different phase of the solar cycle. This new context will allow us to address effectively for the first time important science*

questions, including (1) Are EMIC waves a major storm-time loss process for outer zone relativistic electrons? (2) How does the inner portion of the outer zone evolve during the descent to solar minimum? And (3) Why do fewer storms affect higher-energy electrons (2 to 8 MeV) than lower energy electrons (0.5 to 2 MeV)?

2.2. Auroral electron acceleration and ion outflow region

General problem: Research has shown that the immediate cause of the aurora is secondary electrons striking atoms and ions in the near-vacuum of the Earth's ionosphere, much as happens in a fluorescent light. We know that these secondary electrons are created by primary electrons accelerated between 1.5 and 4 R_E altitude [Reiff *et al.* 1993, Shelley and Collin 1991, Mozer 1981, Koskinen and Malkkai 1993]. We know in turn that these primary electrons are accelerated by electric fields and waves associated with field-aligned currents driven by magnetospheric dynamics. Yet for all this progress, the key high-altitude auroral acceleration region remains only poorly probed, and in the absence of solid observational guidelines, competing theories of the aurora abound. There remains today no quantitative and self-consistent theory of the auroral circuit that agrees with all observations. Fortunately, Polar's eccentric orbit as it precesses will be ideal over the next 2 years to study in depth the mid- and upper-auroral acceleration region at unprecedented high temporal resolution for these altitudes.

Alfvén waves, double layers, solitons, acceleration of electrons and ions, and ion outflows occur at heights above 2000 km. FAST probed this region below its apogee of 4175 km, resulting in many advances in understanding the auroral acceleration region. In the period 2006–2007, Polar will probe the auroral acceleration region between altitudes of ~ 5000 km to 4 R_E , i.e., the region above the apogee of FAST that needs to be explored (see Fig. 1.3). Polar's healthy particle and field instruments can take advantage of All-Sky Imagers that have been established over the North American sector in preparation for the upcoming THEMIS mission. The correlative observations between Polar and the All-Sky Imagers will establish the spatial location of active aurora relative to the Polar conjugate point in the ionosphere.

The auroral acceleration regions and ion outflow from the ionosphere are intimately related. Escaping heavy ions (O^+ and N^+) measured by Polar can be mapped to bright regions of the aurora. These observations will allow systematic studies of the time history of auroral acceleration with much better spatial resolution than previously achieved. Moreover, by coupling Polar measurements of ion outflows and THEMIS ground-based observations, with radar observations and conductances derived from auroral precipitation intensities, an end-to-end study of ionospheric response to auroral acceleration can be achieved. Combined with global auroral FUV images from IMAGE and intermediate resolution images from the Polar cameras when available, these studies will provide a picture of how the local processes work relative to the larger-scale dynamics of the distant magnetospheric system.

The following specific questions will be addressed:

- What are the energy sources at the top of the auroral acceleration region?
- How is the energy apportioned into the various auroral related phenomena?
- Where (e.g., at what intermediate altitude) are auroral electrons accelerated?
- What fraction of energy available in the convection electric field is converted to precipitating electron energy?
- What are the relationships between particular types of auroras and specific auroral particle acceleration mechanisms?
- To what parts of the field-aligned current system is aurora-producing electron precipitation the current carrier?
- What are the physical processes that lead to ion outflow from the ionosphere?

Recent advances: Correlative studies between FAST and airplane observations show that the narrow features in the electron energy fluxes of precipitated electrons each correspond to visible arcs [Stenbaek-Nielsen *et al.* 1998]. In situ particle observations have further shown that precipitated ion fluxes are associated with the proton aurora observed in global images from IMAGE [Frey *et al.* 2001]. These observations are important because particle precipitation is often the result of field-aligned currents and intimately associated with plasma mechanisms occurring above the aurora and in the distant magnetospheric regions. Alfvén waves communicate to the ionosphere new magnetic configurations imposed by merging in the magnetotail. These signatures include highly structured field-aligned currents and wave Poynting flux. Analyses of Polar’s observations by Wygant *et al.* [2000] have shown the importance of polarized electric field variations and that Alfvén waves are associated with discrete structures in auroras (Fig. 2.6). The Poynting flux of electromagnetic (EM) field is observed directed along the geomagnetic field propagating into the ionosphere. Wygant *et al.* [2000] utilized Polar observations and the Tsyganenko magnetic field model to show that there is a sufficient amount of energy (~ 100 ergs/cm²-s) in the EM fluxes to adequately drive the auroral processes (see Fig 1.3). The new high temporal resolution observations of Alfvén wave Poynting flux at Polar and its correlation to auroral structures from All-Sky Imagers will enable a systematic study of the role of Alfvén wave-associated auroras.

Statistical studies have established the ionospheric auroral zone as the source of upflowing ions [Giles *et al.* 1994]. Upflowing ions observed by TIDE compared with auroral forms by UVI have shown that regions of bright aurora often have large parallel velocities of outflowing O⁺ [Hirahara *et al.* 1998, Stevenson *et al.* 2001]. Wilson *et al.* [2001] compared the characteristics of suprathermal outflowing O⁺ ions to the auroral forms seen at the foot point of the associated field line as observed by UVI. They showed that the flux of escaping O⁺ ions increases by over a factor of 100 as the auroral intensity in the Lyman-Birge-Hopfield (LBH) band increases from 0 to ~ 4 kR (Fig. 2.7). More recently, it was shown that the total nightside auroral zone outflow depends on the size of the

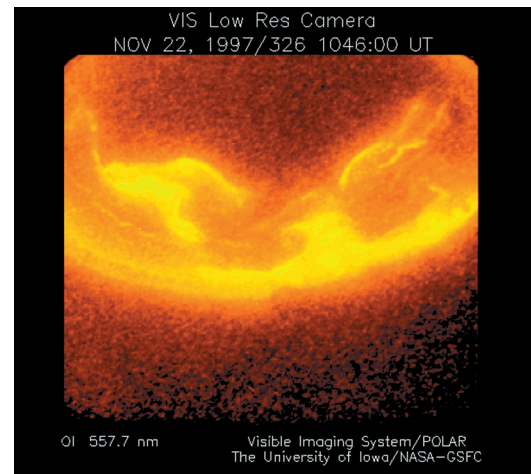


Fig. 2.6 Example of highly detailed auroral structures from the Polar/VIS. The THEMIS ground-based All-Sky Imager network will provide images with spatial resolution improved by a factor of ~ 10 .

substorm, and that the outflow flux increases on average by about a factor 2 after onset [Wilson *et al.* 2004].

New opportunities: During the proposed Polar extended mission, new assets will be available for coordinated auroral acceleration studies. These new assets either did not exist or were in the opposite hemisphere during Polar’s traversal through the southern auroral acceleration region early in the mission. The new ground-based assets include the THEMIS network of All-Sky Imagers which is currently partially installed and will be nearly complete by the fall of 2005 (Fig. 2.8). Thus, it will be available as the Polar orbit sweeps through the night magnetosphere above Canada and Alaska. The THEMIS array provides an imaging canopy from Labrador to Alaska and the USA–Canadian border to the Arctic Ocean. The THEMIS magnetometer chain covers the auroral regions of the North American continent from the eastern coast of Canada through to Alaska. Images are obtained every 10 s. Magnetometer data are sampled every 0.5 s. Campaign investigations of conjunctive observations between Polar and the THEMIS ground-based observations will benefit both missions. Prior to launch of its spacecraft, the THEMIS mission will benefit by exercising its ground-based network on coordinated scientific campaigns in an operational mode driven by outside factors. Polar, in turn, will benefit by having a temporal–spatial reference frame for its observations. When the THEMIS All-Sky Imagers are in sunlight or are clouded out, coordinated observations utilizing the THEMIS magnetometer chain and the expanded SuperDARN network can continue with knowledge of ionospheric currents associated with auroral activity. Thus, the prime time observational periods are from September 2005 through March 2006 and September 2006 through March 2007.

In September 2006, the Polar orbit plane will lie in the noon–midnight meridian with perigee at mid-northern latitudes at noon and apogee at southern latitudes on the night-side. The Polar inbound pass on its way to perigee cuts through auroral field lines in the critical 2-to 4- R_E geocentric distance range. The plan is to exploit the orbit plane that sweeps over

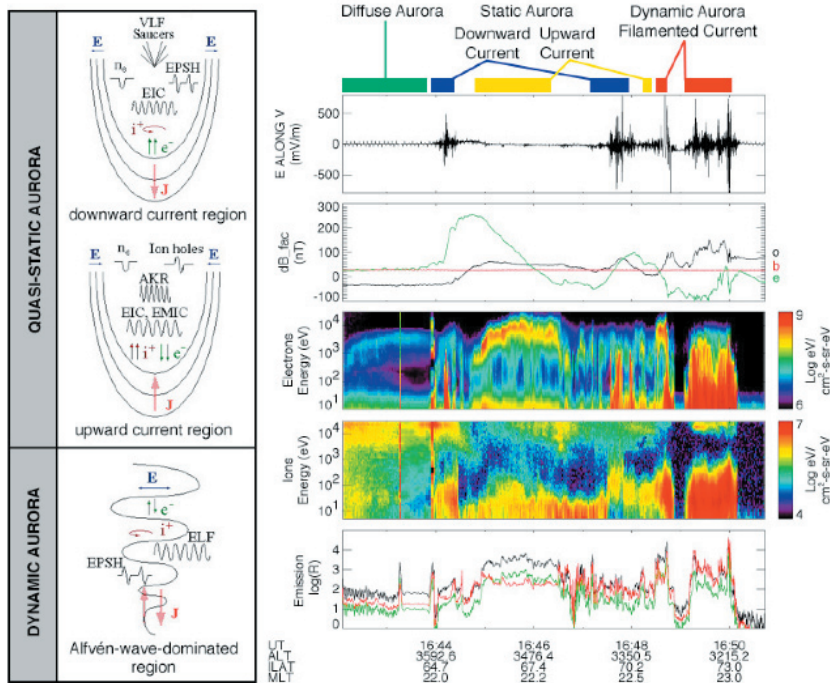


Fig. 2.7 The highly varying and structured auroral formations may be caused by differing auroral accelerations mechanisms, as shown in these FAST and Polar/UVI data and discussed by *Paschmann et al.* [2002].

the midnight-to-dusk sector and observe the critical auroral acceleration region for substorm onset. From January through March in 2006 and in 2007, the orbit perigee passes over the dawn-to-midnight sector. In both local time sectors, Polar will obtain high-temporal-resolution fields and particle data in science mode 2 while magnetically connected to the THEMIS network and to SuperDARN.

The configuration of Polar with its high-temporal-resolution science mode 2 telemetry, FAST, DMSP, the THEMIS All-Sky Imager and magnetometer network, IMAGE, TIMED, the expanded SuperDARN network and the THEMIS and ST5 spacecraft after their launches offers an unprecedented opportunity for focused auroral research.

Approach: During fall 2006, Polar perigee will be in the northern hemisphere, while FAST will also be in the north but at a lower altitude. Thus, both spacecraft are ideally situated to provide complementary measurements of particles and fields with Polar traversing the upper auroral acceleration region and FAST near its lower boundary. The high temporal resolution of FAST coupled with Polar's greater energy range of plasma/particle instruments and its increased particle and fields telemetry using science mode 2, offers a new powerful combination of observations not previously available. In addition, the THEMIS ground system facilities will provide measurements of ground-based observations at the foot of the auroral flux tubes. Polar observations of auroral field-aligned currents inferred from magnetic fields will give us the high-altitude information of the upward and downward current regions, while FAST will observe those at lower altitudes. The combined observations will enable us to investigate the mapping of electric fields, currents, and ion outflows from

Polar to FAST altitudes and comparisons with the All-Sky Imagers will reveal important high-resolution information about their association with the aurora.

Measurements made during the early part of the Polar mission studied mainly the behavior of the global auroral dynamics. Although perigee passes obtained higher-resolution images, the auroral oval was traversed very quickly (~10 min) and data were not obtained for periods long enough to study the smaller-scale auroral structures. The THEMIS ground-based All-Sky Imagers, in conjunction with the acquisition of the high-resolution Polar data, FAST data at lower altitudes, and high-resolution auroral images from TIMED/GUVI offer new opportunities to conduct the high-resolution science studies not previously possible.

The magnetosphere and ionosphere are coupled by means of field-aligned currents, precipitation and ion outflows. The physics of this MI-coupling is fundamental to our understanding of how the solar wind interacts with the geomagnetic field and energy dissipated through auroral substorms and magnetic storms.

Our correlative observations will be organized and related to varying solar wind dynamics, including IMF orientation, clock angle, and solar wind disturbances, coronal mass ejections (CMEs), and phases of substorms and storms.

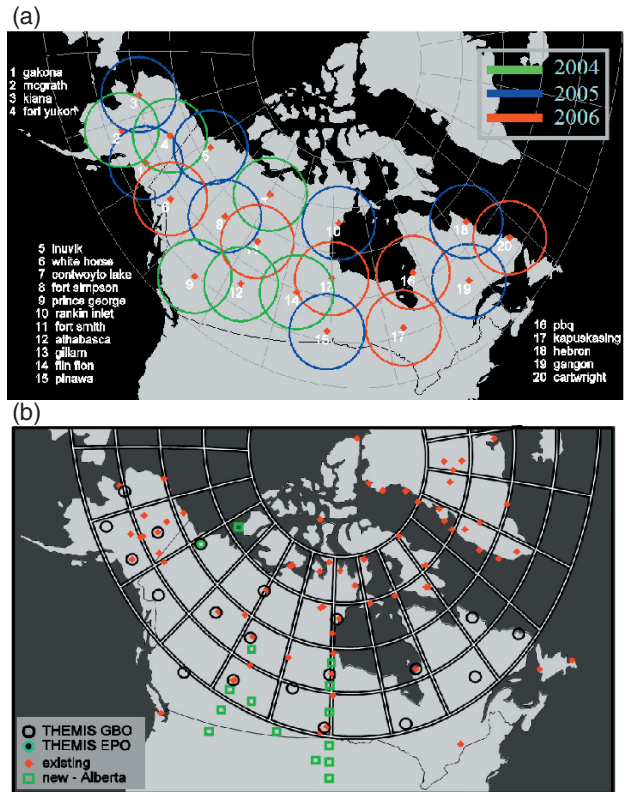


Fig. 2.8 The THEMIS ground-based (a) All-Sky Imager and (b) Magnetometer Network covers the complete auroral region from the Atlantic Coast of Canada to the Pacific Coast of Alaska and the Bering Sea (Figure courtesy of Eric Donovan).

The new configuration of Polar with the S³C Great Observatory will provide an opportunity to investigate the key auroral acceleration region in a way not possible until now.

Expected results: The research proposed here is designed to enhance our understanding of the auroral acceleration region, the MI-coupling process, the sources of ion outflows and physics of the different auroral structures, thin auroral arcs, omega bands and pulsating patches on the dawn side, and westward surges on the dusk side. Coordinated studies of Polar and THEMIS ground based All-Sky Imagers will advance our understanding of the detailed physics of the cause–effect relationship of the auroral acceleration processes, field-aligned currents, Alfvén waves, and plasma processes that are active in the regions above the aurora (Fig. 2.9).

Polar, in combination with DMSP, FAST, THEMIS, and Double Star, will determine the energy partitioning between the fields and particles as a function of altitude in the auroral acceleration region. The conversion of electric and magnetic field energy to the kinetic energy of the precipitating electrons is expected to increase as Polar makes successively lower-altitude cuts through the auroral acceleration region. These high-temporal-resolution observations of the auroral acceleration region are unprecedented and are important for determining the relative importance of the many auroral acceleration mechanisms that have been postulated.

The detailed relationships of the large-scale auroral acceleration structure to the smaller-scale auroral structure are still not well understood. The new high-time-resolution fields and particle observations obtained by Polar, coupled with FAST particle and field measurements, and data from the THEMIS ground-based All-Sky Imagers are critical for finding that elusive connection to fundamentally advance our knowledge of auroral physics. New science results from these observations can be used to improve existing models and as inputs to the development of next-generation MI-coupling models. This contribution of Polar to the Great Observatory is critical to understanding the magnetosphere–ionosphere component of the Sun–Solar System.

Section 2.2 summary: *Extension of the Polar Mission through March 2007 will enable compelling new science, especially significant because acceleration of particles is a fundamental process throughout the universe. The investigation of the auroral acceleration region and ion outflow will occur in a significantly different context than in the early phase of the Polar mission. Higher-temporal-resolution observations at Polar’s perigee over the northern hemisphere will be combined with new ground-based datasets such as those of the THEMIS ground network and an expanded SuperDARN. A robust fleet of orbiting assets including IMAGE, TIMED, THEMIS, Double Star, FAST, and DMSP will provide complementary observations. This new context will allow the Polar mission to address effectively for the first time important science questions, including (1) What are the energy sources at the top of the auroral acceleration region? (2) How is the energy apportioned into the various aurora-related phenomena? (3) Where (e.g., at what intermediate altitude) are auroral electrons accelerated?*

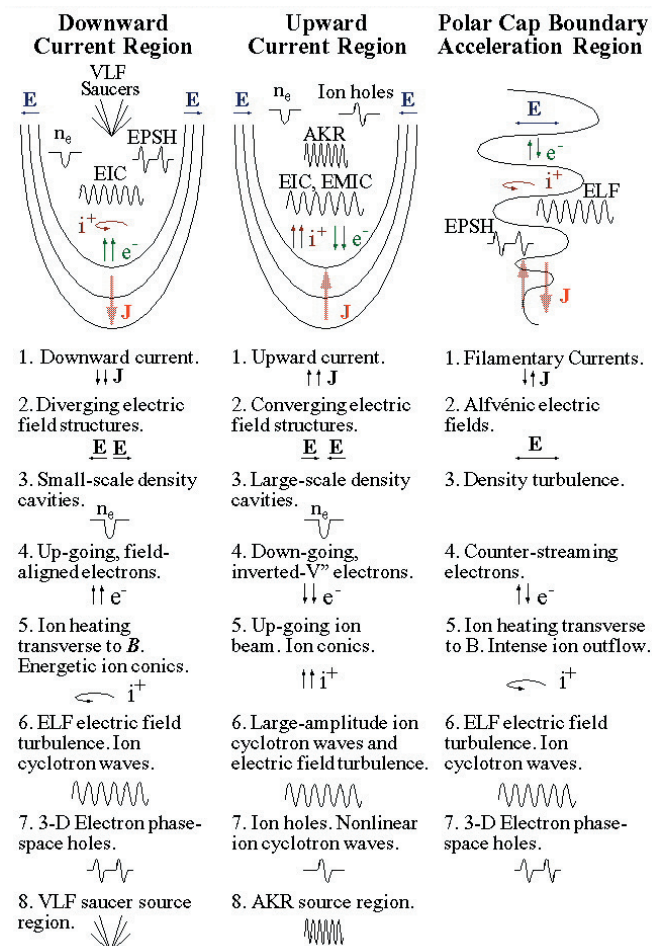


Fig. 2.9 The proposed focused scientific investigation of the auroral acceleration region will determine the conditions under which each of these auroral models is applicable and the fraction of time for their applicability (Figure courtesy of C. Carlson and the FAST team).

2.3. Microscale and macroscale physics of the high-latitude dayside region

Microscale: Signatures of reconnection at high latitudes and in the cusp

General problem: Understanding the processes of magnetic reconnection is of fundamental importance for solar atmospheric and heliospheric processes, solar wind–magnetosphere and magnetosphere–ionosphere coupling. At locations where magnetic reconnection occurs, the fundamental assumptions for magneto-hydrodynamic (MHD) models are violated. Reconnection at the magnetopause is clearly the dominant mechanism by which plasmas from different magnetic topologies mix, allowing particle and electromagnetic field energy and momentum to be exchanged between the solar wind and the magnetosphere. Microphysically, reconnection is enabled by the *demagnetization* of the thermal electrons, a situation that precludes the electron fluid from acting as a field line label, and the motion of a given field line in time no longer makes sense.

Until recently it was thought that this demagnetization could be accomplished either by collisions, wave–particle

effects, or the incidence of scales of the DC magnetic field shorter than the electron's thermal gyroradius. Recent analyses using the reallocated science mode 2 data sets [Mozer *et al.* 2004, Scudder and Mozer 2005, Scudder *et al.* 2005, Scudder and Daughton 2005] have shown the importance of short scale length inhomogeneities of the electric field for thermal electron demagnetization, giving the Polar mission a new, strong lever in the search for the site of the reconnection process. These signatures are very prominent in low β_e magnetopause crossings that may involve component reconnection. In the absence of collisions and suitable wave-particle processes, a generalized view of demagnetization will involve the scale of the *electromagnetic field* compared with the gyroradius of the electron around the magnetic field and will involve the scale of the electric structures and the ratio of the electric force to magnetic force on a thermal electron within these structures. An important goal at these layers is to understand from first principles what enables the process of collisionless reconnection and causes such short-scale layers to occur.

At the nose of the magnetopause, these layers may be only ~ 70 m and be transited in a few milliseconds. As the apogee of the Polar orbit approaches high southern latitudes and the southern cusp region, the direction of the magnetospheric magnetic field will change dramatically from being approximately perpendicular to the solar wind flow to much more oblique angles at higher latitudes. Consequently, we will be able to test whether the reconnection mechanisms discovered at low latitudes near the magnetopause are modified by the magnetic configuration at high latitudes or whether different reconnection mechanisms are in operation. Using the reallocated telemetry of science mode 2, *the occurrence and scale size of the reconnection regions must be studied at all latitudes in order to understand the global macrophysics that emanates from these local microphysical processes.*

Recent Advances: Magnetic reconnection is an important process not only in Earth's magnetosphere, but also on the surface of the Sun and elsewhere in the universe where magnetized low β_e plasmas interact. Instruments on the Polar satellite have provided the first direct observations of antiparallel reconnection at the null line (i.e. $B \sim 0$) and thus, the electron diffusion region associated with magnetic field reconnection [Scudder *et al.* 2002]. This is a region in which neither electrons nor magnetic field lines move with the $\mathbf{E} \times \mathbf{B}/B^2$ velocity, in which magnetic field reconnection occurs, and in which electromagnetic energy is converted to particle kinetic energy. Direct comparisons between measured electron bulk velocities and the fully measured $\mathbf{E} \times \mathbf{B}/B^2$ velocity documented intervals of significant disagreement that were interpreted as the pressure gradient drifts supporting the Hall currents of the reconnection layer [Scudder *et al.* 2002]. During a null line crossing, direct measurements showed that the thermal electron gyroradius exceeded the electron skin depth by at least a factor of 25. The distribution of electrons also showed clear departures from cylindrical symmetry about the magnetic field direction, a condition known as *agyrotropy* that is a measurable index of electron demagnetization.

In an exciting new development concerning demagnetization of electrons and hence the microphysics of collisionless reconnection, Mozer *et al.* [2004] has reported the incidence of abrupt (few milliseconds), intense (>100 mV/m), electric field enhancements (EFEs) that are largely perpendicular to the local magnetic field. Using the 1600-Hz samples of EFI made possible by science mode 2, these structures were distinguished from the solitary waves discovered in the aurora, where the parallel component of the wave is prominent in the wave form. These structures usually are accompanied by a depression in the density, although it is not always in phase with the EFE. From their time duration and typical magnetopause speeds, their thickness was inferred to range from Debye length (10 m) to electron inertial length (4 km). Figure 2.10 illustrates the discovery of EFEs using science mode 2 data recovery to its fullest extent; it is a *spatial reconstruction* of sampled time series of this region – found by transforming into the rest frame of the nearby MHD structures using EFI, MFE, and Hydra data [Scudder and Mozer 2005]. Fiducial scales such as Debye length and gyroradii are determined from most proximate samples of Hydra. Figure 2.10 dramatically shows the strong enhancement of E_{\perp} in the thermal gyroradius layer that is much shorter than the electron inertial scale length. While the thermal electron gyroradius is small compared with the skin depth, the electrons are nonetheless not magnetized in this region – because the short scale of E_{\perp} is disruptive to their guiding center motion. In the 4th panel from the bottom the science mode 1 E_{\perp} data (in black) are superposed upon the concurrent high-temporal-resolution data (in red) enabled in science mode 2. Without the enhanced resolution of the (red) science mode 2 burst time series, the entire upper panels in green would have been lost and the spike in the black profile

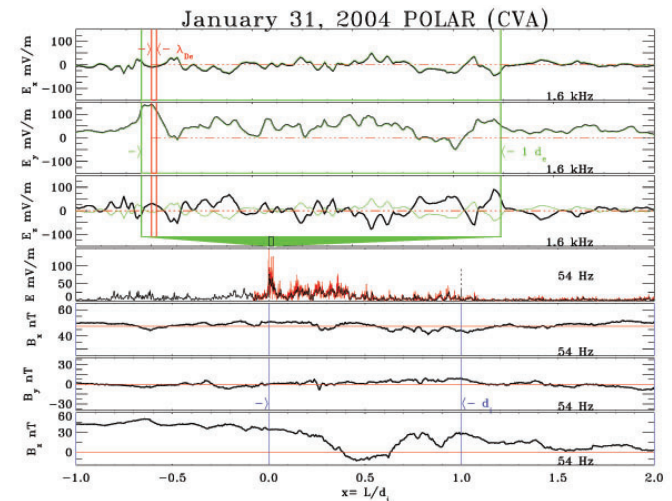


Fig. 2.10 Spatial portrait of discovery EFE that is actually one of the strongest DEFES discovered to date. Upper panels show the spatial profile of E as determined from science mode 2 burst data from EFI. The green perimeter of upper panels is one local electron inertial length. This telescopes into the narrow region below the black rectangle in the expanded spatial scale portrait of the lower four panels. These depict E_{\perp} and B at standard science mode 2 cadences of electric (80 Hz) and magnetic (54 Hz) fields converted into ion inertial lengths. The spatial scale of the E_{\perp} spike is 2 ion skin depths in front of a slow mode disturbance shown in the lower three panels.

discounted as a “noise”; the physics of demagnetization described here would be lost.

Theoretically EFEs with a sufficiently vigorous electric field concentrated in such a short scale should be able to demagnetize the thermal electrons, preferentially energizing the Cartesian momentum along E_{\perp} – in spite of the fact that the electrons have a thermal gyroradius much smaller than the electron skin depth. These EFEs are said to be “demagnetizing” EFEs (DEFEs). Scudder and Mozer [2005] concluded that DEFEs have gyroradius scale lengths that are above the local electron Debye length, which in this low β_e regime can be comparable to the electron thermal gyroradius. Such DEFEs can consistently be considered as demagnetizing agents in low β_e collisionless magnetic reconnection, the same condition that exists on the surface of the sun.

Full particle in cell (PIC) simulations of self-consistent reconnection layers have corroborated this picture derived from Polar data of the demagnetizing of thermal electrons by DEFEs in the presence of a guide field (i.e., component reconnection) [Scudder et al. 2005, Pritchett 2005, Daughton and Scudder 2005, and Scudder and Daughton 2005]. Figure 2.11 presents a snapshot of the analysis from Daughton’s simulation, where the units of the axes of the contour plot are electron skin depths, the mass ratio for the simulation is 25, and a guide field is present equal in size to the reconnection field. Such geometry is prototypical for component reconnection. The PIC EFEs occur just behind the separatrices on the outflow side and extend into the separator regions [Daughton and Karamibadi 2005]. As shown by the upper left contour, E_{\perp} is strongly and narrowly enhanced behind the separatrices and has a spatial scale along the normal of the order of the electron thermal gyroradius, a conclusion similar to that measured in the Polar event in Fig. 2.10. Using the full pressure tensor in the PIC code, the suggestion derived from the Polar observations that the electron pressure tensor is deformed from cylindrical symmetry has been recovered using the PIC simulation’s electron pressure tensor \vec{P}_e . The lower left-hand color contour illustrates in the same format as that for E_{\perp} the distribution of agyrotropy, A_0 , across the solution plane; it too is strongly enhanced just behind the mathematical separatrices of the reconnection pattern in near coincidence with the locale of enhanced E_{\perp} . Along this ridge of agyrotropy behind the separatrices the electromagnetic field exceeds the threshold surmised for demagnetization from the Polar EFE events. Interestingly, the PIC simulations show that the parallel electric field is generally weak compared with the perpendicular fields in these layers, and the density is locally depressed, precisely as found in the Polar data.

Three new insights arise from these studies: (1) The suggestion that the non-ideal region may not just be localized “at” the separator, but extends out along the separatrices (this has positive implications for the Magnetospheric MultiScale mission, in that the size of the reconnection region presents a bigger target, thus increasing the likelihood of MMS encountering these important reconnection regions on each orbit). (2) The intense, electron thermal gyroradius scaled E_{\perp} layers provide suitable structures to demagnetize the electrons in very low β_e plasmas, the regimes favored by component reconnection

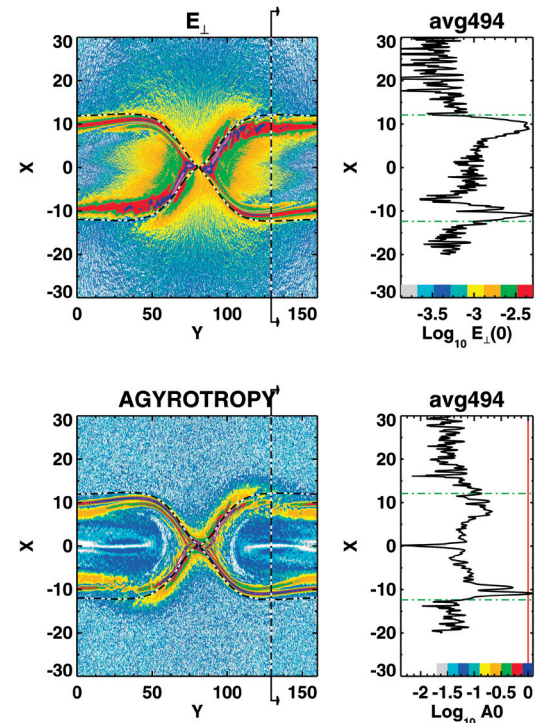


Fig. 2.11 Recent simulations have reproduced the critical features of the Polar observations near the reconnection sites in the presence of a guide field. Intense thin layers of perpendicular electric field are stretched along to the inside surface of the separatrices as shown in the upper left panel. The E_{\perp} along the vertical cut in the upper left panel is displayed in the upper right panel showing the strong, thin E_{\perp} regions just inside the separatrix crossing (dashed green line). The bottom two panels show that strong agyrotropy is associated with E_{\perp} layers. The spatial dimensions of the panels are in electron skin depths.

scenarios where the separator is not a magnetic null line. And, (3) in contrast with magnetic null line separators, where electrons can easily become demagnetized in the high β_e skin depth current channels [Scudder et al. 2002], low β_e plasmas at component reconnection sites are seemingly guaranteed to have the thermal electron gyroradius $\rho_e \equiv \beta_e^{1/2} d_e$ smaller than the skin depth of the current channel and hence the guiding center is ordered relative to the variations of the magnetic field, but not necessarily to that of the electric field. The new concept here is that a simple guiding ordered picture of the electrons that preserves the concept of a moving magnetic field line is violated if the electron thermal gyroradius is larger than the shortest scale of the magnetic or the electric field, not just that of the magnetic field.

New opportunities and specific goals: In the next two dayside apogee seasons, Polar will be at high latitudes where the extensions of the same techniques and search methods that were used to identify the low-latitude EFEs and other disruptive layers in the magnetopause will be used to probe the scale size of possible demagnetization layers in and near the polar cusp. Signatures of agyrotropy will be identified both in simulations and in the new Polar Hydra data looking for signatures of disruption of gyrotropy. These new observations will be compared with recently developed models to aid in the interpretation of the results. The high-time-resolution data

in telemetry science mode 2 will be utilized for the first time in this important magnetospheric region. Many interpretations of geophysical data require high-latitude reconnection in this region. Polar is the first and only satellite that is capable of such discoveries, because a non-zero parallel electric field is a first-order requirement for such a layer and Polar, with its three-axis field measurement, is the only satellite in orbit capable of directly measuring the parallel electric field.

Thus, the goal of this investigation is to understand the microphysics of high-latitude reconnection and its impact on magnetospheric dynamics through the analyses of these new high-temporal-resolution measurements of high latitude and cusp layer spatial scales, which are observed to be disruptive to thermal electrons, where parallel electric fields are observed.

Approach: High-latitude field and particle measurements were made early in the Polar mission when the data were transmitted in telemetry science mode 1 and in which a typical electron diffusion region lasted about one data point of the electric field measurement and a fraction of a data point of the magnetic field measurement. The advantage of the coming high-latitude passes is that Polar will operate in telemetry science mode 2, where the electric field data rate is twice that of mode 1. In addition, all three components of the magnetic field data are transmitted in mode 2 at 54 samples/s through the Hydra experiment, as compared with 9 samples/s of the mode 1 data. The 54-Hz data through Hydra is low-pass filtered at 11 Hz, which is more than twice the ~4-Hz filter rate of the mode 1 data, so the magnetic signature of electron diffusion regions and the microphysics of the cusp will be much better resolved in the coming seasons than was done early in the mission. This is particularly important in deriving the time-to-space conversions that use frame transformation properties of \mathbf{E} and \mathbf{B} that are different, but are compromised when these two time series are not sampled with comparable time resolution.

Candidate intervals with measurable E_{\parallel} that occur in the magnetopause current layer will be segregated based on the scale of the structure and its ability to demagnetize the thermal electrons measured by Hydra in the most proximate vicinity of the abrupt structure. New techniques devised to bring anisotropy and agyrotropy measurements to 1.15-s time resolution will be used to probe for proximate and localized enhancements of agyrotropy in the vicinity of abrupt candidate structures. Similar diagnostics will be attempted on PIC codes to test the investigative approach.

Expected results: The nature and occurrence rate of EFEs in their associated demagnetizing layers of reconnection is not known at high latitudes. Because of the large changes in magnetic field direction at high latitudes relative to the plasma flows in the magnetosheath, the physical nature of these layers at high latitude may be dramatically different than those measured near the equator. Based on the 3-year EFE search and initial searches for non-EFE electron diffusion regions at low latitudes, it is expected that 85 EFE and ~40 non-EFE electron diffusion regions will be found each spring season when the satellite is located at or near the dayside cusp. The new observations will provide information on the

incidence of microphysics required for reconnection to occur at high latitudes, the frequencies of reconnection events, and the plasma parameters that are conducive to the formation of electron diffusion regions and will have implications for analogous reconnection regions on the surface of the Sun, which will never be probed in situ.

Macroscale: The location of the reconnection line

General problem: After decades of research, evidence is incontrovertible that magnetic reconnection occurs at the Earth's magnetopause both when the IMF is southward [e.g., Sonnerup et al. 1981, Fuselier et al. 1991, Phan et al. 1996] and when it is northward [e.g., Gosling et al. 1991, Kessel et al. 1996, Fuselier et al. 2000a,b].

A major outstanding question about magnetic reconnection is where reconnection will occur at the magnetopause for specific IMF conditions. Two scenarios are discussed in the literature: (1) antiparallel reconnection, which occurs where the magnetospheric field and the IMF are antiparallel (shear angle of approximately 180°); and (2) component or guide field reconnection, where one component of \mathbf{B} remains constant across the magnetopause and the remaining two components are antiparallel, resulting in shear angles <180 between the magnetospheric field and the draped IMF. An example as low as 50° shear [Gosling et al. 1990] has been reported.

Recent advances: The antiparallel reconnection sites for northward IMF conditions are relatively small regions poleward of the cusps at high latitudes. Recent Polar observations during northward IMF conditions have revealed the existence of very long reconnection lines extending over several hours of MLT [Onsager et al. 2001, Trattner et al. 2004a] which led to the conclusion that both antiparallel and component reconnection occur simultaneously across distributed locales that make up the reconnection line.

The antiparallel reconnection site for strictly southward IMF conditions covers the entire dayside magnetosphere along the magnetic equator. When a strong B_y component is present, the antiparallel reconnection site splits, producing two separate reconnection lines in different hemispheres [e.g., Crooker 1979]. Alternatively, the component reconnection tilted X-line model for southward IMF conditions predicts that a neutral line runs across the dayside magnetosphere through the sub-solar point, regardless of the magnitude of the B_y component [Cowley and Owen 1989]. The magnitude of the B_y component only determines the tilt of the X-line relative to the equatorial plane.

Simulated ionospheric emissions for the antiparallel and the tilted X-line reconnection model are shown in Fig. 2.12 [e.g., Petrinec et al., 2003]. While there is a continuous ionospheric precipitation response for the tilted X-line model, there is a gap in the ionospheric response across local noon for the antiparallel reconnection model that can be used to determine which scenario is most appropriate when the IMF is not purely southward.

Trattner et al. [2005] used cusp observations by the Cluster satellites to determine the location of the reconnection sites.

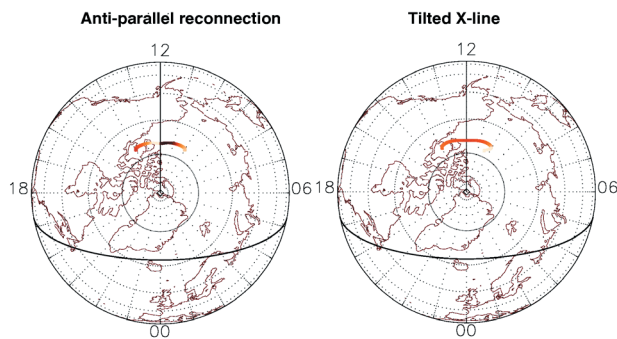


Figure 2.12 Simulated ionospheric response to precipitating cusp ion flux into the dayside ionosphere from an antiparallel and a tilted X-line reconnection model. While there is a continuous ionospheric precipitation response for the tilted X-line model, there is a discontinuous change of precipitating flux across local noon for the antiparallel reconnection model (from *Trattner et al.* [2005]).

Three-dimensional ion observations were used to calculate the distance to the reconnection line for two ion-energy dispersions observed during this Cluster cusp crossing, which were subsequently traced back to the magnetopause along geomagnetic field lines. Two separate reconnection sites in different hemispheres, in agreement with the antiparallel reconnection model, were determined for the two cusp structures.

New opportunities and specific goals: During the final period of Polar operations (2006–2007), the orbit of the Polar spacecraft will have precessed enough to routinely observe the southern hemisphere cusp. This provides a unique opportunity to systematically analyze the location of the reconnection line for various IMF conditions using all assets of the S³C Great Observatory including Polar, Cluster, and IMAGE. Plasma analyzers on the Polar spacecraft, such as the Toroidal Imaging Mass Angle Spectrograph (TIMAS), the Thermal Ion Dynamics Experiment (TIDE), and Hydra are used to estimate the distance to the reconnection line from the southern cusp, which is subsequently traced back to the magnetopause along geomagnetic field lines [e.g., *Trattner et al.* 2004a, *Fuselier et al.* 2000a]. In a similar way, observations by the Cluster Ion Spectrometer (CIS) on the Cluster spacecraft in the northern cusp will be used to supplement and confirm the reconnection locations derived from the Polar measurements in the southern hemisphere. The results can be further confirmed with observations by IMAGE/FUV [e.g., *Fuselier et al.* 2002, *Trattner et al.* 2005].

The goal of the proposed science focus is to distinguish between antiparallel and component reconnection for various IMF conditions and thereby make a critical step forward in understanding the fundamental properties of reconnection.

The following specific questions will be addressed:

- What solar wind and IMF conditions will cause reconnection to occur in the antiparallel or component (tilted X-line) regions of the magnetopause?
- What is the influence of the IMF clock angle on the reconnection scenario?
- What is the influence of the solar wind dynamic pressure on the reconnection scenario?

The results are especially interesting for the orbit-planning effort of the upcoming NASA MMS mission, the goal of which is to sample the reconnection diffusion region. A clear understanding of the location of the reconnection line for different solar wind and IMF conditions is fundamentally important for maximizing the encounters of MMS with its designated target, the reconnection region.

Approach: Figure 2.13 (top) shows a 2D cut through the 3D distribution measured by Polar/TIMAS for 15:24:43 to 15:24:55 UT on Oct. 17, 1997. The distribution is plotted in the frame where the bulk flow velocity perpendicular to the magnetic field is zero. The plane of the 2D cut contains the magnetic field direction (y axis) and the axis parallel to the Sun–Earth line. 3D flux measurements from TIMAS within $\pm 45^\circ$ of this plane are rotated into the plane by preserving total energy and pitch angle to produce the distribution.

Below the 2D distribution is a slice through the distribution along the magnetic field direction (along the y-axis of the top panel). The solid line shows the measured flux level. For both panels, distributions with positive velocities are moving parallel to the geomagnetic field towards the ionosphere, while distributions with negative velocities are moving away from the ionosphere, antiparallel to the magnetospheric field. The peak of the precipitating magnetosheath distribution in Fig. 2.13 is easily identified as the only peak at positive velocities (420 km/s). At negative velocities, two peaks are identified, representing the mirrored magnetosheath distribution (–680 km/s) and, at lower velocities, ionospheric ion outflow which is often

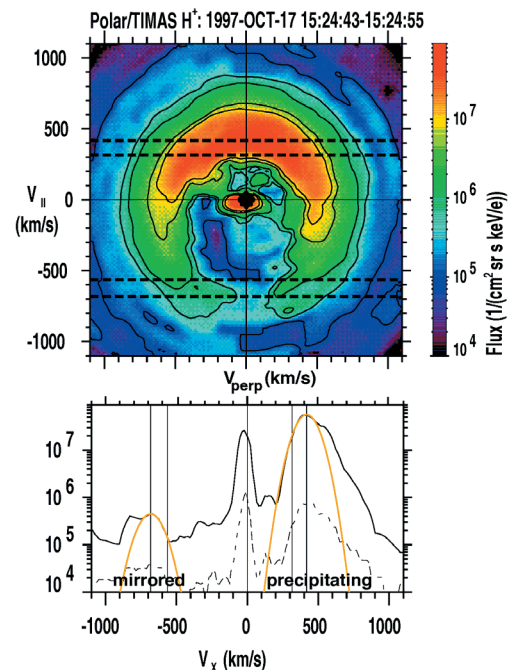


Fig. 2.13 2D representation of the 3D H⁺ ion flux distribution observed by Polar/TIMAS. Top: Velocity space distribution in a plane containing the magnetic field direction (y-axis) and the plane parallel to the Sun–Earth line. Bottom: The one-dimensional cut of the distribution above along the magnetic field direction. The dashed line represents the one-count level. Both distributions are fitted with Gaussian distributions (yellow curve) to ensure consistent 1/e velocity cutoff definitions.

observed at these latitudes [e.g. *Yau et al. 1985, Lennartsson et al. 2004*]. The low-velocity cutoffs of the precipitating and mirrored distributions are defined at the low-speed side of each beam, where the flux is 1/e less than the peak flux [see also *Fuselier et al. 2000b*]. The slowest ions of the two magnetosheath distributions are nearest the reconnection site.

It is possible to estimate the distance to the reconnection line by using the low-velocity cutoffs of the precipitating and mirrored magnetosheath populations in the cusp together with a time-of-flight model [e.g., *Onsager et al. 1991*] and the Tsyanenko 1996 (T96) semi-empirical magnetospheric field model [*Tsyanenko 1995*]. The distance along the magnetic field line from Polar to the reconnection line is X_r , where

$$X_r / X_m = 2 V_e / (V_m - V_e)$$

and X_m is the distance from Polar to the ionospheric mirror point, V_e is the cutoff velocity of the precipitating (earthward propagating) ions, and V_m is the cutoff velocity of the mirrored distribution. X_m is determined by using the position of the spacecraft in the cusp and tracing the geomagnetic field line at this position down to the ionosphere using the T96 model. The resulting distance, X_r , is subsequently traced back along the magnetic field line to the magnetopause using the T96 model.

An example of such a trace is shown in Fig. 2.14. Plotted are the magnetopause shear angles for the March 3, 2003, cusp crossings by the Polar (left) and the Cluster (right) spacecraft, as seen from the Sun. Square symbols in the shear-angle plots show the location of a section of the reconnection lines at the magnetopause. The black circle represents the location of the terminator plane. The magnetopause shear angle is calculated from the magnetospheric field directions and the IMF field directions at the magnetopause using models for the shear angle at the magnetopause and the draping of the IMF across a model of the magnetopause that is parameterized for solar wind conditions.

Red regions represent antiparallel magnetic field regions at the magnetopause, while black regions represent

parallel magnetic field conditions. The Polar and Cluster cusp crossings are more than 8 hours apart but occurred during similar IMF clock angles (about 255°), which results in almost identical shear angle plots. The location of the reconnection line derived from the Polar crossing of the southern cusp is in the southern hemisphere close to the antiparallel reconnection region. The location of the reconnection line derived from the Cluster crossing of the northern cusp is also in the southern hemisphere at about the same location as the Polar trace result. As shown in Fig. 2.14, despite the proximity to the antiparallel reconnection region (in red), the location of the trace points on the magnetopause (yellow and green regions) lead to the conclusion that this event is in agreement with a tilted X-line (shown in white) [*Trattner et al. 2004b*].

Expected results: The use of the 3D plasma instruments on Polar and Cluster in opposite hemispheres will allow the first systematic investigation of the location of the reconnection line for all IMF conditions. For this purpose, true cusp conjunctions between Polar and Cluster would be ideal; however, they are not required to achieve the desired result of knowing the location of the reconnection line for various solar wind and IMF conditions. As is evident from the example above, events with similar clock angles can also be directly compared. Events with similar clock angles observed in different MLT sectors are of special interest for probing the entire length of the reconnection line. Selected events will be compared with ionospheric emissions observed by IMAGE/FUV to cross-check the field-line tracing results.

Based upon the cusp database for the northern cusp regions, we expect to have about 200 Polar and 80 Cluster cusp events in the data survey for January–March 2006 and 2007, which will sufficiently span the parameter space of interest. An understanding of the location of the reconnection line will not only benefit the ongoing effort in unlocking the secrets of magnetic reconnection but is also of great interest to future missions and can be used to maximize the encounters of the MMS mission with the diffusion region.

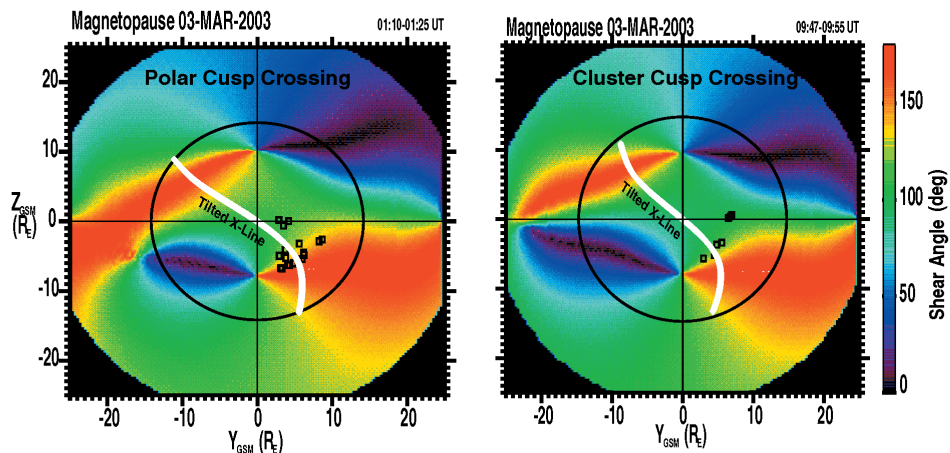


Figure 2.14 The magnetic field shear angle at the magnetopause as seen from the Sun, calculated from the magnetic field direction of the Tsyanenko 96 model and the draped IMF conditions [*Cooling et al. 2001*] during a southern Polar (left) and northern Cluster (right) cusp crossings on March 3, 2003. Square symbols represent the locations of the reconnection line at the magnetopause. The locations were determined by tracing the calculated distances to the reconnection line back to the magnetopause, along the geomagnetic field line in the Tsyanenko 96 model, starting at the position of the satellites in the magnetosphere.

Section 2.3 summary: *The extension of the Polar mission through March 2007 will enable compelling new science in the study of high-latitude magnetic reconnection and the cusp. The new science mode 2 will allow for the first time high-temporal-resolution observations of the high-latitude magnetopause and cusp region. The oblique configuration of the magnetic field at those high latitudes will present new configurations in which to study the thin filamentary structure of reconnection regions. Collaborations with S³C assets such as Cluster, which were not in orbit when Polar first visited this region, will allow probing of the high-latitude dayside magnetopause and cusp over a much longer baseline in the same and opposite hemispheres. These new opportunities will allow us to address effectively for the first time important science questions, including (1) How do the occurrence and nature of separatrix/diffusion region crossings vary as a function of latitude and external IMF magnetic geometry where component reconnection is expected to be increasingly common at higher magnetic latitudes? (2) What are the electron demagnetization mechanisms that allow component reconnection at high latitudes? Do these mechanisms include thin layers of strong E_FE_s that have been observed at lower latitudes? (3) How does the orientation of the magnetic field in the magnetosheath impact the relative fraction and rates of antiparallel reconnection versus component reconnection in the presence of a guide magnetic field? (4) What is the spatial/temporal coherence of the dayside magnetosphere under steady solar wind conditions?*

2.4. Polar and the Sun-Solar System Connections Great Observatory

Value to the Science Mission Directorate science themes: The Polar mission has been a fundamental component of NASA's Sun Earth Connection (SEC) program. The currently proposed objectives have direct impact on each of the new S³C Research Focus Areas discussed in the *Sun-Solar System Connection Science and Technology Roadmap 2005–2035* (August 2005 draft). These are:

- Open the Frontier (F) to Space Environment Prediction: Understand the fundamental physical processes of the space environment – from the Sun to Earth, to other planets, and beyond to the interstellar medium.
- Understand the Nature of our Home (H) in Space: Understand how human society, technological systems, and the habitability of planets are affected by solar variability and planetary magnetic fields.
- Safeguard the Journey (J) of Exploration: Maximize the safety and productivity of human and robotic explorers by developing the capability to predict the extreme and dynamic conditions in space.

Under each of the roadmap focus areas there are several S³C Priority Investigations. The connections between those investigations and Polar's extended mission objectives are shown in Table E.1 of the Executive Summary.

The proposed Polar science investigations highlight Polar's role in the S³C Great Observatory. Reconnection plays a

fundamental role in the acceleration and transport of plasmas in the Earth's magnetosphere and on the surface of the Sun. In situ measurements of the microphysics of reconnection on the Sun will not be possible for the foreseeable future. However the Earth's magnetosphere provides the only accessible laboratory for directly observing reconnection. Knowledge gained from Polar's high-time-resolution observations of the high-latitude dayside reconnection region will be applied to reconnection on the Sun. Understanding the details of energization of radiation belt particles to MeV levels and modeling of the radiation belts will be important for human and robotic explorers leaving low Earth orbit on their way to the Moon and Mars. Finally, the organized interaction of the magnetic and electric fields with particles as in the auroral acceleration region is important for its impact on our home in space – the Earth – and may have important implications for particle acceleration elsewhere in the solar system and the universe.

Polar as an SMD strategic asset: The strategic objectives addressed in the current S³C roadmap (draft available) is “intrinsically one of connections . . . extending over vast distances to produce dramatic effects throughout the solar system.” Because these connections are mediated locally by largely invisible agents, the plasmas and magnetic fields, the science must be based on multiple in situ measurements from several platforms throughout the system. The Polar satellite has played an important role in supporting the system science objectives by characterizing and analyzing the processes that occur throughout the inner magnetosphere and its high-latitude and dayside boundaries. Since its launch, Polar's orbit has evolved such that it sampled the near-Earth equatorial regions, high latitudes at both low and high altitudes, plus the equatorial and mid-latitude inner magnetotail. In the process, the Polar observations have provided new, detailed views of these regions and have answered many pressing science questions. Polar has not done this in a vacuum; it is part of an existing flotilla of satellites, each contributing critical observations. Likewise, Polar's observations have been important to other science missions, especially those focused on S³C science.

The continuing evolution of the Polar orbit brings the spacecraft back to a configuration similar to that of its early years but with apogee over the South Pole. Here, Polar will again make the type of high-latitude observations that were intended to support Cluster observations circa 1996–1999. However, the first Cluster launch failure denied that opportunity. Continued operation of Polar through December 2006 returns this originally envisioned ISTP science goal of having high polar region observations while Cluster traversed the mid-altitude polar regions plus mid- and high-altitude equatorial regions. In 2005 to 2007 Polar will also be sampling the equatorial regions of the inner magnetosphere from near Cluster perigee and lower. The joint operation of Polar, Cluster, ACE, IMAGE, and soon TWINS will provide unprecedented radial in situ and remote observations of the inner magnetosphere and its boundaries. These combined assets will allow testing of radiation-belt and ring-current particle source and transport models that have evolved based in a large part on the earlier Polar observations. Continuing Polar operations offers

the only opportunity in the foreseeable future to make critical in situ high-energy phase space density particle plus fields and EMIC wave measurements deep in the inner magnetosphere simultaneously with complementary measurements by other spacecraft of the current Great Observatory.

The Polar mission has been in place for almost 10 years and, as a result, the science investigators have made significant impact on the space physics literature. There have been nearly 1000 refereed publications by the Polar investigators. The pace of publication continues at a healthy rate – about 150 papers in the last 2 years. Many more publications featuring Polar science in a primary role have been published by researchers outside of the Polar mission team. A full publication list may be found at the Polar web site (<http://pwg.gsfc.nasa.gov/polar/>).

The Polar principal investigators are internationally known leaders of the S³C science community. Two of our PIs and two co-investigators are among the most highly cited space sciences researchers (<http://ishighlycited.com>). The PI teams supply data for collaborative studies, for image conversions, and for model boundary conditions. The imaging teams provide definitive information on the timing of substorm phases and media-ready descriptions of the magnetospheric response to solar events. Special journal issues and meeting sessions are sponsored in addition to semiannual workshops, often held in cooperation with other missions.

The Polar payload continues to be of special value to the S³C community because it is the only mission to provide multispectral imaging of the ionosphere's response to energy inflow simultaneously with the phenomena the in situ instrumentation are observing. In addition, it is the only mission to successfully observe the 3D electric and magnetic field along with full 3D ion and electron distributions. By end of mission, Polar will provide this information over the entire northern and, with this extended mission, the southern MI-coupled system under a wide variety of solar input conditions. Because future Solar-Terrestrial Probe (STP) and LWS initiatives necessarily target different aspects of the Sun–Earth connected system, this observational database will be an important resource for decades to come.

2.5. What have we learned from Polar?

Originally conceived as a keystone of the “Origins of Plasmas in the Earth’s Neighborhood” (OPEN) Program, Polar was designed to expand our understanding of solar wind coupling to the ionosphere, mediated by the magnetosphere, particularly by means of plasma transport and exchange between the two media [ISTP *Red Book*]. Unique design features supporting this objective include diagnostic instrumentation with energy range extending down to ionospheric energies (0.3 eV), continuous (despun) auroral imaging, spacecraft neutralization, the first vector electric fields, and a high standard of electrostatic and magnetic cleanliness. Thanks to these unique features and the evolution of its orbit, Polar has yielded, and continues to yield, new and important scientific results after almost a decade. We featured many of our recent accomplishments in sections 2.1–2.3; in the following “vignettes,”

we summarize the progress that Polar has made in this important foundational area of S³C.

Radiation belt time variations: The effect of geomagnetic storms on radiation belt fluxes is a delicate and complicated balance between the effects of particle acceleration and loss. *Reeves et al.* [2003] investigated 276 moderate and intense geomagnetic storms observed by Polar and found that only about half of the storms increased the fluxes of relativistic electrons, one quarter decreased the fluxes, and the final quarter produced little or no change, suggesting that storms do not simply “pump up” the radiation belts (see Fig. 1.2). In contrast, higher solar wind velocities increased the probability of large flux increases. Using Polar, SAMPEX, and other data, *Blake et al.* (2005a) have searched for those characteristics of geomagnetic storms that lead to new, long-lasting radiation belts. It was found that stable belts require injection inside $L \sim 2.5$, and associated with such injections is an unusually rapid rise in the magnetic field impulse as seen by ground-based magnetometers (Fig. 2.15).

Two broad classes of mechanisms are thought responsible for relativistic electron enhancements: radial transport and local acceleration. Recently, through theoretical and empirical means, great strides have been made toward resolving the relative importance of these two types of mechanisms [e.g., *Meredith et al.* 2002, *O’Brien et al.* 2004, *Horne and Thorne* 2003, *Green and Kivelson* 2004; *Taylor et al.* 2004].

Green [2002] showed the strongest evidence to date that local electron acceleration takes place in the inner magnetosphere: namely, that evolving storm-time phase-space-density peaks are inconsistent with radial transport alone. This study showcased the kind of science that can only be done on a robust platform like Polar. The likely mechanism involved in the formation of this phase-space-density peak is VLF chorus heating of the electron distribution. VLF chorus are the most intense, naturally occurring discrete waves; they occur

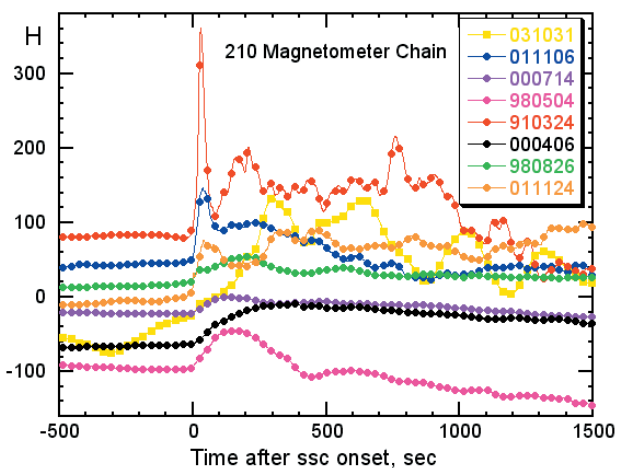


Fig. 2.15 Data from Polar and other satellites showed that stable radiation belts (lifetimes of a month or more) were associated with rapid rise times in ground magnetograms. Here data from the 210 Magnetometer chain is plotted; stable radiation belts were created at the onset of the 910324, 011106, and 011124 events and not others; the difference in rise time between the geoeffective and nongeoeffective events is striking.

regularly within the inner and outer radiation belts and appear before an injection process can take place. The emission propagates without exception away from the geomagnetic equator. The absence of a reflected component within these closed field line regions indicates the chorus is absorbed before reflection, thereby determining the lifetime of radiation belt particles and producing enhanced precipitation [LeDocq *et al.* 1998]. Polar/PWI detected VLF chorus emissions near the dawn meridian in rapid response (<60 s) to magnetospheric pressure pulse events [LeDocq *et al.* 1998, Lauben *et al.* 1998]. Meredith *et al.* [2002] determined that chorus emissions correlate well with magnetic storm-time-accelerated electrons within the radiation belts. Such correlative studies are now being conducted using Polar/PWI and Hydra/CEPPAD data. Understanding how these emissions are generated is important for assessing their role in radiation belt dynamics [Lauben *et al.* 2001; Bell *et al.* 2002; Bortnik *et al.* 2002, 2003a,b].

Magnetic conjunctions between Polar and SAMPEX demonstrated a close relationship between VLF chorus waves and MeV microburst precipitation, and showed how VLF chorus plays a role in both the acceleration and loss of energetic electrons [Lorentzen *et al.* 2001]. This study enables the use of MeV microbursts as a proxy for VLF chorus, which is helpful since long-term observations of chorus with high time and L-shell resolution are difficult. Using Polar and SAMPEX data, O'Brien *et al.* [2004] showed that electron precipitation via microbursts could empty the outer zone of MeV electrons in about 1 day during the main and early recovery phases of three geophysical electromagnetic (GEM) storms. In a follow-up study, Thorne *et al.* [2005] showed that observed lifetimes for loss via microbursts for a range of L shells in the outer zone were comparable to those predicted by quasilinear diffusion theory. In both studies, Polar provided the trapped content of >1 MeV electrons in the outer zone, while SAMPEX provided instantaneous loss rates to microburst precipitation.

The importance of pitch-angle scattering of radiation belt electrons during magnetic storms was shown in the pitch-angle distributions measured by the CEPPAD/SEPS instrument [Walt 2004]. With angular resolution of about 1.5° the pitch-angle distributions clearly showed diffusion of electrons into the loss cone during magnetic storms when electron fluxes and ELF/VLF wave fields were strongly enhanced. This confirmed the original ideas of Kennel and Petschek [1966], although the wave measurements using Polar/PWI show that the waves are not field aligned as those authors assumed. Thus waves and particles on different L shells are coupled by the interactions, and large regions of the outer electron radiation belt decay in unison.

Measurements of pitch-angle distributions of protons during five magnetic storms in 1998 also demonstrated the importance of pitch-angle scattering in the loss of ring current protons [Walt and Voss 2001, 2004]. In some cases diffusion was strong enough that the loss cone fluxes were isotropic and equal to the trapped fluxes. When this scattering occurs, the local lifetime of protons is only about 15 min. Ring current models now being developed include pitch-angle scattering, but most models do not predict wave growth and proton scattering strong enough to fill the loss cone.

Charged particle acceleration as an additional source for the outer radiation belts: The high-altitude dayside cusp is an extremely dynamic region in geospace. Cusp energetic particles (CEPs) observed there [Chen *et al.* 1997, 1998; Fritz *et al.* 1999] have shown orders of magnitude increases of ion intensities with energies from 20 keV up to 10 MeV [Chen and Fritz 2005]. Competing theories relate to the acceleration mechanism for CEPs [Chen and Fritz 1998, Trattner *et al.* 1999, 2003; Fritz and Chen 1999; Sheldon *et al.* 2003; Chen *et al.* 2003; Chang *et al.* 2003]. Chen *et al.* [1997, 1998, 1999] and Sheldon *et al.* [1998] argued for local energization in the high-altitude dayside magnetosphere, near and perhaps in the cusp. Chang *et al.* [1998, 2001] and Trattner *et al.* [1999, 2001] noted that energization of ions to over 100 keV routinely occurs in the Earth's bow shock region, during specific IMF orientations, as a result of the Fermi acceleration process. In addition, numerical simulations [e.g., Delcourt and Sauvaud 1999, Blake 1999] have suggested a ring current source of CEPs.

Delcourt *et al.* [2005] investigated the dynamics of these charged particles in the dayside magnetosphere in response to abrupt variations of the solar wind dynamical pressure. Using test particle simulations, they show that the electric field induced by the compression of the frontside magnetosphere causes prominent energization of plasma sheet ions as well as trapping at high latitudes. Ions that are initially bouncing from one hemisphere to the other are found to experience nonadiabatic energization up to the hundred keV level while being injected into the outer cusp. The energetic particles produced in the outer cusp during such events subsequently circulate about the field minimum at high latitudes without intercepting the equatorial plane and contribute to the high-energy populations observed in this region of space.

Understanding the microphysics and macrophysics of reconnection: Magnetic field reconnection is the process that converts electromagnetic energy to particle energy to drive the Earth's magnetosphere, solar flares, and astrophysical energetic processes. The Polar team has made excellent progress delineating candidate microphysical reconnection layers and illustrating the importance of making explicit tests of the ways that collisionless magnetic reconnection occurs. Mozer *et al.* [2002] demonstrated the presence of opposed electric fields along the normal to reconnecting layers. Scudder *et al.* [2002] provided the first documented penetration by a spacecraft of the separator and, hence, the electron diffusion region, the "holy grail" of magnetic field reconnection.

A rare guide field traversal of the magnetopause on April 1, 2001, provided a snapshot of the ion diffusion region and a rare observation of a small guide magnetic field; as contrasted with particle inferences of the possibility of guide field reconnection, these are the first direct constructions of layer geometry that show the passive component of B orthogonal to the plane of interconnection (i.e., component reconnection) [Scudder *et al.* 2002]. Magnetic field reconnection can and does occur in low- β plasmas, where strong inhomogeneous electric fields demagnetize the electrons in spite of the strong magnetic field. More detailed discussions of these results

were presented in the recent advances section on page 14 of this proposal.

Using Polar and Cluster plasma, electric, and magnetic field measurements, *Maynard et al.* [2003] established wave Poynting flux as an additional necessary, but not sufficient, discriminator for merging at the dayside magnetopause.

Two competing models of magnetic reconnection are anti-parallel reconnection and component reconnection. *Trattner et al.* [2004a] found that both reconnection scenarios occur for the same IMF conditions. *Trattner et al.* [1999, 2002a, 2002b] have shown that during periods of steady IMF, reconnection is steady and occurs over long X-lines as suggested by *Crooker et al.* [1985]. At other times *Trattner et al.* [2002a] demonstrated significant, quantifiable intervals of pulsed plasma entry as predicted by *Lockwood and Smith* [1992, 1994] and *Lockwood et al.* [1995, 1998]. *Fuselier et al.* [1999, 2000a, 2000b, 2001, 2002], *Avanov et al.* [2001], and *Topliss et al.* [2000] used particle observations to quantify reconnection stability in space during steady IMF. A survey of 13 events observed by Polar, Cluster, and SuperDARN places merging at high latitudes whenever the IMF clock angle is less than $\sim 150^\circ$ [*Maynard et al.* 2003]. They also showed that dipole tilt may cause merging sites to move off the equator, even for 180° clock angles. *Trattner et al.* [2002a,b; 2004a] and *Petrenic et al.* [2003] utilizing data from Polar/TIMAS and other satellites presented evidence that reconnection under steady solar wind conditions is primarily steady, not primarily pulsed as previously thought. *Maynard et al.* [2004, 2005] associated the keV field-aligned precipitating electrons from active merging sites with high-resolution all-sky images of 557.7-nm emissions in a dark dayside cusp. They concluded that merging occurs at multiple sites simultaneously and asynchronously on time scales of 30 s to a few minutes, having characteristics of both a temporally varying continuous process and pulsed responses. While the process is ongoing on the large scale, structure and dynamics continue on the mesoscale. The studies proposed in section 2.2, which are now possible because of the evolving Polar orbit, will provide further insight into the nature of solar wind entry and reconnection.

Impact of the ionosphere on geospace processes:

Since our 2003 discovery that the geopause – the boundary inside of which terrestrial plasmas dominate – is often present just inside the magnetopause [*Chandler and Moore* 2003], we have more recently learned that these plasmas exhibit sporadic high-speed sunward flow bursts that are related to southward IMF [*Chen and Moore* 2004] as shown in Fig. 2.16. These flow bursts approach the local Alfvén wave speed, which is substantially depressed by the presence of the relatively dense cold plasmas. This stark comparison reveals the principal significance of these observations: cold ionospheric plasma is present at the subsolar magnetopause, with densities that vary over orders of magnitude, depending upon deep convection of plasmaspheric plumes in the magnetosphere. Thus, the magnetospheric convective response to reconnection with the IMF contains a negative feedback. When deep convection transports sufficient plasmaspheric material to the dayside reconnection region, it reduces the Alfvén speed and hence

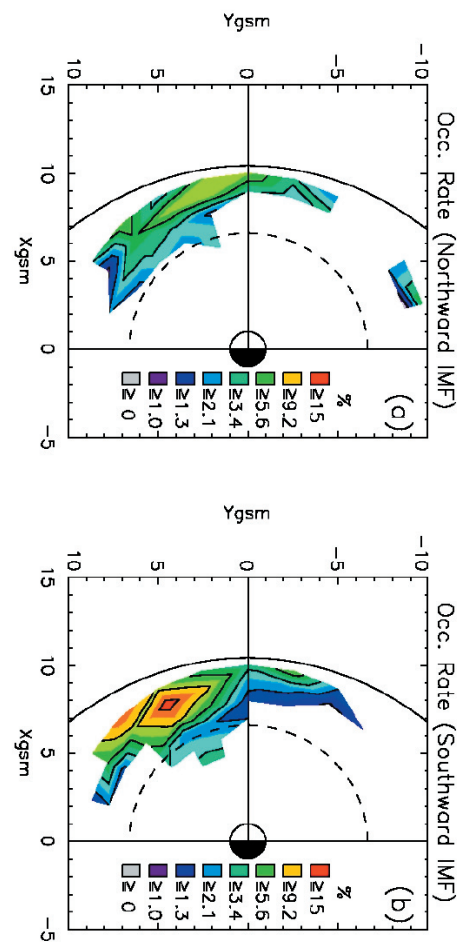


Fig. 2.16 The statistical occurrence probability of cold convecting ions in the magnetopause region is plotted for northward IMF (top left) and for southward IMF (bottom left). The overall distribution is diffuse for northward IMF, but strongly peaked in afternoon local times for southward IMF, with a substantially higher overall probability for the latter case.

limiting the rate of reconnection. This negative feedback possibility was alluded to by *Freeman et al.* [1977], albeit in connection with heavy ions, and may be related to saturation of the transpolar potential at large values, as discussed by *Siscoe et al.* [2004].

We have revisited the supply of proton plasma to the magnetosphere from the ionospheric polar wind, including its circulation throughout the magnetosphere [*Huddleston et al.* 2005]. The results show that, when the full polar wind outflow flux is properly assessed, it supplies enough proton plasma to be comparable with the solar wind contribution in terms of density. On the other hand, independent modeling results [*Moore et al.* 2005] indicate that the solar proton source to the magnetosphere is typically more energized by magnetospheric processes, and therefore tends to dominate the proton pressure in the inner magnetosphere. Thus, it is clear that the ionospheric polar wind outflows can no longer be dismissed or ignored in magnetospheric plasma dynamics.

A survey of cold ion observations in the near-Earth magnetotail using data from Polar/TIDE [*Liemohn et al.* 2005] showed that the “polar” wind becomes the “lobal” wind in

the magnetotail, with low-energy (<300 eV) ions streaming from the ionosphere downtail. These lobal winds pass through the plasma sheet, forming bi-directional streams at lower latitudes. These results show that the ionosphere is a continuous supplier of plasma to the near-Earth magnetosphere. The high occurrence rate of these streams means that during geomagnetic disturbances, it is not necessary to wait for outflow and magnetospheric circulation to supply the inner magnetosphere with ionospheric ions; these cold streams are an immediately available supply of ionospheric-origin particles.

A statistical study of the ion outflow versus energy input was performed using multi-instrument data (TIDE, EFI, MFI, Hydra) from Polar during its perigee auroral passes in 2000 [Zheng *et al.* 2005]. Several important physical quantities connected to the ion outflow have been investigated, including the Poynting flux from the perturbation fields (below 1/6 Hz), the electron density, temperature, and the electron energy flux. Our results show that the field-aligned ion outflow flux correlates best with the Earth-directed Poynting flux and the precipitating electron density and also demonstrates almost no correlation with the electron energy flux and temperature. The findings from this Polar study are qualitatively similar to those from FAST [Strangeway *et al.* 2005].

Tu *et al.* [2005] used a dynamic fluid semi-kinetic (DyFK) model to simulate the cleft ion fountain. Ion field-aligned flows were modeled for a flux tube convecting along an empirical model-specified convection trajectory across the polar ionosphere from the cusp/cleft region. The simulated field-aligned flow pattern is in qualitative agreement with the observations from TIDE during a typical Polar satellite southern perigee pass. The day–night asymmetry of the O⁺ density across the polar cap from dayside to nightside is directly controlled by the cleft ion fountain, while the H⁺ density asymmetry is probably caused by day–night variations in solar illumination.

When observations of ion outflow from Earth are arranged according to the polarity of the IMF B_z [Lennartsson *et al.* 2004] and limited to times with B_z > 3 nT or B_z < –3 nT, the total rate of ion outflow is seen to be significantly enhanced with negative B_z, typically by factors of 2.5 to 3 for the O⁺ and 1.5 to 2 for the H⁺, more than previously reported from similar but less extensive comparisons. With either IMF B_z polarity, the rate of ion outflow is well correlated with the solar wind energy flow density, especially well with the density of kinetic energy flow. The rate of ion outflow reaches 10²⁶ ions per second or more per hemisphere.

Understanding substorms and auroral associated phenomena: Over nearly 10 years, the Polar mission has figured prominently in the development of our understanding of substorm processes and auroral phenomena. For example, the timing of substorm onset [Liou *et al.* 1999, 2000a, b; 2002], location of the substorm onset region and corresponding magnetotail plasma dynamics [Frank and Sigwarth 2000a, b; Frank *et al.* 2000; 2001a, b; 2002], and the Polar observations of polarized electric field variations associated with strong magnetic field fluctuations within the outer boundary of the local midnight plasmashet at 4 to 6 RE [Ober *et al.* 2001, Wygant *et al.* 2000]. The associated Poynting flux was directed

along the average magnetic field direction coinciding with intense auroral structures (~20 to 30 ergs/cm²-s). The energy flux in the Alfvénic structures, when mapped to ionospheric altitudes, provided sufficient power (~100 ergs/cm²-s) to drive all auroral processes, including acceleration of upward-flowing ion beams, electron precipitation, auroral kilometric radiation (AKR), and Joule heating of the ionosphere [Wygant *et al.* 2000].

Pressure pulses in the solar wind have been shown to cause global brightenings of the auroral oval luminosities on short time scales [Spann *et al.* 1998, Zhou and Tsurutani 1999, Brittnacher *et al.* 2000]. The open polar cap magnetic flux is found to decrease by 50% in time periods as short as 30 min [Sigwarth *et al.* 2005a]. Liou *et al.* [2003, 2004] reported that interplanetary shocks might trigger auroral electrojets enhancements (compression bays) but not auroral breakups. They also show that compression bays are associated with a directly driven process rather than a loading–unloading process.

Statistical studies of substorms have established the seasonal effects on the frequency and magnitude of substorms. By analyzing over 300 substorms using global auroral images taken by Polar/UVI, Chua *et al.* [2004] found that substorms that occur during winter last on average twice as long as substorms that occur during summer. These results suggest that the background ionospheric conductivity plays a vital role in determining how long a substorm lasts. Wu *et al.* [2004] studied 23 storms and 167 concurrent substorms and found that substorms occur more frequently in the main phase (60%) than in the recovery phase (40%) of storms.

Until the advent of the Polar mission, advances in exploring interhemispheric asymmetries of the magnetosphere were mainly characterized by recognition of the existence of such asymmetries rather than in understanding their causes. Using the global Polar/VIS Earth camera to capture the northern and southern nighttime hemisphere aurora oval segments simultaneously in single frames (Fig. 2.17), Frank and Sigwarth [2003] determined that auroral substorm onsets in the northern and southern hemispheres differed in timing by up to 2 min, that the intensities were significantly different, and that the locations of the conjugate onsets were shifted in longitude from that expected by tracing along the standard magnetic field models such as Tsyganenko 89. Images of the aurora acquired with Polar/VIS and Image/FUV have been used to determine the locations of substorm features and auroral arcs in the northern and southern aurora [Ostgaard *et al.* 2004, 2005] and the control of the IMF on the shift of the centroid of the auroral oval [Stubbs *et al.* 2005 and associated NASA press release]. Fox *et al.* [2005] found that the offsets of the substorm onset longitudes in the two hemispheres are controlled by the IMF B_y component and follow the “twist” configuration of ionospheric flows. Standard magnetospheric models are found to underestimate the amount of twist between the two hemispheres due to uncertainties in the level of shielding that should be represented. Using Polar/UVI and IMAGE/FUV, Fillingim *et al.* [2005] observed gross morphological differences in the dayside aurora in the northern and southern hemispheres. The differences are not controlled by

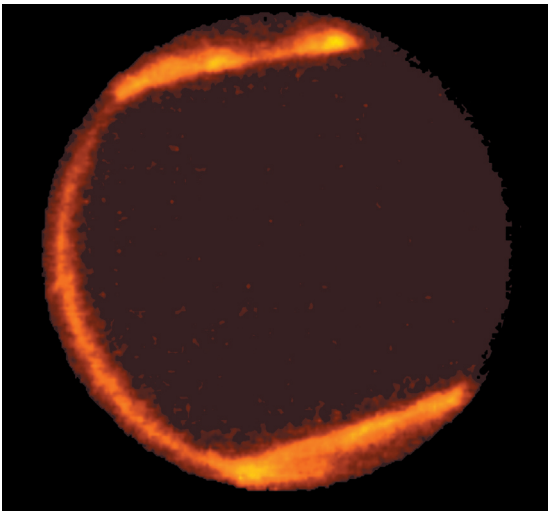


Fig. 2.17 During this magnetospheric storm, the simultaneous observations of the northern and southern auroral ovals exhibit vastly different behavior. In the north, a portion of the auroral oval has dimmed, while in the south, the auroral band remains bright across the entire nighttime sector and brightens in the region that is magnetically conjugate to the dim auroral segment in the north (VIS Earth Camera, 21 Oct 2001, 18:49:32 UT 130.4 nm).

the background ionospheric conductivity because the observations were made near equinox.

Understanding the source of AKR spectral fine structure is critical to understanding details of the generation mechanism. Most recently *Menietti et al.* [2005a] performed linear analysis of the growth of EMIC waves using Polar electron observations (Hydra) within an AKR source region during the observation of AKR striations. In addition, *Menietti et al.* [2005b] reported the similarities between AKR fine structure and Saturn kilometric radiation fine structure observed by the Cassini plasma wave instrument.

Franz et al. [2005] have analyzed Polar/PWI data for electrostatic solitary waves in the high-altitude polar magnetosphere. They find these structures have typical scale sizes of the order of a Debye length, velocities of the order of the electron thermal speed, and electrostatic potentials that are small compared with the electron thermal energy per charge. In addition, *Chen et al.* [2005] investigated a width-amplitude inequality which sets limits on the morphology of observed electron phase space holes relative to measured plasma properties. Such electrostatic structures may be ubiquitous and play a fundamental role in both particle and wave physics.

Examination of energetic electron data from Polar, Cluster, and Chandra at three widely spaced locations with separation $\sim 20 R_E$ across the magnetotail revealed that energetic electrons (>35 keV) appeared simultaneously at all three locations, and that the appearance was 10 min after the injection into geostationary orbit (GEO) as determined by examination of drift dispersion at several local times in GEO orbit (Fig. 2.18) [*Blake et al.* 2005b]. In addition to the substorm-associated electrons, time-correlated electron bursts were observed by the magnetotail spacecraft sporadically for a few hours prior to the substorm.

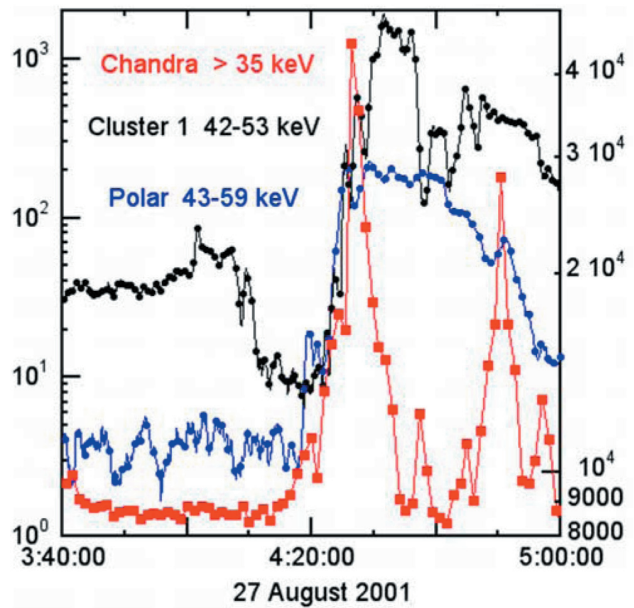


Fig. 2.18 Energetic electrons appeared simultaneously at ~ 0420 UT at three widely spaced positions in the magnetotail: Polar at 0200 local time (LT) and 9 RE; Cluster at midnight LT and 18 RE; and Chandra at 2000 LT and 18 RE. The magnetotail onset was ~ 15 min after GEO spacecraft observed a substorm injection of energetic particles.

From the Sun to the Earth: Studies of the great storms:

An important technical accomplishment of the combined S^3C spacecraft fleet is the systematic tracking of transient events from their birth on the Sun to their effectiveness in producing magnetic storms, accelerating magnetospheric plasmas, and depositing energy into the atmosphere. The power of the S^3C Great Observatory as it evolves is demonstrated with each new storm event, as each mission adds new information toward understanding the overall system dynamics. For example, Polar observations during the April 2002 event showed large depletions in the dayside low-altitude O/N₂ ratio correlated with increased geomagnetic activity and auroral brightenings [*Sigwarth et al.* 2005b]. The observed changes are due to the energy deposition of auroral precipitation and the associated Joule heating of the upper atmosphere which occurred ~ 6 to 12 hours prior to the neutral composition change.

With the May and September 1998 magnetic cloud encounters, Polar investigators were able to separate the response of the magnetosphere to intense solar wind pressure increases as compared with extremes in the IMF direction. The Polar team found that rapid shock-like compressions shrink the magnetosphere in size, increasing the overall magnetic field strength and rapidly moving plasma downstream along the affected field lines [*Russell et al.* 1998]. Increased plasma pressure down the throat of the cusp increases its width in local time and latitude [*Zhou et al.* 2000]. This event also produced an immediate, intense ionospheric mass ejection with the mass flux from the Earth to northern lobe altitudes increasing by more than 2 orders of magnitude [*Moore et al.* 1999]. This, combined with observations from Dynamics Explorer, indicates that fluctuations in solar wind pressure control the outflow of heavy ions from the ionosphere, while the IMF more directly controls the subsequent dispersal of that flow across

polar cap latitudes by controlling transport processes. Surprisingly, field-aligned and region 1 currents connecting the ionosphere to the magnetopause have little reaction to pressure pulse passages, but are strongly enhanced during southward orientations of IMF [Le and Russell 1998]. This finding emphasizes the importance of reconnection as a driver for certain internal dynamics over the contribution due to viscous drag.

During the so-called Halloween storm period (October 29–November 4, 2003) Polar and IMAGE observed that the oxygen outflow from the ionosphere supplied an overwhelming contribution to the hot ring-current plasmas (Fig. 2.19) [Nosé et al. 2005, Moore et al. 2005]. These plasmas form in the magnetotail and are transported into the inner magnetosphere, where they dominate inner magnetospheric storm plasmas of the ring current. The strong tracking of ionospheric outflow, plasma sheet, and ring current O^+ content with the magnitude of storm disturbances clearly demonstrates the terrestrial origin of such plasmas.

Polar's unique orbit, in which it explores nearly the complete volume of the magnetosphere while staying inside it, has proven to be particularly useful for studying the effect of extreme solar events on the magnetosphere, since Polar will almost always be in some place interesting during the event. During the Halloween events of 2003, Polar made many radial passes through the magnetosphere, probing the fluctuations in the magnetic field strength caused by dynamic pressure fluctuations [Russell et al. 2004]. These wave powers increased a factor of 2000 at times inducing rapid radial diffusion that may have been responsible for both particle loss and particle acceleration [Cartwright et al. 2004]

These types of analysis efforts applied to the storms expected during the approach to solar minimum will further define the specific elements of geospace dynamics responsive to one type of solar input or another. In this manner, event by event, Polar, along with the other missions in the Great Observatory, will build a catalogue of the magnetosphere's response to a large variety of solar input conditions.

A thorough survey of the magnetosphere: The precession of Polar's line of apsides over the course of the mission has provided extensive coverage of the Earth's magnetosphere. Le et al. [2004] used this coverage to map the distortion of the magnetic field by the ring and field-aligned currents and from these distortions determine how the currents in the magnetosphere varied with the strength of the geomagnetic field. This study and work by Ganushkina et al. [2003, 2004] also showed that a significant portion of the changes in the Dst index comes from the currents in the near tail. Chi et al. [2003] developed new techniques to identify and characterize ULF waves and surveyed activity as a function of

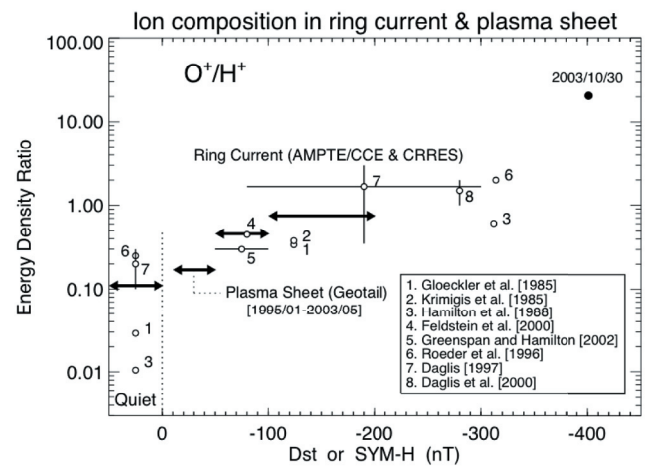


Figure 2.19 Summary of ion composition observations of the ring current, including work by Nosé et al. [2005] who found that O^+ dominates the ring current for superstorms like the Halloween storm of 2003. A similarly extreme outflow flux of low-energy neutral atoms was observed by Polar/TIDE during this event.

solar wind conditions over the northern hemisphere [Chi and Russell 2005].

Polar observations in the equatorial plane (2001–2003) revealed a highly variable magnetic field with values occasionally dropping as low as 1 nT near the current sheet when the IMF is southward and the solar wind velocity is near 800 km/s [Ge and Russell 2005b]. Ge and Russell [2005b] reported frequent dipolarizations of the magnetic field causing compressions of the field at low latitudes and plasma sheet expansions away from the current sheet. Coordinated studies with GOES and Cluster also showed this dynamic behavior, and thus we expect successful studies with the THEMIS mission when the locations of the spacecraft are coordinated [Ge et al. 2005]. Some of the wave phenomena in this equatorial region were totally unexpected. Mirror mode waves like those seen at comets, in the Io wake, and in the Earth's magnetosheath are common in this region. More rare but spectacular when they occur are narrowband low-frequency (periods of minute) waves that arise when the IMF is radially outward from the Sun [Ge and Russell 2005a].

Polar's long dwell time at apogee and line of apside precession over the course of the mission have enabled detailed studies of key magnetospheric regions. This has allowed a more complete picture of the magnetosphere to emerge as Polar samples different regions. In collaboration with missions from the Great Observatory, Polar continues to add pieces to the very complicated puzzle.

3. Technical and Budget

3.1. Status of the space assets

Health of the spacecraft

The Polar satellite, launched on February 24, 1996, is in a highly elliptical orbit with a period of approximately 18.5 hours. The inclination is 83.7° , apogee is at $9.4 R_E$, perigee is at $1.7 R_E$ geocentric, and the precession rate of the line of apside is 16° per year. Over the next 2 years, the Polar apogee will precess to nearly polar southern latitudes. It will pass through midnight local times at southern latitudes in the fall of each year and noontime cusp–southern hemisphere latitudes each spring (see Fig. 1.1).

As the orbit evolves, Polar will have the opportunity to acquire data appropriate for new science questions. The traversals of the radiation belts and the heart of the ring current will continuously progress inward as apogee moves to high southern latitudes. The well-instrumented spacecraft will scan the crucial $L = 6$ to $3 R_E$ through the heart of the radiation belts. This scan will be performed with the benefit of unprecedented high-time-resolution observations made possible by the switch to the new science mode 2 telemetry format. The previous scan of this region occurred at lower temporal resolution and during solar maximum, whereas the upcoming scan will occur during the period of high-speed streams as the Sun approaches solar minimum. Polar will continue to skim the high-latitude dayside magnetopause and will obtain new high-temporal resolution passes through the southern dayside cusp to complement the northern cusp work early in the mission. With the local time phasing of the Polar and Cluster orbits, simultaneous cusp and magnetopause crossings will occur with Polar and Cluster in the same hemisphere and in opposite hemispheres. In effect, Polar becomes the “Fifth Cluster member,” providing a very long baseline for measurement comparisons.

The spacecraft subsystems are operating nominally. All three batteries are very healthy, and have successfully serviced the spacecraft through the longest eclipses of the mission. Polar has lost one of its two digital tape recorders through failure of the recorder’s power supply. Despite this loss, the Polar mission continues to acquire data with greater than 90% coverage with the remaining tape recorder fully capable of servicing the mission. The transponder used since launch has lost some output power, but the margin remains adequate without switching to the backup transponder. The despun platform continues to operate nominally with no degradation of performance.

Operations at ecliptic normal attitude

Early in the mission life of Polar, the spacecraft was oriented with its spin axis perpendicular to the orbital plane. Every 6 months the Polar spin axis was inverted by a spin axis precession maneuver (180° flip) to maintain the spacecraft batteries and the imaging platform in shadow for thermal and power regulation. By careful management of the fuel resource, including a 6-month period of operations with the spin axis oriented normal to the solar ecliptic, the fuel reserves were stretched to cover the 7.5 years of flip maneuvers. As the onboard fuel

supply sized for the 3-year design life plus a 2-year extended mission phase was nearing depletion in February 2004, Polar was maneuvered to place the spin axis perpendicular to the ecliptic plane for the final time. Since then three small maneuvers per year have been required to compensate for the gravity gradient drift of the spin axis. The new orientation has had no adverse effect on our ability to address the science objectives of the Polar mission.

The remaining amount of fuel is expected to be sufficient to maintain the ecliptic normal configuration until March 2007. After that time, the drift of the spin vector will point the spacecraft radiators at the Sun. Thermal effects are unknown but overheating of spacecraft subsystems is expected at that time and spacecraft operations will cease.

In October 2006 all of the remaining fuel will be expended in an engineering test to determine the amount of unusable fuel and the effectiveness of using the inert gas that pressurizes the tanks as a non-reactive propellant. The spacecraft engineers will find this information extremely useful in planning for operations of other spacecraft with long mission lives. An added benefit will be extended auroral viewing for the final 3 months of the Polar mission.

High resolution telemetry operations (science mode 2)

Since going to ecliptic normal attitude, Polar has utilized its alternate telemetry format, called “science mode 2” to maximize the science return for the mission. The science mode 2 telemetry format approximately doubles the telemetry allocation for each of the fields and particles instruments at the expense of the imagers. This format was implemented and tested pre-flight as a contingency mode in the event of failure of Polar’s despun platform. The mode is invoked with an on-board software command and has been utilized in the ecliptic normal configuration, on a time-share basis with the imaging, primarily during those portions of the orbit when the imaging platform cannot achieve pointing lock on the Earth due to loss of horizon sensor coverage. The EFI, MFE, and Hydra instruments all take advantage of the additional telemetry allocation by increasing the electric field sampling to 80 Hz, the magnetic field sampling to 25 Hz, and via Hydra, even higher sampling of the full magnetic field vector at 54 Hz.

Health of the instrumentation

Nine of Polar’s eleven science experiments are operational and providing high-quality science data products (see Tables 1.1 and 3.1). Polar carries five types of charged particle detectors to sample electron and ion populations and perform mass identification, from thermal to relativistic energies. Polar’s electric and magnetic field instruments include dual high-resolution fluxgate magnetometers and the first successful triaxial electric field instrument with ultra-high time resolution burst-mode capability. Two imagers continue to provide spectral imaging in ultraviolet and visible wavelengths; these are mounted on a despun platform to optimize viewing of the aurora and other targets.

Table 3.1 Instrument-by-instrument availability of data products. Note that full science analysis products are available in every case. In the future, Polar has agreed to partner with proposers to the “Virtual Observatory” Announcement of Opportunity that will enable increased use of the Polar, Wind and Geotail data sets by the S³C science community.

Instrument	Browse Products/ Key Parameters	Open access to High Resolution Calibrated Data	Summary Plot Web Interfaces	Custom Plot Interfaces
MFE	via CDAWeb KP is high res product	via CDAWeb KP is high res product	on PI server, several resolutions	via PAPCO
EFI	via CDAWeb KP is high res product	via CDAWeb, & PI server KP is high res product	KP only	via PAPCO
PWI	via CDAWeb	via CDAWeb many high res products	Many products at various resolutions	create many types of spectrograms via PAPCO, or web interface
CAMMICE	via CDAWeb	via CDAWeb PAPCO compatible	Many types of summary plots	via PAPCO
CEPPAD	via CDAWeb	via CDAWeb PAPCO compatible	Many types of summary plots	via PAPCO
Hydra	via CDAWeb	via CDAWeb PAPCO compatible	DDEIS spectrograms	Create many types of spectrograms, moments and distribution plots via PAPCO
TIMAS	via CDAWeb	via CDAWeb PAPCO compatible	Summary spectrograms on PI server, high resolution spectrograms via CDAWeb	via PAPCO
TIDE	via CDAWeb	via CDAWeb PAPCO compatible	Several types of summary spectrograms, high resolution spectrograms via CDAWeb	create many types of spectrograms, moments and distribution plots via PAPCO
UVI	via CDAWeb	via CDAWeb	Full sets of images online	
PIXIE	via CDAWeb	via CDAWeb	Full sets of movies and images online	custom auroral movies via web
VIS	via CDAWeb	via CDAWeb	Full sets of images online	

Two of our science investigations are no longer operational but continue to serve as valuable data resources. The PIXIE imager provided global X-ray wave-length images through November of 2002; the PWI Plasma Wave Instrument provided complete 0.1-Hz to 800-kHz wave vector characteristics for the first 18 months of the mission.

MFE status: The Magnetic Field Experiment (MFE) continues to return precise high-resolution three-component measurements of magnetic fields. The instrument does not show any sign of aging or degradation. In the new science mode 2, the time resolution of MFE data is enhanced to 24 Hz from the present high rate of approximately 8 Hz. MFE data also help to organize and interpret the data measured by other experiments on the Polar spacecraft, especially the energetic particles, plasmas, and electric field experiments.

EFI status: The 3-axis Electric Field Experiment (EFI) on Polar continues to operate with no degradation or loss of function. It remains the only operational 3-axis electric field experiment in space and is not expected to be duplicated until MMS is launched. With optimal utilization of onboard fuel to minimize the time that the electric field sensors will be shadowed by the spacecraft during the remainder of the mission, EFI will continue to provide high-quality data for topics such as reconnection, electromagnetic energy conversion, plasma entry, convection, auroral particle acceleration, etc.

Hydra status: The Hydra instrument continues to function well, with all but one subsystem functioning. The electron portion of one of the two sensor heads of the Duo-Deca-Electron-Ion Spectrometer (DDEIS) is no longer working. Alternate approaches have been developed to determine the

electron density, temperature anisotropy, and agyrotropy of the electrons despite the failure. The inter-detector gains of the DDEIS are changing with time in an expected way with the large number of total counts these detectors have registered. Relative balancing on these detectors is accomplished by software on the ground. Absolute calibration is assisted by comparison with ion estimates of density and intercomparison with solar wind monitors when we occasionally encounter the solar wind. The Parallel Plate Analyzer (PPA) sensor articulated for high-resolution samples of electrons along the magnetic field direction continues to work well and is cross calibrated with the DDEIS.

TIMAS status: The Toroidal Imaging Mass-Angle Spectrograph (TIMAS) instrument continues to return high-quality 3D resolved data on the energy, mass, pitch angle, and composition of energetic (15 eV < E/q < 25 keV) ions. The sensitivity in the energy range <700 eV, however, was degraded by a discharge event in December 1998. The effective gain of the detector drifted slowly until September 2003 and has remained stable since then. The 3D instrumental angular response was optimized for orbit normal operation. However, data obtained during ecliptic normal observations retain nearly 4π coverage and have only slightly degraded angular resolution compared with orbit-normal operations.

TIDE status: The Thermal Ion Dynamics Experiment (TIDE) continues to return excellent quality data in an energy range (0.3 to 450 eV) that has never before been explored from a high-altitude orbit like that of Polar. It continues to provide observations of the polar wind, auroral ion outflows,

plasmaspheric material, and low-velocity magnetosheath boundary layer and cusp entry plasmas from the solar wind. TIDE lost its mass analysis capability in 1996 owing to loss of secondary electron yield from its carbon start foils, but has since served as a superb automatic aperture electrostatic analyzer for ions. Its detector sensitivity has decayed very slowly over the 9 years since launch. During 2004, a detector gain adjustment restored the TIDE sensitivity to within a factor of 2 of its original value. The plasma source neutralizer has been inoperative, apparently owing to thruster contamination of the cathode, since April 20, 2000, and no additional attempts to operate it are planned. We look forward to continuing TIDE operations through the life of the spacecraft.

CAMMICE status: The Charge and Mass Magnetospheric Ion Composition Experiment (CAMMICE) consists of two sensor systems and two data processing units. The sensors are known as the Magnetospheric Ion Composition Spectrometer (MICS) and the Heavy Ion Telescope (HIT). The HIT is returning valuable data on the energetic total ion intensity. An interface circuit of the MICS sensor failed in 2002, ending its useful contribution to the Polar mission. By instrument command, the telemetry allocated to MICS was reallocated to the HIT sensor.

CEPPAD status: The three Comprehensive Energetic Particle and Pitch Angle Distribution (CEPPAD) sensors and the data processing unit (DPU) continue nominal operation. There is no evidence of degradation that would limit the utility of the CEPPAD data for science. The Imaging Electron Sensor (IES) and High-Sensitivity Telescope (HIST) sensors are behaving as they did at launch; no change in performance has been observed. The Imaging Proton Sensor (IPS) silicon detectors, being openly exposed to the radiation environment, have suffered from radiation damage. The radiation damage increases the noise threshold of the silicon detectors; the DPU is commanded to raise the threshold when noise contaminates the lowest energy channel. The energy threshold has been increased from 18 keV at the time of launch to approximately 50 keV at the present time. The rate of increase has been decreasing as expected. In summary, CEPPAD performs much as it did at launch and can be expected to operate nominally as long as the Polar mission continues.

VIS status: The Visible Imaging System (VIS) continues to acquire images of the aurora, dayglow, and nightglow at an average rate of approximately 1 image/min during the imaging periods of each orbit. To date, the VIS has acquired approximately 3.3 million visible and ultraviolet images. The VIS instrument continues to be healthy with no significant degradation in performance of the visible sensors. The ultraviolet-sensitive VIS Earth Camera has developed a high background noise floor, but continues to produce quality images for scientific analyses. A small decrease in sensitivity of ~10% has occurred over the life of the mission. The VIS is fully capable of continuing in service for the life of the Polar spacecraft.

UVI status: The Ultraviolet Imager (UVI) is stable and fully capable of meeting its scientific mission. The backup detector, activated in December 1996 after the failure of the primary detector, shows no measurable sign of degradation. The only

other failure was the microswitch used to position the filter wheel, which occurred early in the mission, but it has not affected operations because a backup switch was available. A light leak in the back of the housing was detected early in the mission but this is a problem only for short periods twice a year when the Sun is directly behind the UVI housing. In summary, UVI is healthy and obtaining high-quality images.

PIXIE status: The Polar Ionospheric X-ray Imaging Experiment (PIXIE) instrument's capability to distribute collected X-Ray fluxes across the image plane failed in November 2002. PIXIE leaves as its legacy a 6-year database of time-tagged and energy-resolved X-ray counts (2 to 10 keV in 64 channels), localized in the instrument's image plane so as to permit projection back to their source points on the Earth's ionosphere.

PWI status: The Polar Plasma Wave Instrument (PWI) power supply began to exhibit an undervoltage condition on September 16, 1997. This condition was likely caused by an "open" circuit at the power inductor in the power supply. This power supply is the only means of providing power to both of PWI's data processors (low- and high-rate). The low-rate processor requires less power to operate and is able to process Multichannel Analyzer (MCA) and Sweep Frequency Receiver (SFR) data when the power supply voltage is slightly elevated during long periods of extreme cold. These times occur twice per year during the Polar eclipse seasons when the base plate that holds the power supply falls below 20°C.

3.2. Status of the combined Polar-Wind-Geotail ground system

From ISTP to streamlined Polar-Wind-Geotail mission operations: After the 2001 review of operating Sun-Earth Connection (SEC) missions, the International Solar-Terrestrial Program (ISTP), along with its Central Data Handling Facility (CDHF), was discontinued. Polar funding in FY02 was used to develop a low-cost approach to operations and data processing for Polar, Wind, and Geotail. These changes reduced the combined mission operations and data analysis (MO&DA) annual costs for Global Geospace Science (GGS) by about 3.5 million dollars. Wind and Geotail budgets contain only some "incremental support" for the Polar project-funded operations infrastructure.

The ground data processing, command planning, and command management for Polar, Wind, and Geotail were performed in several shared facilities, some of which also supported other missions (SOHO, Cluster, IMP-8, and UARS). The services of the ISTP Science Planning and Operations Facility (SPOF) and Command Management Facility (CMF) were consolidated within the Polar/Wind Mission Operations Center (MOC) with associated reduction in personnel.

Re-hosting and fully automating the data processing and distribution functions previously performed by the CDHF has been fully functional since the CDHF was closed in September 2002, saving an *additional* \$1.2M annually over ISTP/GGS levels. The data processing environment for the Polar, Wind, and Geotail spacecraft is now streamlined onto two

computers (a data server and a data processor with hot spares) and fully automated to eliminate the need for data technicians. The environment is maintained part time by two civil servants at a very low cost. Our “CDHF on a rack” serves all the functions provided by the ISTP system, including the service of near-real-time data streams from Wind and Polar, processing of key parameters, and data distribution through ftp transfers and automatically produced and labeled CDs/DVDs.

An effort to similarly streamline and automate the production of Level-0 data for Wind and Polar is nearly complete. Level-0 data production is already efficient to the point that this task is not expected to yield significant short-term cost savings. However, consolidation of this function within the “CDHF on a rack” will provide the Wind mission with a very compact and cost effective stand-alone data processing system after the end of the Polar mission.

Further cost savings for the Polar, Wind, and Geotail MOC have come from the implementing unattended spacecraft contacts and data playbacks without serious impact on the health and safety of the Polar and Wind spacecraft. Current tended operations are provided 7 days a week with 12 hours per day. Re-engineering is ongoing to achieve further cost reductions by converting to tended operations 5 days a week for 8 hours per day with automated lights-out operations on weekends and nights. Other re-engineering projects in the MOC will provide greater mission operation cost savings in the interest of preserving data analysis funds, including streamlining Deep Space Network (DSN) support costs.

3.3. Data availability

Polar data as a Sun-Solar System Connection data resource: As part of the S³C Great Observatory, the Polar mission’s data policies are predicated on the acquisition of data that is simultaneous, comprehensive, and closely coordinated with the other mission components of the observatory. Polar established an open data policy from the outset as part of ISTP (<http://pwg.gsfc.nasa.gov/rules.html>). At this time we are experiencing unprecedented demand for the Polar data in all forms. Because most of the Polar data are easily accessible online, without the necessity of PI team involvement, it is not easy to monitor the broad range of Polar data users; however, a partial list of scientists and educators that have used the Polar data is included in Appendix C.

The Polar data comprise an extensive set of high-resolution particle and field measurements, covering the full energy and mass ranges of interest, and measured simultaneously with global, multispectral images of the aurora. Polar has one of the most complete sets of instrumentation ever flown as a package and thus represents a unique data source likely to be of value to the S³C science community for the next 1.5 years. The estimated volume of mission data acquired (based on average bits per orbit, an 18-hour orbit, and Level-1 and 2 data products, which are estimated at 20% of the Level-0 volume) to be archived at the NSSDC will be about 3.2 TB over the 11.1-year lifetime of the mission.

Polar end-to-end data flow: The Polar mission maintains a series of World Wide Web pages that provide the latest

information about all aspects of Polar, including the type and accessibility of Polar data. These pages are located at <http://pwg.gsfc.nasa.gov/>.

Data are downlinked three to five times per day using the DSN subnet and forwarded to the MOC, located at Goddard Space Flight Center (GSFC). Once the data from an orbital segment are delivered to the MOC, Level-0 and Level-1 science data processing begin automatically. The resulting products are made available on completion of the processing cycle to anyone via an anonymous ftp site maintained at GSFC. The ftp site is accessible from the Polar web site (URL noted above) or can be accessed directly at <ftp://pwgdata.gsfc.nasa.gov/pub/>. Access is fully open; no accounts, passwords, or registration procedures are required to access the complete set of data products. The products are also immediately forwarded to the NSSDC for permanent archiving and open public distribution via CDAWeb.

In addition, all of the instrument teams have Remote Data Analysis Facilities (RDAFs) and maintain open-access web servers at their institutions, which are used in processing, analyzing, disseminating, and correlating Polar data. Investigators with the appropriate data types routinely generate additional data products that are posted at their web sites.

Browse data products: The ability to quickly survey the vast array of data being generated by each instrument is essential to broader community use of the Polar data set. Level-1 data processing is performed at GSFC and, in select cases, at the instrument RDAFs. Level-1 products include images, spectrograms, and data files of varying resolution referred to as Key Parameter files (KP). All KP data sets are created as Common Data Format (CDF) files using the ISTP Guidelines [Kessel *et al.* 1993,1995] for key parameter data. The Project office, and instrument teams processing Level-1 data, provide the files directly to the NSSDC for distribution by CDAWeb. The site http://pwg.gsfc.nasa.gov/data_products.shtml provides an overview of the Level-1 data products currently available at CDAWeb and elsewhere.

Full science data products: Several forms of calibrated higher-level Polar data products are produced and made available for science analysis. For the most part, binary higher-level data products are also in the ISTP/Common Data Format, although the imaging teams provide single images and movies in the more common JPG and MPG formats. These products are routinely delivered to the NSSDC for long-term archiving and community-wide distribution. They are also available from the individual instrument teams’ web sites. The associated documentation and generation software will be delivered to the NSSDC at end-of-mission for long-term archiving. The site http://pwg.gsfc.nasa.gov/data_products.shtml provides an overview of the higher Level data products currently being archived.

Science analysis tools: Several of the Polar instrument teams have been at the forefront of efforts to provide device-independent data analysis tools. The most well-known and utilized of these is the PAnel Plot COMposer (PAPCO). PAPCO is a free, IDL-based, open-source software package

that allows interactive processing and plotting of data from a variety of instrument sources on the same time base (<http://leadbelly.lanl.gov/ccr/software/papco/papco.html>). There are PAPCO modules for the eight Polar in situ observation instruments. The calibrated data files in each case are available from the instrument web servers and have been archived to the NSSDC for distribution by CDAWeb. Polar teams have exploited the Web and its ability to provide an interface for data analysis that is free of installation procedures.

Polar data availability under limited resources: The Polar Mission Team is making every effort under the limited resources available to maximize the availability of data to the public and science community in useful forms. Due to limitations on staffing and the challenge of processing the high-time-resolution science mode 2 data, some of the Polar investigations have temporarily fallen behind in instrument data processing. These problems have been remedied and the data are being processed at a rate of 2 months of data each calendar month. Processing is expected to be up to date by April 2006. The Polar mission has been approached by virtual observatory proposers for inclusion of the Polar data set and we enthusiastically support these efforts. We look forward to participating in the resident archive activity at the end of the Polar mission. Initial discussions are underway to consider the plan for this participation.

3.4. Polar budget

Polar funding history and the future funding requested in this proposal are consistent with the guidelines given by the former Office of Space Science Mission Extension Paradigm. We request a modest budget over planning guidelines during this final mission extension to continue mission operations for an additional year to March 31, 2007, and to be followed by a year of final data analyses and archiving. This mission extension budget with a projected gradual decreasing level of support for our bare-bones mission and science operations will remain well within the mission extension paradigm.

In evaluating the Polar budget it should be noted that although mission operations are conducted in a shared facility with the Wind spacecraft, and the data processing is performed with equipment and personnel shared with the Wind and Geotail spacecraft, joint cost accounting has not been applied. Rather, the Polar mission bears the majority of the costs for these facilities. The proposed Polar budget covers a disproportionate 58% of the combined Polar, Wind, and Geotail operations and data processing facilities costs. When the Polar mission ends, Wind and Geotail will be required to cover these costs from their respective budgets.

Tables in the budget attachment list the Polar guideline and optimal/requested funding levels following the categories and instructions applicable to this Senior Review. The FY2006-FY2008 “in-guidelines” budget supports a bare-bones mission operation and science operations mission through March 2007 followed by a ramp-down year of data analysis and archiving through March 2008. Compared with the prime mission phase, a significantly higher risk and lower data collection efficiency have been implemented and fewer services are provided to

science investigators (section 3.2). There is minimal support for the science analysis required to understand and maintain optimal performance of the instrumentation.

FY2006–FY2008 Full Cost Guideline and “5-way”

Functional Breakdown: Table I of budget attachment provides Full Cost Guideline. Table II provides Full Cost “5-way” Functional Breakdown, which includes Flight Dynamics Facility (FDF) support, Flight Operations Team (FOT) support, Level-0 (LZ) processing, and MOMS operations contract. FDF, FOT, and LZ support includes 11.9 full-time equivalents (FTEs), the result of staff reductions since FY2003. Staff reductions (13.5 to 11.9 FTEs) are enabled by operations concept changes (re-allocation of duties, cross-training of personnel, utilization of stored commands for tape recorder dumps, more efficient use of stored command tables for instrument commanding, etc.) and implementation of automation. FOT staffing (currently at 12 hours/day for 7 days/week) will transition to 8 hours/day for 5 days/week. This staffing level is the minimum required to ensure the health and safety of the mission assets. Further reductions in science data capture requirements will not impact the staffing level.

FY2006–FY2008 Instrument Team Breakdown: Table III shows the requested Instrument Team Breakdown. Carry-forward from FY2005 is used to offset some instrument team costs in FY2006. In FY2007 the entire costs for the instrument operations are required. Mission Operations costs for the first 6 months of FY2007 are included. This scenario ensures the health and safety of mission assets. Funding to the teams is intended to cover the cost of the facilities, materials, services and personnel required to operate the instruments. This includes commanding the flight hardware and monitoring instrument health; tuning instrument response and processing procedures to accommodate the changing orbit or spacecraft operations; routine processing of data products; maintenance of RDAF and web servers; and, most important, the supply of processed science data, graphics, analyses and interpretation in support of science studies. These activities include the final archiving at the NSSDC. Funding differences between teams reflect special challenges or advantages in their individual environments.

FY2006–FY2008 “5-Way” Breakdown for in-kind

contributions: Table IV provides the in-kind NASA costs. “Space Communications Services” encompasses the cost of DSN support, mission-critical routed data lines, and dedicated voice communications. DSN support costs are based on the User Loading Profile, which is provided by the project to the Deep Space Mission System’s (DSMS) Resource Allocation Planning Group. The costs were provided by JPL and are based on the most recent DSN pricing. “Mission Services” includes hardware maintenance and sustaining engineering services.

FY2006–FY2008 “5-Way” Breakdown for optimal

budget: The Optimal Budget (Table V) for the proposed Polar mission extension is identical to the minimum full cost guidelines budget listed in Table II. The Polar team believes that within the current budget constraints, the minimum mission represents the optimal use of resources to achieve the maximum return.

4. Education and Public Outreach

Building on the foundation of the very successful ISTP E/PO program, the Polar team has continued to commit significant time, energy, and funding (1.2% of total mission budget) into a wide-ranging program. The goal of our program is to excite and inspire the next generation of space explorers and enhance science understanding by creating personal learning experiences for students, educators, and the public. The interaction of Earth's magnetosphere and ionosphere with the Sun and solar wind leads to a wide range of space weather events, such as the aurora, which affect life and society. Thus these subjects can be used to inspire students in science, technology, engineering, and math (STEM).

Linkage to national education standards increases the value of a product to classroom teachers. The Polar mission provides exciting real-world examples for curricula in physical science, Earth and space science, and the history and nature of science, as well as technology, math, and geography. All of our products developed since 2002 directly address education standards. We maximize our nationwide impact through partnerships, with the SOHO project, the SEC Education Forum (SECEF), and the "Living with a Star" (LWS) program. These partnerships help us share resources such as education expertise and funding, create better products and programs based on previous evaluations, utilize proven successful distribution channels, evaluate our projects, and report our work through the Education Program Data Collection and Evaluation System (EDCATS).

Dr. Nicola Fox leads the Polar E/PO program. Ms. Kerri Beisser cultivates opportunities for new partnerships, and Ms. Beth Jacob and Dr. Robert Hoffman lead the effort to produce new E/PO products. All four are exceptionally experienced and committed to NASA E/PO. A number of our instrument teams pursue their own E/PO programs but also contribute concepts and material for Project activities. In addition to these program leaders, a large number of Polar science team members are directly involved in E/PO programs either providing oversight or contributing valuable content.

4.1 Accomplishments

Polar scientists have been enthusiastic participants in a range of formal and informal education programs. We have worked with the Hispanic and African-American communities, Native Americans, professional societies for underserved and underrepresented populations, and rural and inner-city communities.

Earth's Dynamic Space: Solar-Terrestrial Physics & NASA's Polar Mission: The Polar science team created a thorough introduction to geospace physics in the form of a DVD that can be viewed end-to-end or split into individual segments and tailored to lesson plans. This multi-use DVD is intended for audiences ranging from a traditional classroom or after-school club to museums and science centers. The DVD explains subjects such as the aurora, the magnetosphere,

and space weather, while highlighting the ongoing and wide-ranging scope of the Polar science discoveries. This platform introduces the learner to key team members as well as the science principles. Dramatic visualizations are used to illustrate the complex principles that describe Earth's dynamic space. The team poured through existing NASA resources, and created visualizations using Polar data to complement the NASA stock footage, while scientists donated their time to create and review scripts. The DVD was produced by the award-winning audio-visual group at the Johns Hopkins University Applied Physics Laboratory (JHU/APL).

The Polar DVD was featured at the Association of Science and Technology Centers (ASTC) national meeting in September 2004. As a result, we now have a distribution network through ASTC of over 540 science centers in 40 countries. The DVD is also receiving nationwide distribution through the NASA/Jet Propulsion Laboratory SpacePlace network, whose members are non-traditional, rural science centers and libraries that are desperately in need of materials. The DVD also was included in NASA's Sun Earth Day 2005 E/PO program; 10,000 copies were distributed as part of the supporting educational packages; and 2000 copies were used in educator workshops at NASA/GSFC. The DVD was selected by a judging panel to receive an "Award of Distinction" in the "External Communications/Education" category of the Communicator Awards, an international award recognizing noteworthy and highly crafted non-broadcast television programming. The Polar team is delighted with the positive response to the DVD. Through the wide distribution network, it has reached hundreds of thousands of people of all ages.

Sun-Earth Day: This high-leverage program was developed by SECEF, with Polar as a co-leader, to foster sustained partnerships with education communities around the world. Sun-Earth Day focuses on a different topic each year and includes classroom and museum events around the country leading up to live television and web broadcasts. SECEF assembles educator kits with teacher-tested activities, web and print resources connecting real science to national education standards. Polar has supported the annual program with various activities including presentations at the Maryland Science Center (MSC), the Cedar Rapids Science Station in Iowa, and the National Air and Space Museum. *Sun-Earth Day 2003: Live From the Aurora* included a series of live TV interactive experiences for students with Dr. Fox hosting a live show and Polar/VIS providing live auroral images via the website. The Polar-developed flyer *What Causes the Northern Lights?* and the *Aurora* poster (see E/PO Products), along with Polar auroral imagery, went into the 2003 and 2004 educator kits. The Polar DVD was incorporated into the *Sun-Earth Day 2005*



educator kits and featured in the related teacher workshops at NASA/GSFC. Dr. Fox was interviewed live with nationwide news stations in support of the Sun-Earth Day 2005 program.

Other Educator Workshops and Support: The Polar team has presented science content at many educator workshops, including high-profile events at the National Science Teachers Association, National Council of the Teachers of Mathematics, and Maryland State Teachers Association national meetings. Our scientists also gave talks on space weather and aurora at SECEF teacher workshops held at NASA/GSFC. The TIDE team hosts two K-12 teacher workshops each summer at Vanderbilt Dyer Observatory. The topic is solar-terrestrial physics, and 25 teachers participate in each workshop. TIDE team members have made themselves available for long-term support by email and phone to teachers as well as former student interns.

Student Events: Providing students an opportunity to interact directly with a scientist is often the spark that leads to a career in STEM, and the Polar team reaches out to many students. For example, PWI team members give K-16 classroom talks about space physics, life as a space scientist, and a space scientist's role in studying the solar system with robotic spacecraft. TIMAS and CEPPAD team members at the Laboratory for Atmospheric and Space Physics (LASP) have a pooled E/PO effort to support various activities, including several K-12 school trips each year. Polar E/PO materials have been routinely supplied to Dana Middle School, Hawthorne, CA, where CAMMICE team members are involved with the science program. Drs. Fox and Sigwarth presented a high-school student workshop in Baltimore as part of the 2003 Maryland Pre-College Fair held in conjunction with the Black Engineer of the Year awards.

During the two-week Maryland Summer Center for Space Science Education camp for talented 6th and 7th graders run by the Maryland State Department of Education, Dr. Fox introduced students to the excitement of designing their own missions and the opportunities to study space weather.

The TIDE team conducts three 1-week space camps for 5th, 6th, 7th, and 8th graders and has public nights once a month that feature solar-terrestrial topics.

The "Space Academy" series (<http://www.spaceacademy.jhuapl.edu>) – developed by JHU/APL, Comcast Cable, and the Discovery Channel – takes students behind the scenes of actual space missions and introduces them to engineers and

scientists working on some of NASA's most exciting projects. Drs. Fox and Sigwarth hosted a Space Academy on Space Weather, which involved about 100 students from Maryland middle schools. The daylong event included a briefing on the aurora and space weather, a student "press conference," lunch-time discussions with scientists and engineers, tours through "Exploration Stations" including a spacecraft mission control center and satellite communications facility, and science demonstrations.

Museums: Polar has played a leading role in bringing the topics of space weather and the aurora to the informal education community. Our team members provided science content and movies for planetarium shows at the Maryland Science Center (MSC) and the Yamanashi Prefectural Science Center in Japan, and also contributed images, movies, and content to the Space Weather Center exhibit, now showing at the DC Children's museum and the subject of an interactive website.

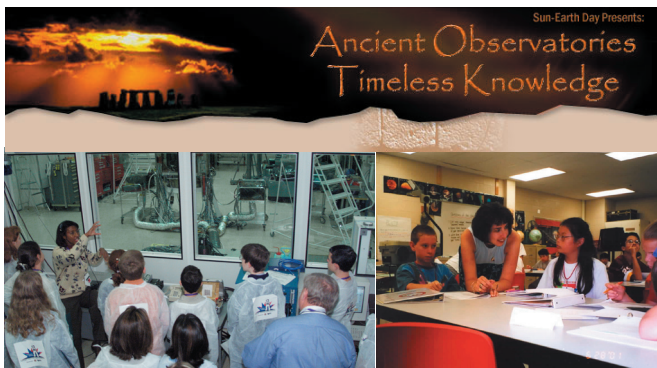
Dr. Fox has participated in "Scientist in Residence" days at MSC's SpaceLink exhibit, answering questions from the public in person. She also hosted MSC's Live from the Sun planetarium show, narrating the live show with taped planetarium segments, and identifying interesting features on observatory Sun images in real time.

4.2. E/PO products

Print products: All of our print products have clear linkage to the Polar science results and were developed with national education standards in mind. They have each been named exemplary NASA OSS E/PO products, having undergone comprehensive evaluation by scientists and educators. As such they are listed in the NASA Space Science Educator Resource Directory (SSERD). In addition to this evaluation, we also field-test our products to ensure that they will prove useful to their intended audience. The popular *Storms from the Sun* poster explores the science of coronal mass ejections and space weather. Spanish-language translations of both the print and online versions of the poster, *Tormentas Solares*, are in wide use by teachers in U.S. Hispanic communities and South and Central America.

The comparable *Aurora* poster tells a more detailed story of the aurora with pictures, history, myths, resources, and a lesson plan that addresses science, math, and geography standards. A companion to the *Aurora* poster, the colorful tri-fold *What Causes the Northern Lights?* covers common questions and myths surrounding the aurora. A second flyer, *What Causes Storms from the Sun?* has recently been released. A third, *Do Killer Electrons Affect You?* is developed and awaits printing.

On The World Wide Web: The *Mission to Geospace* web site, also in the SSERD, continues as a portal for journalists, teachers, and space aficionados to find easy-to-read and engaging materials related to S³C science. The site averages 1000 accesses per day. It contains publicly accessible articles, news releases, and space weather imagery; the images and movies are by far the most popular section. The *Conexión Sol-Tierra* web site, based on *Mission to Geospace*, provides links



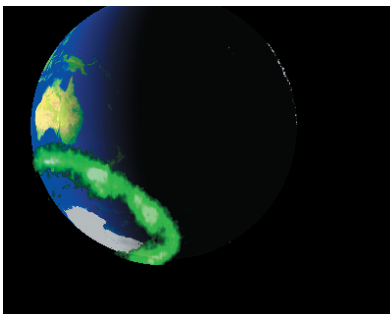
to many Spanish-language Sun-Earth connections resources, including *Tormentas Solares*.

Polar in the Public Eye: *The Press.* The Polar team contributed to the development of a number of press releases in 2003 and 2004. The VIS team provided auroral images for the NASA video feed on the Halloween Storms in October 2003 and also supported a series of three auroral stories: *Auroras Spotted from Space* (http://www.nasa.gov/vision/universe/solarsystem/1121_aurora.html), *An Unusual Light Show* (<http://www.nasa.gov/centers/goddard/solarsystem/aurora110.html>), and *Just in Time for Olympic Lighting, Sun Lights Up the Skies* (http://www.nasa.gov/centers/goddard/earthandsun/olympic_aurora.html).

A Polar-sponsored press release entitled “Solar wind makes waves; killer electrons go surfing?” from September 2003 generated a lot of activity, being picked up at many of the top science news web sites (<http://www.nasa.gov/centers/goddard/news/topstory/2003/0904magwaves.html>).

Print. Members of the Polar team assisted in the production of *What's Out There!*, a guide of 212 seminal astronomical images edited and designed to display the majesty of space phenomena with scientifically sound explanations. Dr. Fox refereed a large section of the book concerning the Earth and Sun and a Polar/VIS image was used in the Earth section to show the aurora at both poles. The book, whose introduction is written by Stephen Hawking, will be published simultaneously in eight languages plus English in October/November 2005. In addition, Polar images were included in a feature “Sun and Aurora” in the July 2004 *National Geographic*. Dr. Fox also provided editorial assistance for this article.

Television. Dr. Fox took part in the NASA SciFiles TV show



The Case of the Technical Knockout, and was featured in a short video submitted to NASA TV on Women’s History Month. Dr. Fox also supported a live shot TV news campaign for the 2005 Sun-Earth Day campaign and was interviewed by 10 TV stations, including Washington, Dallas, Austin, Denver, and Spokane. The Discovery channel recently updated the BBC series *The Planets*. Dr. Fox was interviewed for the program on Earth, and Polar images were used in the series.

Community outreach. Polar scientists took advantage of many opportunities to share with their communities. These activities included presentations at the GSFC Visitor Center, the ICON 29 Science Fiction Convention in Cedar Rapids, the Iowa City Girl Scout Troop, and University of Iowa Hospital and Clinics Child-care Center. At the 2004 Iowa State Fair, the Polar/PWI team supported an exhibit with information on Polar space research projects and student research opportunities in physics and astronomy.

Polar science results have been incorporated into a course on the space environment and its hazards to space systems. The course is jointly sponsored by The Aerospace Institute and the AIAA. The Aerospace Institute provides courses for its staff and the US Air Force in El Segundo, CA, and Chantilly, VA.

4.3. New E/PO efforts

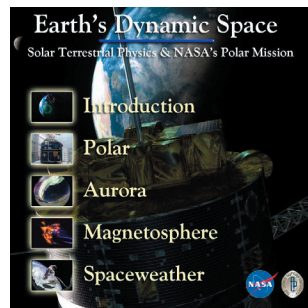
Polar expects to continue pursuing a vigorous and challenging E/PO program. Past activities have shown that we maintain our long-term partnerships and continuously search out new partnerships and opportunities to present exciting S³C science to the public. The team will continue to provide scientist time and E/PO materials for Sun-Earth Day, educator workshops, community and student events, and museums, and will take advantage of other appropriate opportunities as they arise.

Educator Workshops: The Polar Mission E/PO program will participate in the existing space science teacher professional development programs that take place at the Space Sciences Laboratory (SSL) at the University of California in Berkeley (UCB). These workshops are free to educators and teach inquiry-based science with activities about magnetism, the seasons, solar science, and lectures about the Sun and aurora. The workshops take place throughout the year and often coincide with training workshops put on by UCB’s Lawrence Hall of Science (LHS) Great Explorations in Math

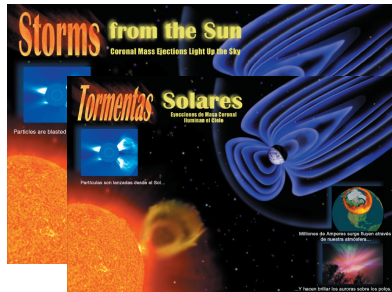


and Science (GEMS) project. Polar will leverage the existing infrastructure of these workshops by helping to support them. These workshops are also funded by other NASA mission E/PO programs, such as THEMIS and STEREO-IMPACT, as well as SECEF (<http://cse.ssl.berkeley.edu/workshops/>).

DVD Website: Following the success of the DVD *Earth's Dynamic Space: Solar-Terrestrial Physics & NASA's Polar Mission*, we are producing a supporting website that will contain further information about each of the science topics covered in the DVD plus teacher and student activities.



Información en Español: With the past successes of the *Tormentas Solares* poster and the *Conexión Sol-Tierra* web site, Polar has taken full advantage of opportunities to translate our E/PO materials into Spanish, reaching a large audience often lacking in good science education materials. Our partnership with the LWS E/PO team is facilitating translation and printing of the *Aurora* poster, as well as the brochures on the northern lights, storms from the Sun, and “killer” electrons. Polar is making all of the Spanish E/PO materials available to the LWS K-14 educator summer workshops at the University of Puerto Rico.



Space Place: We will work with the Space Place program to convert the information in the Polar DVD into the correct format for distribution to their library and small museum display series. Electronic versions of these displays remain on the website indefinitely and have the potential to reach an audience of 27 million, primarily in rural and inner-city locations. We will also pursue converting the DVD content into newspaper columns. Currently the Space Place column is published monthly in seven English-language papers and several Spanish-language papers in major U.S. cities.

Print: Our collaboration with the LWS E/PO office and SECEF allows us to continue development of additional brochures on

topics covering the span of key topics in S³C science. Each will be aligned with national education standards, and they will fill gaps in the developing NASA “Curriculum Quilt” whenever possible. A third in the series of tri-fold flyers has been developed and is awaiting printing. Work has already commenced on two more brochures *How Far Does the Sun Reach?* and *Can You Live Without the Ionosphere?* These new products will join our existing flyers and Aurora poster to be distributed by SECEF at major educator venues.

Polar E/PO at GSFC: To increase the impact of our very limited E/PO funds, we have chosen to partner with other S³C missions at NASA/GSFC—SOHO, RHESSI, Geotail, and Wind – and with the SECEF at Goddard. The upcoming STEREO and SDO missions have agreed to join this partnership as they enter their mission operations and data analysis phases. We plan to develop cross-mission themes and E/PO programs and products from the individual instrument teams. By working across missions, we eliminate duplication of effort, leverage award-winning resources already in operation, and increase the impact of limited E/PO funds for any single mission. In addition, our approach ensures a sustainable E/PO program that emphasizes overall S³C science understanding and how each mission contributes to this integrated picture. In this manner, as older missions retire, new missions (data, science results, and funding) can take their place and add their chapters to the ever-growing story of S³C science.

This consortium of missions will support the SECEF award-winning E/PO programs that meet both science and pedagogy standards and are reviewed by NASA. SECEF will incorporate our mission science results into its larger programs as outlined in Table 4.1.

We will use SECEF’s well-developed network of end users to enhance the reach and impact of these programs. These end users include museums and science centers; national parks; Girl Scouts USA; amateur astronomers (e.g., Astronomical League, AAVSO), and numerous minority and professional groups such as AGU, AAS, La Raza, World Hope, National Society of Black Engineers.

The educational products and programs produced by this consortium will be reviewed annually for scientific accuracy and currency and for pedagogy. This will be done as part of the SECEF annual review process through its membership in the NASA Space Science Education Support Network. We will leverage these existing NASA evaluation programs to ensure that our education products and programs are engaging, effective, and appropriate for the target audiences.

Table 4.1 SECEF incorporates Polar science in its award-winning E/PO programs.

SECEF Program	How it will be used	Impact each year
Sun Earth Day 2006 and beyond	Use mission data to highlight the Sun and eclipses	Tens of millions
Student Observation Network (SON)	Develop learning modules based on mission science	>10,000 students
Space Weather Center	Build a museum kiosk on solar phenomena	>10,000 museum goers >100 teachers in exhibit-based workshops

Appendix A: References

- Albert, J. M., Evaluation of quasi-linear diffusion coefficients for EMIC waves in a multispecies plasma, *J. Geophys. Res.*, 108(A6), 1249, doi:10.1029/2002JA009792, 2003.
- Avanov, L. A. Jr., S. A. Fuselier, and O. L. Vaisberg, High-latitude magnetic reconnection in sub-Alfvénic flow: Interball tail observations on May 29, 1996, *J. Geophys. Res.*, 106(A12), 29491, 10.1029/2000JA000460, 2001.
- Bell, T. F., U. S. Inan, J. Bortnik, and J. D. Scudder, The Landau damping of magnetospherically reflected whistlers within the plasmasphere, *Geophys. Res. Lett.*, 29, 2002.
- Blake, J. B., Comment on “Cusp: A new acceleration region of the magnetosphere” by Jiasheng Chen et al., *Czech. J. Phys.*, 49(4a), 675-677, 1999.
- Blake, J. B., P. L. Slocum, J. E. Mazur, M. D. Looper, R. S. Selesnick, and K. Shiokawa, Geoeffectiveness of shocks in populating the radiation belts, in *Multiscale Coupling of Sun-Earth Processes*, edited by A. T. Y. Lui, Y. Kamide, and G. Consolini, Elsevier BV, p.125, 2005a.
- Blake, J. B., R. Mueller-Mellin, J. A. Davies, X. Li, and D. N. Baker, Global observations of energetic particles around the time of a substorm on 27 August 2001, *J. Geophys. Res.*, in press, 2005b.
- Bortnik, J., U. S. Inan, and T. F. Bell, L-dependence of energetic electron precipitation driven by magnetospherically reflecting whistler waves, *J. Geophys. Res.*, 107, 2002.
- Bortnik, J., U. S. Inan, and T. F. Bell, Energy distribution and lifetime of magnetospherically reflecting whistlers in the plasmasphere, *J. Geophys. Res.*, 108, A5, 11(B99), doi:10.1029/2002JA009316, May 2003a.
- Bortnik, J., U. S. Inan, and T. F. Bell, Frequency-time spectra of magnetospherically reflecting whistlers in the plasmasphere, *J. Geophys. Res.*, 108, A1, 1030, doi:10.1029/2002JA009387, January 2003b.
- Brittnacher, M., M. Wilber, M. Fillingim, D. Chua, G. Parks, J. Spann, and G. Germany, Global auroral response to a solar wind pressure pulse, *Adv. Space Res.*, 25, 1377-1385, 2000.
- Cartwright, M., C. T. Russell, R. Skoug, C. W. Smith, and S. Kanekal, Solar wind control of the compressional fluctuation level in the magnetosphere: How the solar wind controls the radiation belts? *13th Annual GEM Meeting*, Snowmass, CO, June 2004.
- Chandler, M. O., and T. E. Moore, Observations of the geopause at the equatorial magnetopause: Density and temperature, *Geophys. Res. Lett.*, 30(16), 1869, doi:10.1029/2003GL017611, 2003.
- Chang, S.-W., J. D. Scudder, S. A. Fuselier, J. F. Fennell, K. J. Trattner, J. S. Pickett, H. E. Spence, J. D. Menietti, W. K. Peterson, R. P. Lepping, and R. Friedel, Cusp energetic ions: A bow shock source, *Geophys. Res. Lett.*, 25, 3729-3732, 1998.
- Chang, S.-W., J. D. Scudder, K. Kudela, H. E. Spence, J. F. Fennell, R. P. Lepping, R. P. Lin, and C. T. Russell, MeV magnetosheath ions energized at the bow shock, *J. Geophys. Res.*, 106, 19,101-19,115, 2001.
- Chang, S.-W., J. D. Scudder, K. Kudela, H. E. Spence, J. F. Fennell, R. P. Lepping, R. P. Lin, and C. T. Russell, Reply to comment on “MeV magnetosheath ions energized at the bow shock” by J. Chen, T. A. Fritz, and R. B. Sheldon, *J. Geophys. Res.*, 108(A8), 1312, 2003.
- Chen, J., and T. A. Fritz, Correlation of cusp MeV helium with turbulent ULF power spectra and its implications, *Geophys. Res. Lett.*, 25, 4113-4116, 1998.
- Chen, J., and T. A. Fritz, High-altitude cusp: The extremely dynamic region in geospace, *Surveys in Geophysics* (in press), 2005.
- Chen, J., T. A. Fritz, R. B. Sheldon, H. E. Spence, W. N. Spjeldvik, J. F. Fennell, and S. Livi, A new, temporarily confined population in the polar cap during the August 27, 1996 geomagnetic field distortion period, *Geophys. Res. Lett.*, 24, 1447-1450, 1997.
- Chen, J., T. A. Fritz, R. B. Sheldon, H. E. Spence, W. N. Spjeldvik, J. F. Fennell, S. Livi, C. T. Russell, J. S. Pickett, and D. A. Gurnett, Cusp energetic particle events: Implications for a major acceleration region of the magnetosphere, *J. Geophys. Res.*, 103, 69-78, 1998.
- Chen, J., T. A. Fritz, and K. Kudela, Cusp: A new acceleration region of the magnetosphere, *Czech. J. Phys.*, 49(4a), 667-673, 1999.
- Chen, J., T. A. Fritz, and R. B. Sheldon, Comment on “MeV magnetosheath ions energized at the bow shock” by S.-W. Chang et al., *J. Geophys. Res.*, 108(A8), 1311, 2003.
- Chen, L.-J., J. Pickett, J. Franz, P. Kintner, and D. Gurnett, On the Width-Amplitude Inequality of Electron Phase-Space Holes, *J. Geophys. Res.* (in press), June 2005.
- Chen, S.-H., and T. E. Moore, Dayside flow bursts in the Earth’s outer magnetosphere, *J. Geophys. Res.*, 109(A3), A03215, 20, doi: 10.129/2003JA010007, 2004.
- Chi, P. J., and C. T. Russell, Statistical characteristics of the magnetospheric ULF spectrum, presented at *AGU Chapman Conference on Magnetospheric ULF Waves*, San Diego, March 2005.
- Chi, P. J., C. T. Russell, and T. Higuchi, Automatic identification of ULF waves in triaxial magnetic records, *Eos. Trans. AGU*, 84(46), p.F1309, *Fall Meeting Suppl.*, Abstract SM51B-0529, 2003.
- Chua, D., G. Parks, M. Brittnacher, G. Germany, and J. Spann, Auroral substorm timescales: IMF and seasonal variations, *J. Geophys. Res.*, 109, A03207, doi:10.1029/2003JA009951, 2004.
- Cooling, B. M. A., C. J. Owen, and S. J. Schwartz, Role of the magnetosheath flow in determining the motion of open flux tubes, *J. Geophys. Res.*, 106, 18,763, 2001.
- Cowley, S. W. H., and C. J. Owen, A simple illustrative model of open flux tube motion over the dayside magnetopause, *Planet. Space Sci.*, 37, 1461, 1989.
- Crooker, N. U., Dayside merging and cusp geometry, *J. Geophys. Res.*, 84, 951, 1979.

- Crooker, N. U., J. G. Luhmann, J. R. Spreiter, and S. S. Stahara, Magnetopause merging site asymmetries, *J. Geophys. Res.*, *90*, 341, 1985.
- Daughton, W., and H. Karamibadi, Kinetic theory of collisionless tearing at the magnetopause, *J. Geophys. Res.*, A03217, 2005.
- Daughton, W., and J. D. Scudder, Abstract submitted to APS DPP, Boulder, Co, 2005.
- Delcourt, D. C., and J.-A. Sauvaud, Populating of the cusp and boundary layers by energetic (hundreds of keV) equatorial particles, *J. Geophys. Res.*, *104*, 22635, 1999.
- Delcourt, D. C., H. V. Malova, L. M. Zelenyi, J.-A. Sauvaud, T. E. Moore, and M.-C. Fok, Energetic particle injections into the outer cusp during compression events, *Earth Planets Space*, *57*, 125, 2005.
- Dessler, A. J., and R. Karplus, Some effect of the diamagnetic ring currents on Van Allen radiation, *J. Geophys. Res.*, *66*, 2289, 1961.
- Elkington, S. R., M. K. Hudson, and A. A. Chan, Resonant acceleration and diffusion of outer zone electrons in an asymmetric geomagnetic field, *J. Geophys. Res.*, *108*(A3), 1116, doi:10.1029/2001JA009202, 2003.
- Fillingim, M. O., G. K. Parks, H. U. Frey, T. J. Immel, and S. B. Mende, Hemispheric asymmetry of the afternoon electron aurora, *Geophys. Res. Lett.*, *32*, L03113, doi:10.1029/2004GL021635, 2005.
- Fox, N. J., J. B. Sigwarth, R. J. Barnes, G. Chisham, S. W. H. Cowley, L. A. Frank, M. Pinnock, Hemispheric asymmetries in the location and intensity of the auroral ovals and their association with ionospheric convection and IMF, submitted to *J. Geophys. Res.*, 2005.
- Frank, L. A., and J. B. Sigwarth, Findings concerning the positions of substorm onsets with auroral images from the Polar spacecraft, *J. Geophys. Res.*, *105*, 18,919-18,920, 2000a.
- Frank, L. A., and J. B. Sigwarth, Findings concerning the positions of substorm onsets with auroral images from the Polar spacecraft, *J. Geophys. Res.*, *105*, 12,747-12,761, 2000b.
- Frank, L. A., and J. B. Sigwarth, Simultaneous images of the northern and southern auroras from the Polar spacecraft: An auroral substorm, *J. Geophys. Res.*, *108*(A4), 8015, doi:10.1029/2002JA009356, 2003.
- Frank, L. A., W. R. Paterson, J. B. Sigwarth, and S. Kokubun, Observations of magnetic field dipolarization during auroral substorm onset, *J. Geophys. Res.*, *105*, 15,897-15,912, 2000.
- Frank, L. A., J. B. Sigwarth, W. R. Paterson, and S. Kokubun, Two encounters of the substorm onset region with the Geotail spacecraft, *J. Geophys. Res.*, *106*, 5811-5831, 2001a.
- Frank, L. A., W. R. Paterson, J. B. Sigwarth, and T. Mukai, Observations of plasma sheet dynamics earthward of the onset region with the Geotail spacecraft, *J. Geophys. Res.*, *106*, 18,823-18,841, 2001b.
- Frank, L. A., W. R. Paterson, and J. B. Sigwarth, Observations of plasma injection into the ring current during substorm expansive phase, *J. Geophys. Res.*, *107*(A11), 1343, doi:10.1029/2001JA000169, 2002.
- Franz, J. R., P. M. Kintner, J. S. Pickett, and L.-J. Chen, Properties of small amplitude electron phase-space holes observed by Polar, *J. Geophys. Res.* (in press), 2005.
- Fraser, B. J., J. L. Horwitz, J. A. Slavin, Z. C. Dent, and I. R. Mann, Heavy ion mass loading of the geomagnetic field near the plasmopause and ULF wave implications, *Geophys. Res. Lett.*, *32*, L04102, doi:10.1029/2004GL021315, 2005.
- Freeman, J. W., H. K. Hills, T. W. Hill, P. H. Reiff, and D. A. Hardy, Heavy ion circulation in the Earth's magnetosphere, *Geophys. Res. Lett.*, *4*, 195, 1977.
- Frey, H. U., S. B. Mende, C. W. Carlson, J.-C. Gérard, B. Hubert, J. Spann, R. Gladstone, and T. J. Immel, The electron and proton aurora as seen by IMAGE-FUV and FAST, *Geophys. Res. Lett.*, *28*, 1135, 2001.
- Fritz, T. A., and J. Chen, Reply, *Geophys. Res. Lett.*, *26*, 1363-1364, 1999.
- Fritz, T. A., J. Chen, R. B. Sheldon, H. E. Spence, J. F. Fennell, S. Livi, C. T. Russell, and J. S. Pickett, Cusp energetic particle events measured by POLAR spacecraft, *Phys. Chem. Earth (C)*, *24*(1-3), 135-140, 1999.
- Fuselier, S. A., D. M. Klumpar, and E. G. Shelley, Ion reflection and transmissions during reconnection at the Earth's subsolar magnetopause, *Geophys. Res. Lett.*, *18*, 139, 1991.
- Fuselier, S. A., M. Lockwood, T. G. Onsager, and W. K. Peterson, The source population for the cusp and the cleft/LLBL for southward IMF, *Geophys. Res. Lett.*, *12*, 1665, 1999.
- Fuselier, S. A., K. J. Trattner, and S. M. Petrinec, Cusp observations of high- and low-latitude reconnection for northward IMF, *J. Geophys. Res.*, *105*, 253, 2000a.
- Fuselier, S. A., S. M. Petrinec, and K. J. Trattner, Stability of the high-latitude reconnection site for steady northward IMF, *Geophys. Res. Lett.*, *27*, 473, 2000b.
- Fuselier, S. A., S. M. Petrinec, K. J. Trattner, and W. K. Peterson, O⁺ Observations in the cusp: Implications for dayside magnetic field topology, *J. Geophys. Res.*, *106*, 5977, 2001.
- Fuselier, S. A., H. U. Frey, K. J. Trattner, S. B. Mende, and J. L. Burch, Cusp aurora dependence on interplanetary magnetic field Bz, *J. Geophys. Res.*, *107*(A7), doi:10.1029/2001JA900165, 2002.
- Ganushkina, N., T. I. Pulkkinen, M. Kubyshkina, H. Singer, and C. T. Russell, Magnetospheric magnetic field modeling during storms, presented at *EGS-AGU-EUG Joint Assembly*, Nice, France, April 2003.
- Ganushkina, N., Yu. N., T. I. Pulkkinen, M. V. Kubyshkina, M. Ejiri, H. J. Singer, and C. T. Russell, Event-oriented modeling of magnetic fields and currents during storms, in *Adv. Polar Upper Atmos. Res.*, *18*, 105-110, 2004.
- Ge, Y., and C. T. Russell, Mirror mode waves detected by Polar in near-midnight tail, presented at *Joint CEDAR-GEM Workshop*, Santa Fe, NM, June 2005a.
- Ge, Y., and C. T. Russell, Stretching and collapse of the nightside magnetosphere at 9 Re, presented at Spring AGU Meeting, *Eos, Trans. AGU*, *86*(18), *Jt. Assem. Suppl.*, Abstract SM23B-08, JA415, 2005b.

- Ge, Y., C. T. Russell, and T-S. Hsu, Dynamics of the near-Earth tail: Polar, GOES and Cluster coordinated observations, presented at *European Geosciences Union General Assembly*, Vienna, April, 2005.
- Giles, B. L., C. R. Chappell, T. E. Moore, R. H. Comfort, and J. H. Waite Jr., Statistical survey of pitch angle distributions in core (0–50 eV) ions from Dynamics Explorer 1: Outflow in the auroral zone, polar cap, and cusp, *J. Geophys. Res.*, *99*, 17843, 1994.
- Goldstein, J., M. Spasojevic, P. H. Reiff, B. R. Sandel, W. T. Forrester, D. L. Gallagher, and B. W. Reinisch, Identifying the plasmopause in IMAGE EUV data using IMAGE RPI in situ steep density gradients, *J. Geophys. Res.*, *108*(A4), 1147, doi:10.1029/2002JA009475, 2003.
- Gosling, J. T., M. F. Thomsen, S. J. Bame, R. C. Elphic, and C. T. Russell, Plasma flow reversal at the dayside magnetopause and the origin of asymmetric polar cup convection, *J. Geophys. Res.*, *95*, 8073, 1990.
- Gosling, J. T., M. F. Thomsen, S. J. Bame, R. C. Elphic, and C. T. Russell, Observations of reconnection of interplanetary and lobe magnetic field lines at the high-latitude magnetopause, *J. Geophys. Res.*, *96*, 14,097, 1991.
- Green, J., *Testing Relativistic Electron Acceleration Mechanisms*, Ph.D. thesis, UCLA, 2002.
- Green, J. C., and M. G. Kivelson, Relativistic electrons in the outer radiation belt: Differentiating between acceleration mechanisms, *J. Geophys. Res.*, *109*, A03213, doi:10.1029/2003JA010153, 2004.
- Hirahara, M., J. L. Horwitz, T. E. Moore, G. A. Germany, J. F. Spann, W. K. Peterson, E. G. Shelley, M. O. Chandler, B. L. Giles, P. D. Craven, C. J. Pollock, D. A. Gurnett, J. S. Pickett, A. M. Persoon, J. D. Scudder, N. C. Maynard, F. S. Mozer, M. J. Brittner, and T. Nagai, Relationship of topside ionospheric ion outflows to auroral forms and precipitation, plasma waves, and convection observed by Polar, *J. Geophys. Res.*, *103*, 17,391, 1998.
- Horne, R. B., and R. M. Thorne, Potential waves for relativistic electron scattering and stochastic acceleration during magnetic storms, *Geophys. Res. Lett.*, *25*, 3011-3014, 1998.
- Horne R. B., and R. M. Thorne, Relativistic electron acceleration and precipitation during resonant interactions with whistler-mode chorus, *Geophys. Res. Lett.*, *30*(10), 1527, doi:10.1029/2003GL016973, 2003.
- Huddleson, M., C. R. Chappell, D. C. Delcourt, T. E. Moore, B. L. Giles, and M. O. Chandler, Understanding the Earth's ionosphere as a source of magnetospheric plasmas, *J. Geophys. Res.* (in press), 2005.
- Kennel, C. F., and H. E. Petschek, Limit on stably trapped particle fluxes, *J. Geophys. Res.*, *71*, 1, 1966.
- Kessel, M., and R. Candey, Visualization of International Solar-Terrestrial Physics Program (ISTP) data, in *Visualization Techniques in Space and Atmospheric Sciences*, NASA SP-519, December 1995.
- Kessel, R. L., R. E. McGuire, H. K. Hill, N. J. Schofield, Jr., and J. Love, ISTP guidelines for CDF, in *International Solar-Terrestrial Physics (ISTP) Key Parameter Generation Software (KPGS) Standards and Conventions, Version 1.2*, W. H. Mish, NASA, 1993.
- Kessel, R. L., S.-H. Chen, J. L. Green, S. F. Fung, S. A. Boarden, L. C. Tan, T. E. Eastman, J. D. Craven, and L. A. Frank, Evidence of high latitude reconnecting during northward IMF: Hawkeye observations, *Geophys. Res. Lett.*, *23*, 583, 1996.
- Kim, H.-J., and A. A. Chan, Fully adiabatic changes in storm time relativistic electron fluxes, *J. Geophys. Res.*, *102*(A10), 22,107-22,116, doi:10.1029/97JA01814, 1997.
- Koskinen, H. E. J., and A. M. Mälkki, Auroral weak double layers: A critical assessment, in *Auroral Plasma Dynamics*, edited by R. Lysak, AGU Monograph 80, p. 97, 1993.
- Lauben, D. S., et al., VLF chorus emissions observed by Polar during the January 10, 1997 magnetic storm, *Geophys. Res. Lett.*, *25*, 2995-2998, 1998.
- Lauben, D. S., U. S. Inan, and T. F. Bell, Precipitation of radiation belt electrons induced by obliquely propagating lightning-generated whistlers, *J. Geophys. Res.*, *106*, 29,745-29,770, 2001.
- Le, G., and C. T. Russell, Initial Polar magnetic field experiment observations of the low-altitude polar magnetosphere: Monitoring the ring current with polar orbiting spacecraft, *J. Geophys. Res.*, *103*, 17,345, 1998.
- Le, G., C. T. Russell, and K. Takahashi, Morphology of the ring current derived from magnetic field observations, *Ann. Geophys.*, *22*, 1267-1295, 2004.
- LeDocq, M. J., D. A. Gurnett, and G. B. Hospodarsky, *Geophys. Res. Lett.*, *25*, 4063-4066, 1998.
- Lennartsson, O. W., W. K. Peterson, and H. L. Collin, Solar wind control of Earth's H⁺ and O⁺ outflow rates in the 15-eV to 33-keV energy range, *J. Geophys. Res.*, *109*(A12), A12212 doi:10.1029/2004JA010690, 366, 2004.
- Liemohn, M. W., T. E. Moore, P. D. Craven, W. Maddox, A. F. Nagy, and J. U. Kozyra, Occurrence statistics of cold streaming ions in the near-Earth magnetotail: Survey of Polar-TIDE observations, *J. Geophys. Res.*, *110*, A07211, doi:10.1029/2004JA010801, 2005.
- Liou, K., C.-I Meng, T. Y. Lui, P. T. Newell, M. Brittner, G. D. Reeves, R. R. Anderson, and K. Yumoto, On relative timing in substorm onsets, *J. Geophys. Res.*, *104*, 22,807-22,817, 1999.
- Liou, K., C.-I Meng, P. T. Newell, K. Takahashi, S.-I. Ohtani, A. T. Y. Lui, M. Brittner, and G. Parks, Evaluation of low-latitude Pi2 pulsations as indicators of substorm onset using Polar ultraviolet imagery, *J. Geophys. Res.*, *105*, 2495-2505, 2000a.
- Liou, K., C.-I Meng, A. T. Y. Lui, P. T. Newell, and R. R. Anderson, Auroral kilometer radiation at substorm onset, *J. Geophys. Res.*, *105*, 25325-25331, 2000b.
- Liou, K., C.-I Meng, A. T. Y. Lui, P. T. Newell, and S. Wing, Magnetic dipolarization with substorm expansion onset, *J. Geophys. Res.*, *107*, 1131, doi:10.1029/2001JA000179, 2002.
- Liou, K., J., P. T. Newell, C.-I Meng, C.-C. Wu, and R. P. Lepping, Investigation of external triggering of substorms with

- Polar ultraviolet imager observations, *J. Geophys. Res.*, *107.*, doi:10.1029/2003JA009984, 2003.
- Liou, K., P. T. Newell, C.-I. Meng, C.-C. Wu, and R. P. Lepping, On the relationship between shock-induced polar magnetic bays and solar wind parameters, *J. Geophys. Res.*, *108.*, doi:10.1029/2004JA010400, 2004.
- Liu, W., G. Rostocker, and D. Baker, Internal acceleration of relativistic electrons by large amplitude ULF pulsations, *J. Geophys. Res.*, *104*, 17,391, 1999.
- Lockwood, M., and M. F. Smith, The variation of reconnection rate at the dayside magnetopause and cusp ion precipitation, *J. Geophys. Res.*, *97*, 14,841, 1992.
- Lockwood, M., and M. F. Smith, Low- and mid-altitude cusp particle signatures for general magnetopause reconnection rate variations, 1, Theory, *J. Geophys. Res.*, *99*, 8531, 1994.
- Lockwood, M., C. J. Davis, M. F. Smith, T. G. Onsager, and W. F. Denig, Location and characteristics of the reconnection X-line deduced from low-altitude satellite and ground-based observations, Defense Meteorological Satellite Program and European Incoherent Scatter data, *J. Geophys. Res.*, *100*, 21,803, 1995.
- Lockwood, M., C. J. Davis, T. G. Onsager, and J. D. Scudder, Modelling signatures of pulsed magnetopause reconnection in cusp ion dispersion signatures seen at middle altitudes, *Geophys. Res. Lett.*, *25*, 591, 1998.
- Lorentzen, K. R., M. D. Loper, and J. B. Blake, Relativistic electron microbursts during the GEM storms, *Geophys. Res. Lett.*, *28*(13), 2573-2576, 2001.
- Maynard, N. C., D. M. Ober, W. J. Burke, J. D. Scudder, M. Lester, M. Dunlop, J. A. Wild, A. Grocott, C. J. Farrugia, E. J. Lund, C. T. Russell, D. R. Weimer, K. D. Siebert, A. Balogh, M. Andre, and H. Reme, Polar, Cluster and SuperDARN evidence for high latitude merging during southward IMF: Temporal/spatial evolution, *Annales Geophys.*, *21*, 2233-2258, 2003.
- Maynard, N. C., J. Moen, W. J. Burke, M. Lester, D. M. Ober, J. D. Scudder, K. D. Siebert, D. R. Weimer, C. T. Russell, and A. Balogh, Temporal-spatial structure of magnetic merging at the magnetopause inferred from 557.7-nm all-sky images, *Annales Geophysicae*, *22*, 2917-2942, 2004.
- Maynard, N. C., W. J. Burke, J. D. Scudder, D. M. Ober, D. R. Weimer, K. D. Siebert, C. T. Russell, M. Lester, F. S. Mozer, and N. Sato, Electron signatures of active merging sites on the magnetopause, *J. Geophys. Res.* (in press), 2005.
- Menietti, J. D., O. Santolik, J. S. Pickett, and D. A. Gurnett, High resolution observations of continuum radiation, *Planet. Space Sci.*, *53*, 283-290, 2005a.
- Menietti, J. D., R. L. Mutel, O. Santolik, J. D. Scudder, I. W. Christopher, and J. Cook, Striated drifting AKR bursts II: Possible stimulation by upward traveling EMIC Waves, submitted to *J. Geophys. Res.*, 2005b.
- Meredith, N. P., R. B. Horne, R. H. A. Illes, R. M. Thorne, D. Heynderickx, and R. R. Anderson, Outer zone relativistic electron acceleration associated with substorm-enhanced whistler mode chorus, *J. Geophys. Res.*, *107*(A7), 1144, doi:10.1029/2001JA900146, 2002.
- Moore, T. E., W. K. Peterson, C. T. Russell, M. O. Chandler, M. R. Collier, H. L. Collin, P. D. Craven, R. Fitzenreiter, B. L. Giles, and C. J. Pollock, Ionospheric mass ejection in response to a CME, *Geophys. Res. Lett.*, *26*(15), 2339, 1999.
- Moore, T. E., M.-C. Fok, M. O. Chandler, S.-H. Chen, S. P. Christon, D. C. Delcourt, J. A. Fedder, M. W. Liemohn, W. K. Peterson, and S. Slinker, Ionospheric plasmas in the ring current, *Yosemite 2004 Monograph* (in press), May 2005.
- Mozer, F. S., ISEE-1 observations of electrostatic shocks on auroral zone field lines between 2.5 and 7 Earth radii, *Geophys. Res. Lett.*, *8*, 823, 1981.
- Mozer, F. S., S. D. Bale, and T. D. Phan, Evidence of diffusion regions at a subsolar magnetopause crossing, *Phys. Rev. Lett.*, *89*(1), 015002-1-4, 2002.
- Mozer, F. S., S. D. Bale, T. D. Phan, and J. A. Osborne, Observations of electron diffusion regions at the subsolar magnetopause, *Phys. Rev. Lett.*, *91*, 245002, 2003.
- Mozer, F. S., S. D. Bale, and J. D. Scudder, Large amplitude, extremely rapid, predominately perpendicular electric field structures at the magnetopause, *Geophys. Res. Lett.*, *31*, L15802, doi:10.1029/2004GL020062, 2004.
- Nosé, M., S. Taguchi, K. Hosokawa, S. P. Christon, R. W. McEntire, T. E. Moore, and M. R. Collier, Overwhelming O⁺ contribution to the plasma sheet energy density during the October 2003 superstorm: Geotail/EPIC and IMAGE/LENA observations, *J. Geophys. Res.* (in press), 2005.
- O'Brien, T. P., M. D. Looper, and J. B. Blake, Quantification of relativistic electron microburst losses during the GEM storms, *Geophys. Res. Lett.*, *31*, L04802, doi:10.1029/2003GL018621, 2004.
- Ober, D. M., N. C. Maynard, W. J. Burke, W. K. Peterson, J. B. Sigwarth, L. A. Frank, J. D. Scudder, W. J. Hughes, and C. T. Russell, Electrodynamics of the poleward auroral border observed by Polar during a substorm on April 22, 1998, *J. Geophys. Res.*, *106*, 5927-5943, 2001.
- Onsager, T. G., M. F. Thomsen, R. C. Elphic, and J. T. Gosling, Model of electron and ion distributions in the plasma sheet boundary layer, *J. Geophys. Res.*, *96*, 20,999, 1991.
- Onsager, T. G., J. D. Scudder, M. Lockwood, and C. T. Russell, Reconnection at the high-latitude magnetopause during northward interplanetary magnetic field conditions, *J. Geophys. Res.*, *106*(A11), 25467-25488, doi:10.1029/2000JA000444, 2001.
- Østgaard, N., S. B. Mende, H. U. Frey, T. J. Immel, L. A. Frank, J. B. Sigwarth, and T. J. Stubbs, Interplanetary magnetic field control of the location of substorm onset and auroral features in the conjugate hemispheres, *J. Geophys. Res.*, *109*, AO7204, doi:10.1029/2003JA010370, 2004.
- Østgaard, N., N. A. Tsyganenko, S. B. Mende, H. U. Frey, T. J. Immel, M. Fillingim, L. A. Frank, and J. B. Sigwarth, Observations and model predictions of substorm auroral asymmetries in the conjugate hemispheres, *Geophys. Res. Lett.*, *32*, L05111, doi:10.1029/2004GL022166, 2005.
- Paschmann, G., S. Haaland, and R. Treumann (eds.), Auroral plasma physics, *Space Sci. Rev.*, *103*, 1-475, 2002.

- Petrinec, S. M., K. J. Trattner, and S. A. Fuselier, Steady reconnection during intervals of northward IMF – implications for magnetospheric properties, *J. Geophys. Res.*, *108*(A12), 1458, doi:10.1029/2003JA009979, 2003.
- Phan, T.-D., G. Paschmann, and B. U. Ö. Sonnerup, Low latitude dayside magnetopause and boundary layer for high magnetic shear 2. Occurrence of magnetic reconnection, *J. Geophys. Res.*, *101*, 7817, 1996.
- Pritchett, P. L., Externally driven magnetic reconnection in the presence of a normal magnetic field, *J. Geophys. Res.*, *110*, A05209, doi:10.1029/2004JA010948, 2005.
- Reeves, G. D., K. L. McAdams, R. H. W. Friedel, and T. P. O'Brien, Acceleration and loss of relativistic electrons during geomagnetic storms, *Geophys. Res. Lett.*, *30*(10), 1529, doi:10.1029/2002GL016513, 2003.
- Reiff, P. H., G. Lu, J. L. Burch, J. D. Winningham, L. A. Frank, J. D. Craven, W. K. Peterson, and R. A. Heelis, On the high- and low-altitude limits of the auroral electric field region, in *Auroral Plasma Dynamics*, AGU Monograph 80, edited by R. L. Lysak, p. 143, 1993.
- Russell, C. T., J. A. Fedder, S. P. Slinker, X.-W. Zhou, G. Le, J. G. Luhmann, F. R. Fenrich, M. O. Chandler, T. E. Moore, and S. A. Fuselier, Entry of the POLAR spacecraft into the polar cusp under northward IMF conditions, *Geophys. Res. Lett.*, *25*, 3015-3018, 1998.
- Russell, C. T., G. Delory, M. Dougherty, D. Lario, J. G. Luhmann, R. Skoug, and C. W. Smith, Heliospheric response to the solar events of October and November, 2003, presented at the *EGU First General Assembly*, Nice, France, April 2004.
- Scudder, J. D., F. S. Mozer, N. C. Maynard, and C. T. Russell, Fingerprints of collisionless reconnection at the separator: I. Ambipolar-Hall signatures, *J. Geophys. Res.*, *107*(A10), SMP 13-1: SMP 13-38, doi:10.1029/2001JA000126, 2002.
- Scudder, J. D., Z. W. Ma, and F. S. Mozer, Debye length structures in Earth's reconnection layer: Observations and simulations, to be submitted, *Phys. Plasmas*, 2005
- Scudder, J. D., and F. S. Mozer, Electron demagnetization and collisionless magnetic reconnection in $\beta_e = 1$ plasmas, *Phys. Plasmas* (in press), 2005.
- Scudder, J. D., and W. Daughton, Abstract APS DPP, Boulder, CO, October 2005.
- Sheldon, R. B., H. E. Spence, J. D. Sullivan, T. A. Fritz, and J. Chen, The discovery of trapped energetic electrons in the outer cusp, *Geophys. Res. Lett.*, *25*, 1825-1828, 1998.
- Sheldon, R. B., J. Chen, and T. A. Fritz, Comment on "Origins of energetic ions in the cusp" by K. J. Trattner et al., *J. Geophys. Res.*, *108*(A7), 1302, 2003.
- Shelley, E. G., and H. L. Collin, Auroral ion acceleration and its relationship to ion composition, in *Auroral Physics*, edited by C.-I. Meng, M. J. Rycroft, and L. A. Frank, Cambridge University Press, 1991.
- Sigwarth, J. B., N. J. Fox, and L. A. Frank, Global auroral response to dynamic pressure impulses in the solar wind, submitted to *J. Geophys. Res.*, 2005a.
- Sigwarth, J. B., G. Crowley, J. C. Foster, and N. J. Fox, Global observations of O/N₂ in Earth's thermosphere during Sun-Earth storms, submitted to *J. Geophys. Res.*, 2005b.
- Siscoe G., J. Raeder, and A. J. Ridley, Transpolar potential saturation models compared, *J. Geophys. Res.*, *109*, A09203, doi:10.1029/2003JA010318, 2004.
- Sonnerup, B. U. Ö., G. Paschmann, I. Papamastorakis, N. Sckopke, G. Haerendel, S. J. Bame, J. R. Asbridge, J. T. Gosling, and C. T. Russell, Evidence for magnetic field reconnection at the Earth's magnetopause, *J. Geophys. Res.*, *86*, 10049, 1981.
- Spann, J. F., M. Brittnacher, R. Elsen, G. A. Germany, and G. K. Parks, Initial response and complex polar cap structures of the aurora in response to the January 10, 1997 magnetic cloud, *Geophys. Res. Lett.*, *25*, 2577-2580, 1998.
- Stenbaek-Nielsen, H. C., T. J. Hallinan, D. L. Osborne, J. Kimball, C. Chaston, J. McFadden, G. Delory, M. Temerin, and C. W. Carlson, Aircraft observations conjugate to FAST: Auroral arc thicknesses, *Geophys. Res. Lett.*, *25*(12), 2073-2076, doi:10.1029/98GL01058, 1998.
- Stevenson, B. A., J. L. Horwitz, G. Germany, T. E. Moore, B. L. Giles, P. D. Craven, M. O. Chandler, Y.-J. Su, and G. K. Parks, Polar observations of topside field-aligned O⁺ flows and auroral forms, *J. Geophys. Res.*, *106*, 18,969-18,979, 2001.
- Strangeway, R. J., R. E. Ergun, Y.-J. Su, C. W. Carlson, R. C. Elphic, Factors controlling ionospheric outflows as observed at intermediate altitudes, *J. Geophys. Res.*, *110*, doi:10.1029/2004JA010829, 2005.
- Stubbs, T. J., R. R. Vondrak, N. Østgaard, J. B. Sigwarth, and L. A. Frank, Simultaneous observations of the auroral ovals in both hemispheres under varying conditions, *Geophys. Res. Lett.*, *32*, L03103, doi:10.1029/2004GL021199, 2005.
- Summers, D., and C.-Y. Ma, A model for generating relativistic electrons in the Earth's inner magnetosphere based on gyroresonant wave-particle interactions, *J. Geophys. Res.*, *105*, A2, 2625-2639, 2000.
- Summers, D., and R. M. Thorne, Relativistic electron pitch-angle scattering by electromagnetic ion cyclotron waves during geomagnetic storms, *J. Geophys. Res.*, *108*(A4), 1143, doi:10.1029/2002JA009489, 2003.
- Summers, D., R. M. Thorne, and F. Xiao, Relativistic theory of wave particle resonant diffusion with application to electron acceleration in the magnetosphere, *J. Geophys. Res.*, *103*, 20,487, 1998.
- Taylor, M. G. G. T., R. H. W. Friedel, G. D. Reeves, M. W. Dunlop, T. A. Fritz, P. W. Daly, and A. Balogh, Multi-satellite measurements of electron phase space density gradients in the Earth's magnetotail, *J. Geophys. Res.*, *109*, A05220, doi:10.1029/2003JA010294., 2004.
- Thorne, R. M., T. P. O'Brien, Y. Y. Shprits, D. Summers, and R. B. Horne, Timescale for MeV electron microburst loss during geomagnetic storms, *J. Geophys. Res.* (in press), 2005.
- Topliss, S. M., C. J. Owen, and W. K. Peterson, A simple model of complex cusp ion dispersions during prolonged

- intervals of northward interplanetary magnetic field, *Geophys. Res. Lett.*, *27*, 3587, 2000.
- Trattner, K. J., S. A. Fuselier, W. K. Peterson, and S.-W. Chang, Comment on "Correlation of cusp MeV helium with turbulent ULF power spectra and its implications" by J. Chen and T. A. Fritz, *Geophys. Res. Lett.*, *26*, 1361-1364, 1999.
- Trattner, K. J., S. A. Fuselier, W. K. Peterson, S.-W. Chang, R. Friedel, and M. R. Aellig, Origins of energetic ions in the cusp, *J. Geophys. Res.*, *106*, 5967-5976, 2001.
- Trattner, K. J., S. A. Fuselier, W. K. Peterson, M. Boehm, D. Klumpar, C. W. Carlson, and T. K. Yeoman, Temporal versus spatial interpretation of cusp ion structures observed by two spacecraft, *J. Geophys. Res.*, *107*(A10), 1287, doi:10.1029/2001JA000181, 2002a.
- Trattner, K. J., S. A. Fuselier, W. K. Peterson, and C. W. Carlson, Spatial features observed in the cusp under steady solar wind conditions, *J. Geophys. Res.*, *107*(A10), 1288, doi:10.1029/2001JA000262, 2002b.
- Trattner, K. J., S. A. Fuselier, W. K. Peterson, S.-W. Chang, R. Friedel, and M. R. Aellig, Reply to comment on "Origins of energetic ions in the cusp" by R. Sheldon, J. Chen, and T. A. Fritz *J. Geophys. Res.*, *108*(A7), 1303, 2003.
- Trattner, K. J., S. A. Fuselier, and S. M. Petrinec, The location of the reconnection line for northward IMF, *J. Geophys. Res.*, *109*(A03219), doi:10.1029/2003JA009975, 2004a.
- Trattner, K. J., S. A. Fuselier, S. M. Petrinec, and W. K. Peterson, Tracing the location of the reconnection site from the northern and southern cusps, *AGU Fall Meeting*, San Francisco, USA, 2004b.
- Trattner, K. J., S. A. Fuselier, S. M. Petrinec, T. K. Yeoman, C. Mouikis, H. Kucharek, and H. Reme, The reconnection sites of spatial cusp structures, *J. Geophys. Res.*, *110*, A04207, doi:10.1029/2004JA010722, 2005.
- Tsyganenko, N. A., Modeling the Earth's magnetospheric magnetic field confined within a realistic magnetopause, *J. Geophys. Res.*, *100*, 5599, 1995.
- Tu, J., J. L. Horwitz, and T. E. Moore, Simulating the cleft ion fountain at Polar perigee altitudes, *J. Atmos. Solar-Terr. Phys.*, *67*, 465, 2005.
- Walt, M., Scattering of trapped electrons by VLF waves during a magnetic storm, *AGU Fall Meeting*, San Francisco, USA, 2004.
- Walt, M., and H. D. Voss, Losses of ring current ions by strong pitch angle scattering, *Geophys. Res. Lett.*, *28*, 3839, 2001.
- Walt, M., and H. D. Voss, Proton precipitation during magnetic storms in August through November 1998, *J. Geophys. Res.*, *109*, A02201, doi:10.1029/2003JA010083, 2004.
- Wilson, G. R., D. M. Ober, G. Germany, and E. J. Lund, The relationship between suprathermal outflowing ions and auroral electron energy deposition: Polar/UVI and FAST/TEAMS, *J. Geophys. Res.*, *106*(A9), 18,981-18,993, 2001.
- Wilson, G. R., D. M. Ober, G. A. Germany, and E. J. Lund, Nightside auroral zone and polar cap ion outflow as a function of substorm size and phase, *J. Geophys. Res.*, *109*, doi:10.1029/2003JA009835, A02206, 2004.
- Wu, C.-C., K. Liou, R. P. Lepping, and C.-I. Meng, *J. Atmos. Terr. Phys.*, *66*(2), 125-132, 2004.
- Wygant, J. R., A. Keiling, C. A. Cattell, M. Johnson, R. L. Ly-sak, M. Temerin, F. S. Mozer, C. A. Kletzing, J. D. Scudder, W. Peterson, C. T. Russell, G. Parks, M. Brittnacher, G. Germany, and J. Spann, Polar spacecraft based comparisons of intense electric fields and Poynting flux near and within the plasmashet-tail lobe boundary to UVI images: An energy source for the aurora, *J. Geophys. Res.*, *105*, 18,675, 2000.
- Yau, A. W., E. G. Shelley, W. K. Peterson, and L. Lenchysyn, Energetic auroral and polar ion outflow at DE 1 altitudes: Magnitude, composition, magnetic activity dependence and longterm variations, *J. Geophys. Res.*, *90*, 8417, 1985.
- Zheng, Y., T. E. Moore, F. S. Mozer, C. T. Russell, and R. J. Strangeway, Polar study of ionospheric ion outflow versus energy input, *J. Geophys. Res.*, *110*, A07210, doi:10.1029/2004JA010995, 2005
- Zhou, X., and B. T. Tsurutani, Rapid intensification and propagation of the dayside aurora: large scale interplanetary pressure pulses (fast shocks), *Geophys. Res. Lett.*, *26*, 1097, 1999.
- Zhou, X. W., et al., Solar wind control of the polar cusp at high altitude, *J. Geophys. Res.*, *A1*, 245, 2000.

Appendix B: Acronym List

2D	Two Dimensional	FUV	Far Ultra-Violet
3D	Three Dimensional	GEMS	Great Explorations in Math and Science
ACE	Advanced Composition Explorer	GEO	Geosynchronous Orbit
AGU	American Geophysical Union	GGS	Global Geospace Science
AIAA	American Institute of Aeronautics and Astronautics	GOES	Geostationary Operational Environment Satellite
AKR	Auroral Kilometric Radiation	GPS	Global Positioning System
ASTC	Association of Science and Technology Centers	GSFC	Goddard Space Flight Center
Bz	North-South oriented magnetic field	GUVI	Global Ultra-Violet Imager
CAMMICE	Charge and Mass Magnetospheric Ion Composition Experiment (Polar experiment)	H	Home
CD	Compact Disk	HEO	Highly-Elliptical Orbit
CDAWeb	Coordinated Data Analysis Web (NSSDC)	HIST	High Sensitivity Telescope (part of Polar/CEPPAD)
CDHF	Central Data Handling Facility (part of ISTP)	HIT	Heavy Ion Telescope (part of Polar/CAMMICE)
CDF	Common Data Format	Hydra	not an acronym –Polar’s 3D electron and ion hot plasma instrument
CEP	Cusp Energetic Particle	IMAGE	Imager for Magnetopause to Auroral Global Exploration
CEPPAD	Comprehensive Energetic Particle Pitch-angle Distribution (Polar experiment)	IMF	Interplanetary Magnetic Field
CME	Coronal Mass Ejection	IMP	Interplanetary Monitoring Platform
CMF	Command Management Facility	IMPACT	In-situ Measurements of Particles And CME Transients
DDEIS	Duo-Deca-Electron-Ion-Spectrometer (Polar/Hydra)	ISTP	International Solar-Terrestrial Physics program
DEFE	Demagnetizing Electric Field Enhancements	J	Journey
DMSP	Defense Meteorological Satellites Program	JHU/APL	Johns Hopkins University/Applied Physics Laboratory
DPU	Data Processing Unit	JPG	Joint Photographic Experts Group (file standard)
DSN	Deep Space Network	JPL	Jet Propulsion Laboratory
Dst	Disturbance Storm Time Index	keV	kilo electron volt (unit of measure)
DVD	Digital Versatile Disk	KP	Key Parameter
EDCATS	Education Program Data Collection and Evaluation System (NASA’s E/PO reporting database)	L	L-shell (nominally the McIlwain L-shell)
EFE	Electric Field Enhancement	LANL	Los Alamos National Laboratory
EFI	Electric Field Instrument (on Polar)	LASP	Laboratory for Atmospheric and Space Physics
EM	Electromagnetic	LWS	Living With a Star
EMIC	Electromagnetic ion cyclotron	MCA	Multi-Channel Analyzer
ENA	Energetic Neutral Atom	MEO	Middle Earth Orbit
EP	Energetic Particle	MeV	Mega electron volt (unit of measure)
E/PO	Education and Public Outreach	MFE	Magnetic Field Experiment
ESA	Electro-Static Analyzer	MHD	Magneto Hydro Dynamics
EUV	Extreme Ultra-Violet	MI	Magnetosphere-Ionosphere
F	Frontier	MICS	Magnetospheric Ion Composition Sensor (part of Polar/CAMMICE)
FAST	Fast Auroral Snapshot Explorer	MLT	Magnetic Local Time
FDF	Flight Dynamics Facility	MMS	Magnetosphere Multiscale (a SEC STP mission)
FOT	Flight Operations Team	MO&DA	Mission Operations and Data Analysis
FTP	File Transfer Protocol	MOC	Mission Operations Center

MOMS	Mission Operations and Mission Services	SOHO	Solar and Heliospheric Observatory
MPG/MPEG	Moving Pictures Experts Group (file standard)	SPOF	Science Planning Operations Facility
MSC	Maryland Science Center	SSERD	Space Science Education Resource Director
NASA	National Aeronautics and Space Administration	ST5	Space Test 5
NSSDC	National Space Science Data Center	STEM	Science, Technology, Engineering and Math
OPEN	Origins of Plasmas in the Earth's Neighborhood	STEREO	Solar TERrestrial RELations Observatory
OSS	Office of Space Science	STP	Solar Terrestrial Probes
PAPCO	Panel Plot Composer	SuperDARN	Super Dual Auroral Radar Network
PI	Principal Investigation	THEMIS	Time History of Events and Macroscale Interactions during Substorms
PIC	Particle In Code	TIDE	Thermal Ion Dynamics Experiment
PIXIE	Polar Ionospheric X-ray Imaging Experiment	TIMAS	Toroidal Imaging Mass-Angle Spectrograph (Polar)
PWI	Plasma Wave Experiment	TIMED	Thermosphere, Ionosphere, Mesosphere, Energetics and Dynamics (a SEC STP mission)
RDAF	Remote Data Analysis Facility	TRACE	Transition Region and Coronal Explorer
R _E	Earth Radius (unit of measure)	TV	Television
RHESSI	Reuven Ramaty High Energy Solar Spectroscopic Imager	TWINS	Two Wide-Angle Imaging Neutral-Atom Spectrometers
S ³ C	Sun Solar System Connection	UARS	Upper Atmospheric Research Satellite
SAMPEX	Solar Anomalous and Magnetospheric Particle Explorer	ULF	Ultra-Low frequency (waves)
SEC	Sun Earth Connections	URL	Uniform Resource Locator
SECEF	Sun Earth Connections Education Forum	UV	Ultraviolet
SEPS	Source/Loss-Cone Energetic Particle Spectrometer (on Polar)	UVI	Ultraviolet Imager
SFR	Sweep-Frequency Receiver	VIS	Visible Imaging System
SMD	Science Mission Directorate	VLF	Very low frequency (waves)
SODA	Space Operations Directive Agreement		

Appendix C: Users of Polar Data

At this time we are experiencing unprecedented demand for the Polar data from all instruments. The majority of the data users download the necessary data directly from either NSSDC or the individual team websites. Since most of the Polar data are easily accessible online, without the necessity of PI team involvement, it is not easy to monitor the broad range of Polar data users. The list here represents a partial record of scientists and educators that have used the Polar data since launch. The affiliations quoted are either the current or last known address.

Adrian, M.	NASA/Goddard Space Flight Center, Greenbelt, MD	Burke, W.	Air Force Research Laboratory, Hansom, MD
Aikio, A.	University of Oulu, Finland	Cairns, I.	University of Sydney, Australia
Alothman, M.	University of Bahrain, Bahrain	Campbell, W.	University of Colorado, Boulder, CO
Andersen, C.	University of Alaska, Fairbanks, AK	Cao, X.	The University of Iowa, Iowa City, IA
Anderson, R.	The University of Iowa, Iowa City, IA	Carlowicz, M.	Woods Hole Oceanographic Institute, Woods Hole, MA
Anderson, P.	University of Texas, Dallas, TX	Cartwright, M.	University of California, Los Angeles, CA
Angelopoulos, V.	Space Sciences Laboratory, University of California, Berkeley	Cattell, C.	University of Minnesota, Minneapolis, MN
Argall, M.	Augsburg College, Minneapolis, MN	Chan, S.	University of Maryland, College Park, MD
Arnoldy, R.	University of New Hampshire, Durham, NH	Chandler, M.	NASA/Marshall Space Flight Center, Huntsville, AL
Ashour-Abdalla, M.	University of California, Los Angeles, CA	Chang, S.-W.	NASA/Marshall Space Flight Center, Huntsville, AL
Avanov, L.	NRC/NSSTC/MSFC	Chapman, S.	University of Warwick, U.K.
Baddeley, L.	University of Leicester, U.K.	Chen, F.	University of California, Los Angeles, CA
Bailey, S.	University of Alaska, Fairbanks, AK	Chen, J.	Boston University, Boston, MA
Baker, D.	LASP, University of Colorado, Boulder, CO	Chen, L.-J.	The University of Iowa, Iowa City, IA
Baker, J.	Johns Hopkins University Applied Physics Laboratory, Laurel, MD	Chen, M.	The Aerospace Corporation, El Segundo, CA
Barker, A.	University of Colorado, Boulder, CO	Chen, C.	Stanford University, Stanford, CA
Barnes, R.	Johns Hopkins University Applied Physics Laboratory, Laurel, MD	Cheng, C.-C.	National Formosa University, Taiwan
Beauvais, E.	Augsburg College, Minneapolis, MN	Chi, P.	University of California, Los Angeles, CA
Bell, T.	Stanford University, Stanford, CA	Chua, D.	Naval Research Laboratory, Washington, DC
Bhattacharjya, J.	Boston University, Boston, MA	Cia, H.	The University of Iowa, Iowa City, IA
Boardsen, S.	NASA/Goddard Space Flight Center, Greenbelt, MD	Cladis, J.	Lockheed Martin, CA
Bonnell, J.	Space Sciences Laboratory, University of California, Berkeley	Clauer, R.	University of Michigan, Ann Arbor, MI
Bortnik, J.	University of California, Los Angeles, CA	Clemmons, J.	Aerospace Corporation, El Segundo, CA
Boudouridis, A.	University of California, Los Angeles, CA	Collier, M.	NASA/Goddard Space Flight Center, Greenbelt, MD
Bougeret, J.-L.	Observatoire Paris Meudon, Meudon Principal, France	Connors, M.	Centre for Science, Athabasca University, Alberta, Canada
Bounds, S.	University of Iowa, Iowa City, IA	Contos, A.	Boston University, Boston, MA
Braginsky, S.	Boston University, Boston, MA	Coombs, J.	Massachusetts Institute of Technology, Boston, MA
Brandt, P.-C.	Johns Hopkins University Applied Physics Laboratory, Laurel, MD	Cote, S.	Boston University, Boston, MA
Bridgman, W.	NASA/Goddard Space Flight Center, Greenbelt, MD	Cowley, S.	University of Leicester, U.K.
Brittnacher, M.	University of Washington, Seattle, WA	Craven, J.	University of Alaska, Fairbanks, AK

Crumley, J.	St. John's University, Queen's, NY	Figueroa, A.	NASA/Goddard Space Flight Center, Greenbelt, MD
Cummer, S.	Duke University, Durham, NC	Fillingim, M.	Space Sciences Laboratory, University of California, Berkeley, CA
Cumnock, J.	University of Texas, Dallas, TX	Finkemeyer, B.	Boston University, Boston, MA
Curto, C.	The University of Iowa, Iowa City, IA	Fishbaugh, K.	Brown University, Providence, RI
Davies, J.	Rutherford Appleton Laboratory, U.K.	Fitzenreiter, R.	NASA/Goddard Space Flight Center, Greenbelt, MD
Decreau, P.	CNRS, Orlean, France	Fleishman, M.	University of California, Los Angeles, CA
Deepak, R.	New Horizons Governors School, Hampton, VA	Fok, M.-C.	NASA/Goddard Space Flight Center, Greenbelt, MD
Dejong, A.	University of Michigan, Ann Arbor, MI	Foreman, E.	Boston University, Boston, MA
Delcourt, D.	Centre d'étude des Environnements Terrestre et Planétaires, Saint-Maur des Fossés, France	Fowler, G.	University of California, Los Angeles, CA
Demekhov, A.	IAP Nizhby Novgorod, Russia	Fox, N.	Johns Hopkins University Applied Physics Laboratory, Laurel, MD
Dempsey, D.	Rice University, Houston, TX	Franz, J.	Cornell University, Ithaca, NY
Denton, R.	Dartmouth College, NH	Fujii, R.	Nagoya University, Nagoya, Japan
Desai, M.	University of Maryland, College Park, MD	Gallagher, Hugh	Johns Hopkins University Applied Physics Laboratory, Laurel, MD
Dohrs, E.	The University of Iowa, Iowa City, IA	Ganguli, G.	Naval Research Laboratory, Washington, DC
Dombeck, J.	University of Minnesota, Minneapolis, MN	Ganushkina, N.	Finnish Meteorological Institute, Helsinki, Finland
Dorelli, J.	The University of Iowa, Iowa City, IA	Ge, Y.	University of California, Los Angeles, CA
Draper, N.	University of Leicester, U.K.	Germany, G.	University of Alabama, Huntsville, AL
Dubinin, E.	University of Michigan, Ann Arbor, MI	Gervais, D.	Boston University, Boston, MA
Dudeny, J.	British Antarctic Survey, Cambridge, U.K.	Giles, B.	NASA Headquarters, Washington, DC
Duguay, R.	Massachusetts Institute of Technology, Boston, MA	Gjerloev, J.	Johns Hopkins University Applied Physics Laboratory, Laurel, MD
Dusenbery, P.	Space Science Institute, Boulder, CO	Goldberg, R.	Johns Hopkins University Applied Physics Laboratory, Laurel, MD
Eather, R.	Keo Consultants, Brookline, MA	Goldstein, J.	Southwest Research Institute, San Antonio, TX
Ebihara, Y.	National Institute of Polar Research, Japan	Grabbe, C.	The University of Iowa, Iowa City, IA
Eccles, A.	Dartmouth College, Dartmouth, NH	Green, James	NASA/Goddard Space Flight Center, Greenbelt, MD
El-Alaoui, M.	University of California, Los Angeles, CA	Green, Janet	SEC/NOAA, Boulder, CO
Elkington, S.	LASP, University of Colorado, Boulder, CO	Greene, H.	Augsburg College, Minneapolis, MN
Elliott, H.	University of Alabama, Huntsville, AL	Grocott, A.	University of Leicester, U.K.
Engebretson, M.	Augsburg College, Minneapolis, MN	Gugliotti-Fishman, G.	Boston University, Boston, MA
Escoubet, P.	ESA/ESTEC	Haines-Stiles, G.	GHSP/Passport to Knowledge, Morristown, NJ
Faden, J.	The University of Iowa, Iowa City, IA	Harris, J.	Boston University, Boston, MA
Faifield, D.	NASA/Goddard Space Flight Center, Greenbelt, MD	Hellinger, P.	Institute of Atmospheric Physics, Prague, Czech Republic
Falthammar, C.-G.	Royal Institute of Technology, Stockholm, Sweden	Henderson, M.	Los Alamos National Laboratory, Los Alamos, NM
Farrugia, C.	University of New Hampshire, Durham, NH	Henize, V.	Rice University, Houston, TX
Fedder, J.	George Mason University, Fairfax, VA	Hinds, S.	Boston University, Boston, MA
Fedorov, A.	CESR, Toulouse, France		
Fennel, J.	The Aerospace Corporation, El Segundo, CA		
Fenrich, F.	Space Sciences Laboratory, University of California, Berkeley, CA		

Hirsch, K.	Boston University, Boston, MA	Klida, M.	Boston University, Boston, MA
Hoffman, R.	NASA/Goddard Space Flight Center, Greenbelt, MD	Kliemann, J.-O.	University of California, Los Angeles, CA
Holdaway, R.	The University of Iowa, Iowa City, IA	Korth, H.	Johns Hopkins University Applied Physics Laboratory, Laurel, MD
Hospodarsky, G.	The University of Iowa, Iowa City, IA	Kozlovsky, A.	University of Oulu, Finland
Hsu, T.	University of California, Los Angeles, CA	Krauklis, I.	Mullard Space Science Laboratory, U.K.
Huddleston, M.	Vanderbilt University, Nashville, TN	Laakso, H.	ESA/ESTEC
Huigen, Y.	Polar Research Institute of China	Ladd, G.	Boston University, Boston, MA
Hull, A.	Space Sciences Laboratory, University of California, Berkeley, CA	Lakhina, G.	Indian Institute of Geomagnetism, India
Hunt, K.	The University of Wisconsin, LaCrosse, WI	Lam, M.	British Antarctic Survey, Cambridge, U.K.
Ieda, A.	STEL, Nagoya University, Japan	Lauben, D.	Stanford University, CA
Imhof, W.	SRI, Menlo Park, CA	Le, G.	NASA/Goddard Space Flight Center, Greenbelt, MD
Immel, T.	Space Sciences Laboratory, University of California, Berkeley	LeDocq, M.	Western Wisconsin Technical College, WI
Inan, U.	Stanford University, Stanford, CA	Lee, D.-Y.	Chungbuk National University, Korea
Jacobs, J.	American Geophysical Union, Washington, DC	Lessard, M.	Dartmouth College, Hanover, NH
Jahn, J.-M.	Southwest Research Institute, San Antonio, TX	Lester, M.	University of Leicester, U.K.
Janhunen, P.	Finnish Meteorological Institute, Helsinki, Finland	Lev-Tov, S.	Stanford University, CA
Johnson, J.	Princeton University, Princeton, NJ	Li, X.	LASP, University of Colorado, Boulder, CO
Jordanova, V.	University of New Hampshire, Durham, NH	Li, S.	The University of Iowa, Iowa City, IA
Jorgenson, A.	Los Alamos National Laboratory, Los Alamos, NM	Liehmon, M.	University of Michigan, Ann Arbor, MI
Kalegaev, V.	Moscow State University, Russia	Lin, N.	Space Sciences Laboratory, University of California, Berkeley, CA
Kanekal, S.	LASP, University of Colorado, Boulder, CO	Liou, K.	The Johns Hopkins University Applied Physics Laboratory
Karamabadi, H.	University of California, San Diego, CA	Lockwood, M.	Rutherford Appleton Laboratory, UK
Karra, M.	Boston University, Boston, MA	Lorentzen, K.	The Aerospace Corporation, El Segundo, CA
Kauristie, K.	Finnish Meteorological Institute, Helsinki, Finland	Lu, G.	HAO/NCAR, Boulder, CO
Kavanagh, A.	Lancaster University, U.K.	Lui, A.	Johns Hopkins University Applied Physics Laboratory, Laurel, MD
Kawano, H.	Kyushu University, Japan	Lund, E.	University of New Hampshire, Durham, NH
Keiling, A.	Space Sciences Laboratory, University of California, Berkeley	Lynch, K.	University of New Hampshire, Durham, NH
Keller, K.	NASA/Goddard Space Flight Center, Greenbelt, MD	Lyons, L.	University of California, Los Angeles, CA
Kendra, M.	Radex Inc., Lexington, MA	Martin, M.	National Geographic Television, Washington, DC
Kepko, L.	Boston University, Boston, MA	Masson, A.	ESA/ESTEC
Khazanov, G.	NASA/Marshall Space Flight Center, Huntsville, AL	Matthews, D.	Boston University, Boston, MA
Khotyaintsev, Y.	Swedish Institute of Space Physics, Sweden	Maynard, N.	ATK Mission Research, Nashua, NH
Khoury, D.	Boston University, Boston, MA	McDonald, E.	University of Washington, Seattle, WA
Kintner, P.	Cornell University, Ithaca, NY	McWilliams, K.	University of Saskatchewan, Canada
Klatt, M.	Augsburg College, Minneapolis, MN	Melnick, R.	NASA/Goddard Space Flight Center/TV, Greenbelt, MD

Menietti, J.	The University of Iowa, Iowa City, IA	Peroomian, V.	University of California, Los Angeles, CA
Meredith, N.	Mullard Space Science Laboratory U.K.	Peterson, W.	University of Colorado, Boulder, CO
Milan, S.	University of Leicester, U.K.	Petrenic, S.	Lockheed Martin ATC, CA
Miyashita, Y.	STEL, Nagoya University, Japan	Pfaff, R.	NASA/Goddard Space Flight Center, Greenbelt, MD
Moldwin, M.	University of California, Los Angeles, CA	Pickett, J.	The University of Iowa, Iowa City, IA
Moore, T.	NASA/Goddard Space Flight Center, Greenbelt, MD	Polniaszek, T.	BBC, London, U.K.
Moorer, D.	LASP, University of Colorado, Boulder, CO	Popielawska, B.	Poland
Morgan, D.	University of Iowa, Iowa City, IA	Prakash, M.	SUNY at Stony Brook, NY
Mouikis, C.	University of New Hampshire, Durham, NH	Pritchett, P.	University of California, Los Angeles, CA
Mozer, F.	Space Sciences Laboratory, University of California, Berkeley, CA	Puhl-Quinn, P.	University of Iowa, Iowa City, IA
Mukai, T.	Institute of Space & Astronautical Science, Kanagawa, Japan	Pulkinnen, T.	Finnish Meteorological Institute, Helsinki, Finland
Murata, K.	Southern Osaka Univ., Osaka, Japan	Rae, J.	University of Alberta, Canada
Mursula, K.	University of Oulu, Finland	Raeder, J.	University of New Hampshire, Durham, NH
Nakai, H.	Ibaraki High School, Japan	Rastaetter, L.	NASA/Goddard Space Flight Center, Greenbelt, MD
Narock, T.	Johns Hopkins University, Baltimore, MD	Reeves, G.	Los Alamos National Laboratory, Los Alamos, NM
Nerdahl, R.	Minneapolis Planetarium, Minneapolis, MN	Reiff, P.	Rice University, Houston, TX
Neudegg, D.	University of Leicester, U.K.	Rheinard, A.	University of Washington
Niciejewski, R.	University of Michigan, Ann Arbor, MI	Richards, P.	NASA Headquarters, Washington, DC
Niehof, J.	Boston University, Boston, MD	Richters, M.	Boston University, Boston, MA
Nishitani, N.	Nagoya University, Japan	Rigler, J.	LASP, University of Colorado, Boulder, CO
Niskala, K.	University of Oulu, Finland	Rodger, A.	British Antarctic Survey, Cambridge, England
Nose, M.	Kyoto University, Japan	Rostoker, G.	University of Alberta, Edmonton, Canada
Ntaikos, D.	Boston University, Boston, MA	Rowland, D.	NASA/Goddard Space Flight Center, Greenbelt, MD
Ober, D.	ATK Mission Research, Nashua, NH	Russell, C.	IGPP-University of California, Los Angeles, CA
O'Brien, T. P.	The Aerospace Corporation, El Segundo, CA	Samara, M.	Dartmouth College, Dartmouth, NH
Ohtani, S.-I.	Johns Hopkins University Applied Physics Laboratory, Laurel, MD	Sanborn, J.	Boston University, Boston, MA
Olsson, A.	Swedish Institute of Space Physics, Kiruna, Sweden	Sanchez, E.	SRI International, Menlo Park, CA
Omidi, N.	Solana Scientific Inc., Solana Beach, CA	Sandahl, I.	Swedish Institute of Space Physics, Kiruna, Sweden
Onsager, T.	NOAA/Space Environment Center, Boulder, CO	Santolik, O.	Charles University, Prague, Czech Republic
Opgenoorth, H.	ESA/ESTEC	Sauvaud, J.	CESR, Toulouse, France
Ostgaard, N.	University of Bergen, Norway	Savin, S.	Space Research Inst., Russian Acad. of Sciences, Moscow, Russia
Panov, E.	IKI, Moscow, Russia	Schauf, A.	Hampton University, VA
Papadopoulos, K.	University of Maryland, College Park, MD	Schreiber, R.	Torun, Poland
Parks, G.	University of California, Berkeley, CA	Schrifer, D.	University of California, Los Angeles, CA
Paterson, W.	Hampton University, VA	Schwab, R.	University of Saskatchewan, Canada
Peredo, M.	Raytheon Corporation, MD	Scudder, J.	The University of Iowa, Iowa City, IA
Perez, J.	Auburn University, Auburn, AL		

Seran, E.	Centre d'Etude des Environnements Terrestre et Planétaires, France	Toivanen, P.	Finnish Meteorological Institute, Finland
Sergeev, V.	St. Petersburg, Russia	Tomic, J.	Boston University, Boston, MA
Shay, M.	University of Delaware, DE	Topliss, S.	Mullard Space Science Laboratory U.K.
Shelburne, G.	Augsburg College, Minneapolis, MN	Trakhtengerts, Y.	IAP Nizhby Novgorod, Russia
Sheldon, R.	Wheaton College, Wheaton, IL	Trattner, K.	Lockheed Martin ATC, CA
Shen, C.	University of Iowa, Iowa City, IA	Travnicek, P.	Institute of Atmospheric Physics, Prague, Czech Republic
Shepherd, S.	Dartmouth College, Dartmouth, NH	Tsurutani, B.	NASA/Jet Propulsion Lab, CA
Shirah, G.	NASA/Goddard Space Flight Center, Greenbelt, MD	Tsyganenko, N.	NASA/Goddard Space Flight Center, Greenbelt, MD
Shue, J.-H.	National Central University, Taiwan	Tu, J.	Center for Atmospheric Research, Lowell, MA
Sibeck, D.	NASA/Goddard Space Flight Center, Greenbelt, MD	Tung, Y.-K.	University of California, Berkeley, CA
Sigsbee, K.	University of Iowa, Iowa City, IA	Turner, N.	Florida Institute of Technology, FL
Sigwarth, J.	NASA/Goddard Space Flight Center, Greenbelt, MD	Uchida, N.	MediAtelier USA, Inc., Santa Monica, CA
Simmerer, J.	Boston University, Boston, MA	Uozumi, T.	Kyushu University, Fukuoka City, Japan
Singh, N.	University of Alabama, Huntsville, AL	Urquhart, A.	Rice University, TX
Slinker, S.	Naval Research Laboratory, Washington, DC	Vaisberg, O.	Space Research Inst., Moscow, Russia
Sojka, J.	Utah State University, Logan, UT	Valek, P.	Auburn University, Auburn, AL
Song, P.	University of Michigan, Ann Arbor, MI	Vo, H.	MIT Haystack Observatory, Westford, MA
Spann, J.	NASA/Marshall Space Flight Center, Huntsville, AL	Von Werne, D.	Boston University, Boston, MA
Spasojevic, M.	Space Sciences Laboratory, University of California, Berkeley, CA	Waldrop, L.	University of Illinois, Champagne- Urbana, IL
Spence, H.	Boston University, Boston, MA	Watkins, N.	British Antarctic Survey, U.K.
Stasiewicz, K.	Swedish Inst of Space Physics, Uppsala, Sweden	Weatherwax, A.	Siena College, NY
Stevenson, A.	University of Alabama, Huntsville, AL	Whipple, E.	University of Washington, WA
Storey, L.	Cucuron, France	Williams, H.	BBC, London, U.K.
Storey, J.	University of Alberta, Canada	Williams, J.	University of Washington, WA
Strangeway, R.	University of California, Los Angeles, CA	Wilson, S.	XYTV, Leeds, U.K.
Streltsov, A.	Dartmouth College, Dartmouth, NH	Wilson, G.	Mission Research Corporation, Nashua, NH
Stubbs, T.	University of Maryland, Baltimore County, MD	Wilson, J.	NASA SHARP Program at Hampton University, VA
Su, Y.-J.	University of Alabama, Huntsville, AL	Wilson, M.	University of Leicester, U.K.
Swisdak, M.	University of Maryland, College Park, MD	Wiltberger, M.	NCAR, CO
Tagirov, V.	Polar Geophysical Institute, Apatity, Russia	Winglee, R.	University of Washington, WA
Takahashi, M.	Yamanashi Prefectural Science Center, Kofu, Yamanashi, Japan	Withers, M.	The George Washington University, Washington, DC
Takahashi, K.	Johns Hopkins University Applied Physics Laboratory, Laurel, MD	Wu, B.-H.	
Tanaka, Y.	Nagoya University, Japan	Wu, Q.	University of Michigan, Ann Arbor, MI
Tanskanen, P.	University of Oulu, Oulu, Finland	Wu, Y.	Chinese Academy of Sciences
Taylor, M.	ESA/ESTEC	Wu, C.-C.	NASA/Goddard Space Flight Center, Greenbelt, MD
Titova, E.	Polar Geophysical Institute, Apatity, Russia	Wuest, M.	Southwest Research Institute, San Antonio, TX
		Wygant, J.	University of Minnesota, Minneapolis, MN

Yahnin, A.	Polar Geophysical Institute, Apatity, Russia	Zesta, E.	University of California, Los Angeles, CA
Yeoman, T.	University of Leicester, U.K.	Zheng, Y.	Johns Hopkins University Applied Physics Laboratory, Laurel, MD
Young, A.	University of Minnesota, Minneapolis, MN	Zhou, X.	NASA/Jet Propulsion Laboratory, CA
Zejun, H.	Polar Research Institute of China	Zong, Q.-G.	Boston University, Boston, MA
Zelenyi, L.	Russian Academy of Science, Space Research Institute, Moscow	Zuluaga, C.	Boston University, Boston, MA
Zeng, W.	University of Alabama, Huntsville, AL	Zurbuchen, T.	University of Michigan, Ann Arbor, MI

Appendix D: Young Scientists Benefitting from the Polar Mission

Below is a list of young scientists who have benefitted from the Polar Mission during their undergraduate, graduate, or post-doctoral careers. The affiliations quoted are either the current or last know address.

Adrian, Mark	NASA/Goddard Space Flight Center, Greenbelt, MD	Chen, Curtis	Stanford University, Stanford, CA
Alothman, Mohamed	University of Bahrain, Bahrain	Chi, Peter	University of California, Los Angeles, CA
Anderson, Carl	University of Alaska, Fairbanks, AK	Chua, Damien	Naval Research Laboratory, Washington, DC
Anderson, Phillip	University of Texas, Dallas, TX	Cia, H. J.	University of Iowa, Iowa City
Argall, Matthew	Auburn University, Auburn, AL	Clemmons, James	Aerospace Corporation, El Segundo, CA
Avanov, Levon	NASA/Marshall Space Flight Center, Huntsville, AL	Collier, Michael R.	NASA/Goddard Space Flight Center, Greenbelt, MD
Baddeley, Lisa	University of Leicester, Radio and Space Plasma Physics	Contos, Adam R.	Boston University, Boston, MA
Bailey, Scott M.	University of Alaska, Fairbanks, AK	Coombs, Jeremy	Massachusetts Institute of Technology, Boston, MA
Baker, Joseph	The Johns Hopkins University Applied Physics Laboratory	Cote, Sean	Boston University, Boston, MA
Barker, Austin	University of Colorado, Boulder, CO	Crumley, James	St. John's University, Queen's, NY
Beauvais, Emily	Auburn University, Auburn, AL	Cummer, Steven	Duke University, Durham, NC
Bhattacharjya, Jyotirmoyee	Boston University, Boston, MA	Cumnock, Judy	University of Texas, Dallas, TX
Bonnell, John	Space Sciences Laboratory, Univ. of California, Berkeley, CA	Curto, Canna	University of Iowa, Iowa City, IA
Bortnik, Jacob	University of California, Los Angeles, CA	Deepak, Rae	New Horizons Governors School, Hampton, VA
Boudouridis, Athanasios	University of California, Los Angeles, CA	Dejong, Anna	University of Michigan, Ann Arbor, MI
Bounds, Scott	University of Iowa, Iowa City, IA	Dempsey, D.	Rice University, Houston, TX
Braginsky, Slavik	Boston University, Boston, MA	Desai, Mihir	University of Maryland, College Park, MD
Brandt, Pontus	Johns Hopkins University Applied Physics Laboratory, Laurel, MD	Dohrs, Eric	University of Iowa, Iowa City, IA
Brittnacher, Mitchell	University of Washington, Seattle, WA	Dorelli, John	University of Iowa, Iowa City, IA
Cao, Xuejun	University of Iowa, Iowa City, IA	Draper, Natalie	University of Leicester, U.K.
Cartwright, Megan	University of California, Los Angeles, CA	Duguay, Ryan	Massachusetts Institute of Technology, Boston, MA
Chan, Stephen	University of Maryland, College Park, MD	Eccles, Alicia Ann	Dartmouth College, Dartmouth, NH
Chandler, Michael	NASA/Marshall Space Flight Center, Huntsville, AL	El-Alaoui, Mostafa	University of California, Los Angeles, CA
Chang, Shen-Wu	NASA/Marshall Space Flight Center, Huntsville, AL	Elkington, Scot	LASP, University of Colorado, Boulder, CO
Chen, Jiasheng	Boston University, Boston, MA	Elliott, H.	University of Alabama, Huntsville, AL
Chen, Li-Jen	University of Iowa, Iowa City, IA	Faden, Jeremy	University of Iowa, Iowa City, IA
Chen, Margaret	The Aerospace Corporation, El Segundo, CA	Fillingim, Matt	Space Sciences Laboratory, Univ. of California, Berkeley, CA

Finkemeyer, Barbara	Boston University, Boston, MA	Karra, Maria	Boston University, Boston, MA
Fishbaugh, Kathryn	Brown University, Providence, RI	Kavanagh, Andrew John	Lancaster University, U.K.
Fleishman, Michael	University of California, Los Angeles, CA	Kawano, Hideaki	Kyushu University, Japan
Fok, Mei-Ching	NASA/Goddard Space Flight Center, Greenbelt, MD	Keiling, Andreas	Space Sciences Laboratory, Univ. of California, Berkeley, CA
Foreman, Eric A.	Boston University, Boston, MA	Keller, Kristi	NASA/Goddard Space Flight Center, Greenbelt, MD
Fowler, Galen	University of California, Los Angeles, CA	Kepko, Larry	Boston University, Boston, MA
Fox, Nicola	Johns Hopkins University Applied Physics Laboratory, Laurel, MD	Khoury, Danielle	Boston University, Boston, MA
Gallagher, Hugh	Johns Hopkins University Applied Physics Laboratory, Laurel, MD	Klida, Mike	Boston University, Boston, MA
Ge, Yasong	University of California, Los Angeles, CA	Klatt, Matthew	Auburn University, Auburn, AL
Gervais, David	Boston University, Boston, MA	Kliemann, Jan-Oliver	University of California, Los Angeles, CA
Giles, Barbara	NASA Headquarters, Washington DC	Korth, Haje	Johns Hopkins University Applied Physics Laboratory, Laurel, MD
Gugliotti-Fishman, Gina M.	Boston University, Boston, MA	Krauklis, Ian	Mullard Space Science Laboratory, U.K.
Gjerloev, Jesper W.	Johns Hopkins University Applied Physics Laboratory, Laurel, MD	Laakso, Harri	ESA/ESTEC
Goldstein, Jerry	Southwest Research Institute, San Antonio, TX	Ladd, Gabe	Boston University, Boston, MA
Green, Janet	NOAA/Space Environment Center, Boulder, CO	Lauben, David	Stanford University, Stanford, CA
Greene, Heather	Augsburg College	Le, Guan	NASA/Goddard Space Flight Center, Greenbelt, MD
Grocott, Adrian	University of Leicester, Radio and Space Plasma Physics	LeDocq, Michael	Western Wisconsin Technical College, WI
Harris, John	Boston University, Boston, MA	Lev-Tov, Sean	Stanford University, Stanford, CA
Henize, Vance	Rice University, Houston, TX	Li, Shashan	University of Iowa, Iowa City, IA
Hinds, Suwada	Boston University, Boston, MA	Liehmon, Michael	University of Michigan, Ann Arbor, MI
Hirsch, Karen	Boston University, Boston, MA	Liou, Kan	Johns Hopkins University Applied Physics Laboratory, Laurel, MD
Holdaway, Robert	University of Iowa, Iowa City, IA	Lorentzen, Kirsten	Aerospace Corporation, El Segundo, CA
Hospodarsky, George	University of Iowa, Iowa City, IA	Lu, Gang	HAO/NCAR, Boulder, CO
Hsu, T. S.	University of California, Los Angeles, CA	Lund, Eric	University of New Hampshire, Durham, NH
Huddleston, Matthew	Vanderbilt University, Nashville, MN	Matthews, David	Boston University, Boston, MA
Ieda, Akimasa	STEL, Nagoya University, Japan	McDonald, Elizabeth	University of Washington, Seattle, WA
Immel, Thomas	Space Sciences Laboratory, Univ. of California, Berkeley, CA	McWilliams, Kathryn	University of Saskatchewan, Canada
Jahn, Jorg-Micha	Southwest Research Institute, San Antonio, TX	Meredith, Nigel P.	Mullard Space Science Laboratory U.K.
Jordanova, Vania	University of New Hampshire, Durham, NH	Milan, Steve	University of Leicester, U.K.
Jorgenson, Anders	Los Alamos National Laboratory, Los Alamos, NM	Miyashita, Yukinaga	STEL, Nagoya University, Japan
Kanekal, Shri	LASP, University of Colorado, Boulder, CO	Moldwin, Mark	University of California, Los Angeles, CA
		Moorer, Dan	LASP, University of Colorado, Boulder, CO

Morgan, David	University of Iowa, Iowa City, IA		Center, Greenbelt, MD
Narock, Thomas	Johns Hopkins University, Baltimore, MD	Simmerer, Jennifer	Boston University, Boston, MA
Ntaikos, Dimitrios	Boston University, Boston, MA	Spann, James	NASA/Marshall Space Flight Center, Huntsville, AL
Neudegg, David	University of Leicester, U.K.	Spasojevic, Maria	Space Sciences Laboratory, Univ. of California, Berkeley, CA
Niehof, John	Boston University, Boston, MA	Stevenson, A.	University of Alabama, Huntsville, AL
Nose, Masahito	Kyoto University, Japan	Storey, Jonathan	University of Alberta, Canada
O'Brien, T. Paul	Aerospace Corporation, El Segundo, CA	Stubbs, Timothy	University of Maryland, Baltimore County, MD
Ohtani, Shin	Johns Hopkins University Applied Physics Laboratory, Laurel, MD	Su, Y.-J.	University of Alabama, Huntsville, AL
Ostgaard, Nikolai	University of Bergen, Norway	Swisdak, Michael	University of Maryland, College Park, MD
Paterson, William	Hampton University, Hampton, VA	Takahasi, Kazue	Johns Hopkins University Applied Physics Laboratory, Laurel, MD
Peredo, Mauricio	Raytheon Corporation, MD	Taylor, Matthew	ESA/ESTEC
Peroomian, Vahe	University of California, Los Angeles, CA	Toivanen, Petri	Finnish Meteorological Institute
Petrenic, Steven	Lockheed Martin ATC, Palo Alto, CA	Tomic, Jelena	Boston University, Boston, MA
Pickett, Jolene	The University of Iowa, Iowa City, IA	Topliss, Stephen	Mullard Space Science Laboratory U.K.
Prakash, Manju	SUNY at Stony Brook, NY	Trattner, Karlheinz	Lockheed Martin ATC, Palo Alto, CA
Pritchett, Philip	University of California, Los Angeles, CA	Tu, Jiannan	Center for Atmospheric Research, Lowell, MA
Puhl-Quinn, Pamela	University of Iowa, Iowa City, IA	Turner, Niescja	Florida Institute of Technology, FL
Rae, Jonathan	University of Alberta, Canada	Urquhart, Andrew	Rice University, Houston, TX
Rastaetter, Lutz	NASA/Goddard Space Flight Center, Greenbelt, MD	Valek, P.	Auburn University, Auburn, AL
Rheinard, Alysha	University of Washington, Seattle, WA	Von Werne, David	Boston University, Boston, MA
Richters, Melissa	Boston University, Boston, MA	Waldrop, Lara Susan	University of Illinois, Champagne-Urbana, IL
Rigler, Josh	LASP, University of Colorado, Boulder, CO	Weatherwax, Allan	Siena College, NY
Samara, Marilia	Dartmouth College, Dartmouth, NH	Williams, John	University of Washington, Washington, DC
Sanborn, Jeff	Boston University, Boston, MA	Wilson, Jaron	NASA SHARP Program at Hampton University, VA
Schauf, Andy	Hampton University, Hampton, VA	Wilson, Matthew	University of Leicester, U.K.
Schrivier, D.	University of California, Los Angeles, CA	Wiltberger, Michael	HAO/NCAR, Boulder, CO
Shay, Michael	University of Delaware, DE	Wu, Chin-Chun	NASA/Goddard Space Flight Center, Greenbelt, MD
Shelburne, Geoff	Auburn University, Auburn, AL	Young, Andrew	University of Minnesota, Minneapolis, MN
Sheldon, Robert	Wheaton College, Wheaton, IL	Zeng, W.	University of Alabama, Huntsville, AL
Shen, Chonghui	University of Iowa, Iowa City, IA	Zesta, Eftyhia	University of California, Los Angeles, CA
Shepherd, Simon	Dartmouth College, Dartmouth, NH	Zhou, Xiaoyan	NASA/Jet Propulsion Laboratory, CA
Shue, Jih-Hong	National Central University, Taiwan	Zong, Q.-G.	Boston University, Boston, MA
Sigsbee, Kristine	University of Iowa, Iowa City, IA	Zuluaga, Carlos	Boston University, Boston, MA
Sigwarth, John	NASA/Goddard Space Flight		

On the covers

Front cover left, top to bottom:

Magnetohydrodynamic simulation of the interaction of the solar wind and Earth's magnetosphere

High-resolution, multicolor image of Earth's visible aurora by Polar/VIS

High-resolution image of Earth's Far Ultraviolet Aurora by Polar/UVI for the same period as above

Global X-ray image of Earth's aurora by Polar/PIXIE for the same period as above

Simulation of null line reconnection at Earth's magnetopause

Model of Earth's radiation belts based on Polar and SAMPEX data

Back cover left, top to bottom:

Simulation tracking the motion of ions flowing from Earth's ionosphere into the magnetosphere during a geomagnetic storm

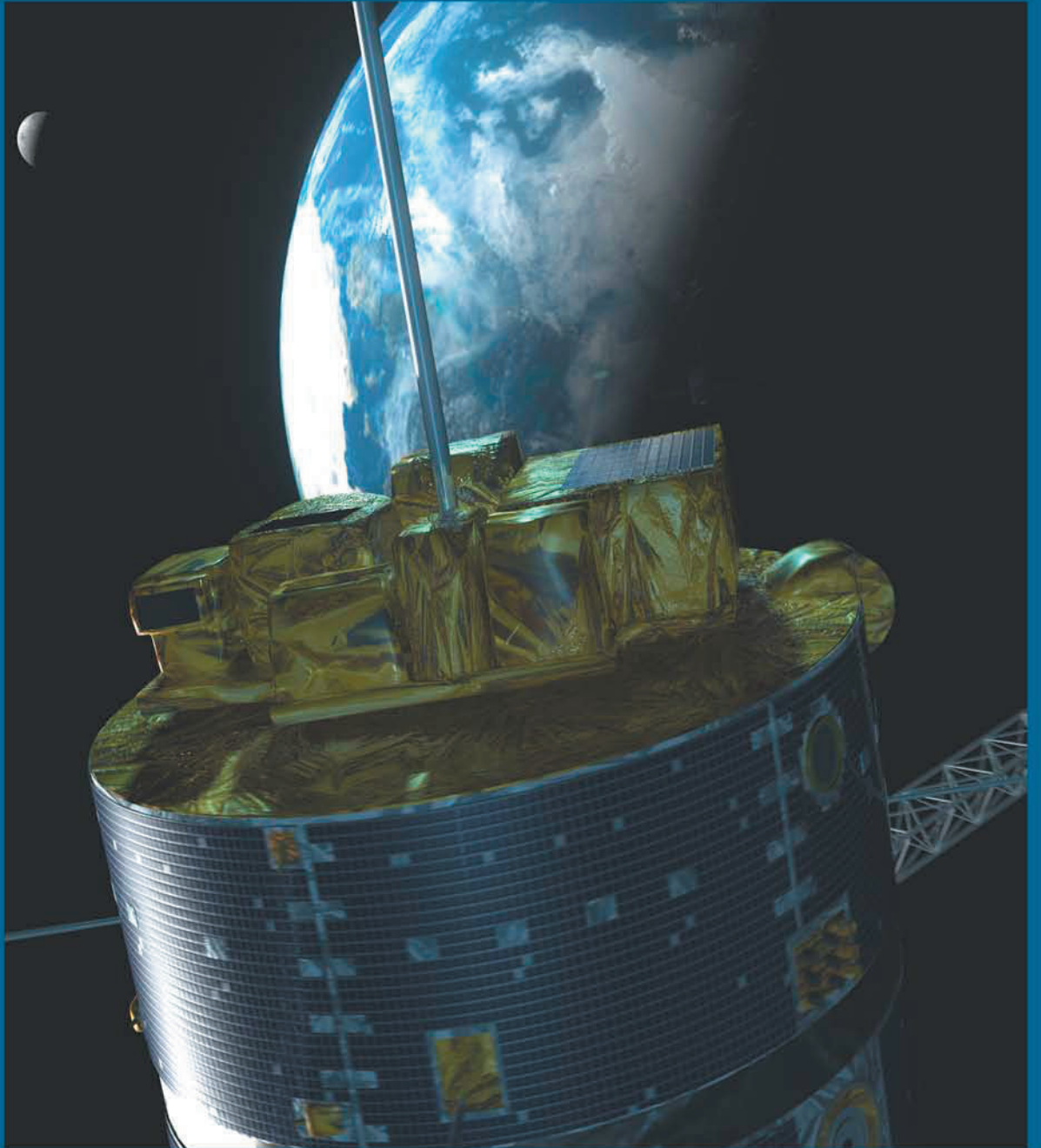
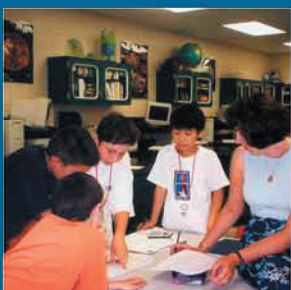
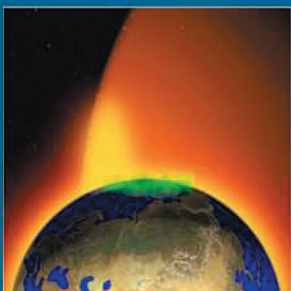
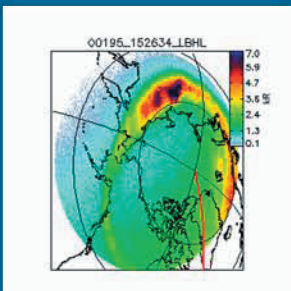
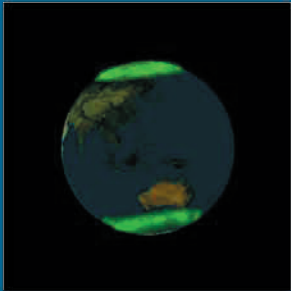
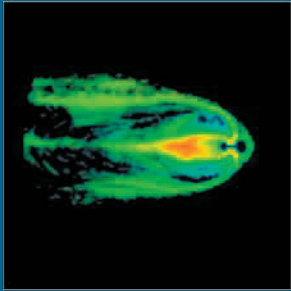
Observation of north and south conjugate far ultraviolet aurora in a single image by Polar/VIS

The Polar spacecraft prior to launch

Auroral substorm observed at far-ultraviolet wavelengths by Polar/UVI

Depiction of cleft-ion fountain where ions flow out from Earth's ionosphere during a geomagnetic storm

Polar scientists have taken an active role in education and public outreach by engaging K-12, undergraduate and graduate students



National Aeronautics and Space
Administration

Goddard Space Flight Center
Greenbelt, Maryland 20771